Primljen / Received: 23.3.2016.
Ispravljen / Corrected: 5.8.2016.
Prihvaćen / Accepted: 1.9.2016.
Dostupno online / Available online: 10.10.2016.

Discrete dome model for St. Jacob cathedral in Šibenik

Authors:

Dalibor Gelo, MCE
Technical college in Zagreb
Department of Civil Engineering
dgelo@tvz.hr

Prof. Mladen Meštrović, PhD. CE
University of Zagreb
Faculty of Civil Engineering
mestar@grad.hr

Preliminary report

Dalibor Gelo, Mladen Meštrović

Discrete dome model for St. Jacob cathedral in Šibenik

Principal features of the non-smooth contact dynamics method, which served as basis for the LMGC90 software formulation, are presented in the paper. The objective of the paper is to present creation of a discrete model using the LMGC90 software. The discrete dome model of the St. Jacob cathedral in Šibenik was created, and dynamic behaviour of the dome was checked by time-history analysis. The results point to a highly nonlinear behaviour of the dome, which would be difficult to detect with the finite element method. The results also reveal critical points, i.e. the maximum displacement and contact force points along the dome.

Ključne riječi:
discrete element, non-smooth contact dynamics, LMGC90, contact law, Gauss-Seidel

Prethodno priopćenje

Dalibor Gelo, Mladen Meštrović

Diskretni model kupole katedrale svetoga Jakova u Šibeniku

U radu su prikazane osnove metode neglatke kontaktne dinamike na temelju koje je formuliran programski paket LMGC90. Cilj rada je prezentirati postupak izrade diskretnog modela u programu LMGC90. Izrađen je diskretni model kupole katedrale sv. Jakova u Šibeniku i na njemu je provedena time-history analiza. Dobiveni rezultati upućuju na značajna nelinearna ponašanja kupole koja je teško obuhvatiti metodom konačnih elemenata. Rezultati upućuju na kritična mjesta, to jest locirana su područja maksimalnih pomaka i kontaktnih sila.

Ključne riječi:
diskretni element, neglatka kontaktna dinamika, LMGC90, kontaktni zakon, Gauss-Seidel

Vorherige Mitteilung

Dalibor Gelo, Mladen Meštrović

Diskretes Modell der Kuppel der Kathedrale des Heiligen Jakob in Šibenik

In dieser Arbeit werden die Grundsätze der nicht-glatten Kontaktdynamik, auf die sich das Softwarepaket LMGC90 stützt, dargestellt. Das Ziel der Arbeit ist, den Aufbau eines diskreten Modells im Programm LMGC90 darzustellen. Ein diskretes Modell der Kuppel der Kathedrale des Heiligen Jakob in Šibenik wurde erstellt und mittels Zeitverlaufsanalysen untersucht. Die Ergebnisse weisen auf ein bedeutend nichtlineares Verhalten hin, das nicht einfach mit finiten Elementen erfasst werden kann. Ebenso deuten die Resultate auf kritische Stellen, so dass Bereiche maximaler Verschiebungen und Kontaktkräfte lokalisiert werden konnten.

Ključne riječi:
diskrete Elemente, nicht-glatte Kontaktdynamik, LMGC90, Kontaktgesetze, Gauss-Seidel

1. Introduction

Complex modelling and lack of adequate software are some of the reasons behind poor acceptance of discrete models in engineering practice. Although the finite element method (FEM) is a good mathematical model for describing the continuum, the discrete method is the preferred choice in the sphere of discontinuous media. The discrete method is based on defining geometry of individual elements, i.e. discrete elements and their mutual contact relationship.

In the territory of the Republic of Croatia, there are many buildings of exceptional cultural and historic significance that are built of stone blocks. Structures made of stone blocks without binder, or with poor binder, are considered to be discontinuous structural systems. St. James Cathedral in Šibenik is made of stone blocks without the use of binder, and it therefore belongs to the group of discontinuous systems. This paper focuses on the development of numerical model of the dome of St. James Cathedral in Šibenik, and on the response of this cathedral to seismic action. Numerical model was developed using the LMGC90 software, which is based on discrete formulation.

2. Discrete element method

The finite-element method (FEM) is widely accepted in all areas of engineering practice. The main property of the FEM is that it considers numerical model as a continuous medium. The geometry and behaviour of a continuous medium is described using pre-defined finite elements. Although behaviour of a great number of problems can be described using the FEM, the use must be made of the discrete element method (DEM) when a discontinuous or intermittent medium is considered. The discrete numerical model is described by a set of individual discontinuous media called discrete elements. They can be observed as absolutely rigid or deformable areas. If deformable discrete elements are considered, then the combined method called finite-discrete element method is used [1]. The finite-discrete element method is aimed at using advantages presented by the FEM and DEM. The interaction between individual discrete elements is described using contact laws.

Laws regulating contact between discrete elements can be defined by means of the smooth and non-smooth contact dynamics. The smooth dynamics attempts to describe deformable behaviour of discrete elements. Contacts between discrete elements are described by means of springs or functions. Behaviour at the contact can depend on the size of overlap, relative speed and relative force.

Spring-based modelling requires the use of time steps that should be smaller than the elastic time response so as to ensure numerical stability [2]. Rigid discrete elements require an increase in spring rigidity, and a shorter time step, which increases the time needed for analysis. Absolutely rigid materials require infinitesimal time steps. Smooth contact dynamics is used for modelling materials with finite rigidity [2]. In the non-smooth contact dynamics, discrete elements are assumed to be absolutely rigid, while elastic behaviour between discrete elements is neglected [2].

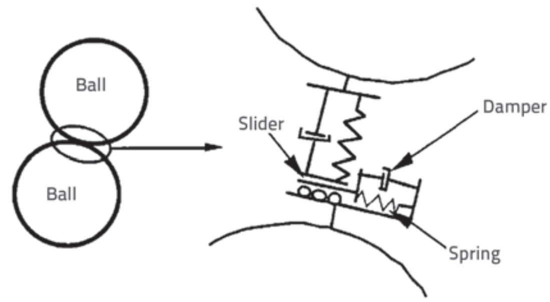

Figure 1. Model of the contact between discrete elements [2]

Unlike the smooth method, the non-smooth method enables the use of a greater time step and can describe "absolutely rigid materials". Proper attention must be paid to the selection of time step. A large time step may result in excessive penetration of discrete elements. An advantage of this method is that it converges quite well, which is otherwise a big problem in case of models with a large number of elements [2]. The non-smooth contact method is implemented in the program LMGC90, which is based on an open source code. The LMGC90 code is written in Fortran and C, and the programming language Python is used for entering the data. It should be noted that the program works exclusively with the operating system Linux, and supports the OpenMP, which enables computing in parallel.

2.1. Equation of motion of non-deformable discrete elements (DE)

Motion of non-deformable discrete elements is described in the Newton-Euler system of equations [3].

$$\begin{aligned} \mathbf{M}\dot{\mathbf{v}}^T &= \mathbf{p}(t) + \mathbf{r} \\ \mathbf{I}\dot{\boldsymbol{\omega}} &= \mathbf{m}(t) + \mathbf{m}_r \end{aligned} \tag{1}$$

Generalized coordinates $\mathbf{q}$ define position of the centre of mass of discrete elements with respect to the origin of the Cartesian coordinate system. The speed of the centre of mass $\mathbf{v}^T$ is defined by deriving coordinates $\mathbf{q}$ along the time t.

$$\mathbf{v}^T = \dot{\mathbf{q}} \tag{2}$$

The speed of the discrete element's rotation around the centre of the mass is defined by means of ω. The values $\mathbf{p}(t)$ and $\mathbf{m}(t)$ describe external resulting force and external resulting moment. The matrices **M** i **I** define the mass matrix and the inertia matrix. The vectors **r** and $\mathbf{m}_r$ are the forces and moments that are caused by contact between two discrete elements.

2.2. Interaction of discrete elements

Each discrete element must have defined contours, interaction points, material characteristics and the law specifying behaviour at the place of contact. The contact of two discrete elements is realised between the selected interaction point and the closest point of the potential interaction body. The term *candidate*, which relates to the body whose interaction point is observed, is introduced to facilitate understanding. The term antagonist, representing the potential interaction body, is also introduced.

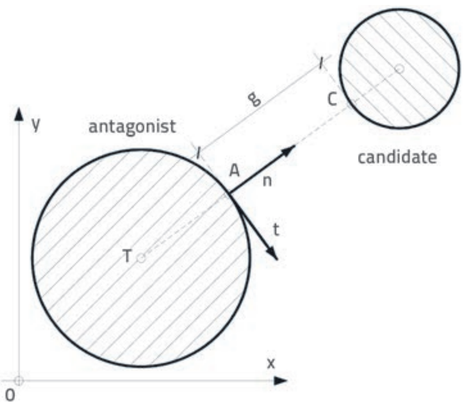

Figure 2. In-plane relation between candidate and antagonist

Figure 2 shows an in-plane problem of relationship between the *candidate* and *antagonist*. Points C and A are potential points of contact. Local axes are linked to the colliding body, while n is normal to the tangential plane. To facilitate presentation, the problem is presented in two-dimensional space, but can simply be extended to three dimensions [3, 4].

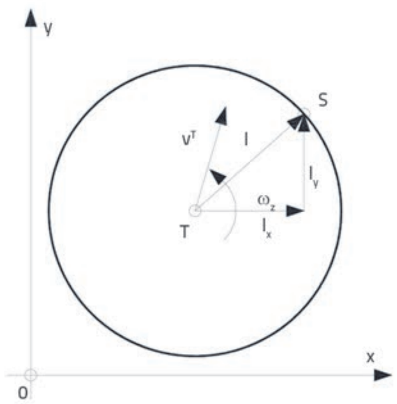

Figure 3. Motion of rigid discrete element

The motion of a rigid discrete element in *x-y* plane is presented in Figure 3. Two points are defined. The point *T* represents the centre of the mass, while the point *S* is situated on the contour of the discrete element. The speed of the point *S* is defined by the speed of the centre of the mass $\mathbf{v}_T$ and by angular velocity ω_z which is related to the rotation around the axis *z*. The velocity of the point *S* can be described by the following expression (3):

$$\begin{bmatrix} v^S{}_x \\ v^S{}_y \end{bmatrix} = \begin{bmatrix} 1 & 0 & -l_y \\ 0 & 1 & l_x \end{bmatrix} \begin{bmatrix} v^T{}_x \\ v^T{}_y \\ \omega_z \end{bmatrix} \tag{3}$$

The two-dimensional problem of the velocity of points on the contour of discrete elements can be extended to a three-dimensional problem, and the velocity of a point is then defined by the expression (4):

$$\mathbf{v}^S = \mathbf{v}^T + \boldsymbol{\omega} \times \mathbf{L} \tag{4}$$

where $\mathbf{v}^S$ is the velocity vector in point *S*, $\mathbf{v}^T$ is the velocity vector of the centre of mass, while $\boldsymbol{\omega}$ is the angular velocity vector. The matrix $\mathbf{L}$ assumes the following form:

$$\mathbf{L} = \begin{bmatrix} 0 & l_z & -l_y \\ -l_z & 0 & l_x \\ l_y & -l_x & 0 \end{bmatrix} \tag{5}$$

It defines the relationship between the angular velocity $\boldsymbol{\omega}$ and velocity in point *S*. In Figure 3, the distance between the potential point of contact between two discrete elements is defined by the vector $\mathbf{g}$, and the change of vector $\mathbf{g}$ in time defines relative velocity between discrete elements. From this point on, the relative velocity between discrete elements will be designated with $\mathbf{U}$. The velocities of potential points of contact between the *candidate* and the *antagonist* are defined in eq. (4), and their difference defines relative velocity as follows

$$\mathbf{U} = \mathbf{v}_C^T + \boldsymbol{\omega}_C \times \mathbf{L}_C - \mathbf{v}_A^T + \boldsymbol{\omega}_A \times \mathbf{L}_A \tag{6}$$

where $\mathbf{v}_C^T$ and $\mathbf{v}_A^T$ are the centre-of-mass velocities of the *candidate* and the *antagonist*, $\boldsymbol{\omega}_C$ and $\boldsymbol{\omega}_A$ are angular velocities of the *candidate* and the *antagonist*. Eq. (6) can be re-formulated as follows:

$$\mathbf{U} = \begin{bmatrix} \mathbf{I} & \mathbf{L}_C & -\mathbf{I} & -\mathbf{L}_A \end{bmatrix} \begin{bmatrix} \mathbf{v}_C^T \\ \boldsymbol{\omega}_C \\ \mathbf{v}_A^T \\ \boldsymbol{\omega}_A \end{bmatrix} \tag{7}$$

or

$$\mathbf{U} = \mathbf{H}^T \mathbf{v} \tag{8}$$

where:

$$\mathbf{H}^T = \begin{bmatrix} \mathbf{I} & \mathbf{L}_C & -\mathbf{I} & -\mathbf{L}_A \end{bmatrix} \tag{9}$$

The matrices $\mathbf{L}_C$ and $\mathbf{L}_A$ correspond to the matrix $\mathbf{L}$ for potential points of contact between the *candidate* and the *antagonist* while $\mathbf{I}$ is the unit matrix measuring 3 x 3. Eq. (8) is the basic equation of the NSCD method, and it links relative velocities between the potential place of contact of two discrete elements and global velocities of the same potential points of contact. The scalar product of Equation 8, with unit vector $[\vec{n}_\alpha \quad \vec{t}_\alpha \quad \vec{m}_\alpha]^T$ that defines the local coordinate system, transforms relative velocities in the direction of local axes, as shown in Figure 3. The index α denoting each potential contact in the system with several discrete elements is introduced. After transformation and introduction of the index α, the Expression 8 assumes the following form:

$$\mathbf{U}_\alpha = \mathbf{H}_\alpha^T \mathbf{v}_\alpha \tag{10}$$

The following relationship can also be established using Eq. (10):

$$\mathbf{r}_\alpha = \mathbf{H}_\alpha \mathbf{R}_\alpha \tag{11}$$

where $\mathbf{r}_a$ is the contact force in the global system while $\mathbf{R}_a$ is the contact force in the local system as defined according to contact law. $\mathbf{H}_a^T$ is the transposed matrix $\mathbf{H}_a$ [3].

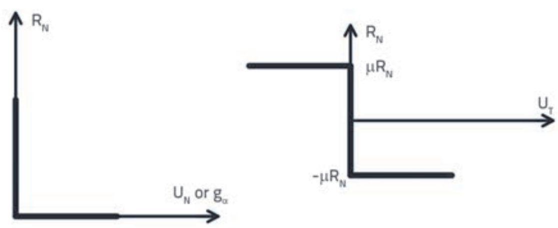

Figure 4. Signorini and Coulomb contact laws

Contact laws define relationships between the relative velocity or distance *g* and the contact force. Although there are many contact laws, the most frequently used ones are the Signorini and Coulomb laws, as shown in Figure 4. The Signorini's contact law is used to determine whether the contact between discrete elements has been realised. If the distance *g* is positive, the contact has not been realised, i.e. the normal contact force $\mathbf{R}_N$ is equal to zero. When the distance *g* is equal to zero, then the normal contact force $\mathbf{R}_N$ is activated, and it can assume infinite values [5]. The value of contact force $\mathbf{R}_N$ depends on the value of forces acting on discrete elements [5]. For the model made of absolutely rigid discrete elements, the normal contact force $\mathbf{R}_N$ is determined by means of impulses, and it depends on the relative velocity $\mathbf{U}_N$ and on the selected value of time step Δt. The Signorini's law can be mathematically described using the following expressions:

$$\begin{aligned} g > 0 &\Rightarrow \mathbf{R}_N = 0 \\ g = 0 &\Rightarrow \mathbf{R}_N \geq 0 \end{aligned} \tag{12}$$

The Coulomb's contact law is shown in Figure 4. In case of dry friction, the value of friction force or tangential contact force $\mathbf{R}_T$ depends on the friction coefficient μ and the normal contact force $\mathbf{R}_N$. The Coulomb's mathematical law can be presented as follows:

$$\begin{aligned} \mathbf{U}_T > 0 &\Rightarrow \mathbf{R}_T = -\mu \mathbf{R}_N \\ \mathbf{U}_T = 0 &\Rightarrow -\mu \mathbf{R}_N \leq \mathbf{R}_T \leq \mu \mathbf{R}_N \\ \mathbf{U}_T < 0 &\Rightarrow \mathbf{R}_T = \mu \mathbf{R}_N \end{aligned} \tag{13}$$

$\mathbf{U}_T$ is the relative tangential velocity.

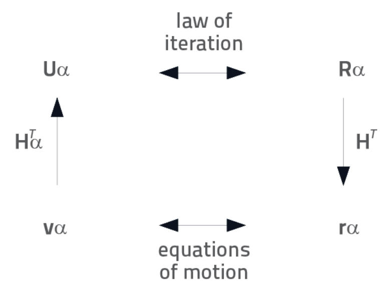

Figure 5. Relationship between global and local unknowns

The relationship between global and local unknowns is shown in Figure 5. Global unknowns are related to the centre of mass of a body or to network points. Global unknowns are displacements **q** velocities $\dot{\boldsymbol{q}}$, resulting forces and moments **r**. Local unknowns are related to the distance between two bodies **g** relative velocity between two bodies **U**, and force **R**.

3. Discrete model of the dome of St. James Cathedral in Šibenik

The drawings of the St. James Cathedral in Šibenik are kept at the Zagreb Institute of History and Art. Tracing-paper drawings on the scale of 1/200 and 1/50 are kept in the Institute's archives; digital versions are currently not available. These drawings consist of four façades, two longitudinal cross-sections, two transverse cross-sections, and the plan view of the structure. Longitudinal cross-sections are defined by planes crossing the cathedral along symmetry axis, and through the side nave. Cross-section planes cut the cathedral through three naves and the central part of the dome. The numerical model development does not require a "perfect" accuracy, i.e. several cm deviation from the as-built state will not significantly alter accuracy of the solution. Drawings on the scale of 1/200 are used in the scope of this paper. They are considered to be accurate enough for development of a good-quality numerical model. Visual inspection of the cathedral was also made, and it enabled collection of additional data for preparation of the model. This visual inspection enabled experts to determine regularity of placement of stone blocks, and the way in which steel ties are arranged.

3.1. Dome geometry

The dome is of octagonal form, and its sides measure 330 cm in length at the base. The height of the dome, measured from cornice to acroterion, amounts to 600 cm. The basic load-bearing system is formed of eight ribs that are linked together at the dome crown. The schematic view of the rib disposition is shown in Figure 6. The ribs are linked together with a central block connecting ribs into a single assembly. The central block and the ribs form an arch. The angle between two rib axes amounts to 45°. Each rib is made of ten elements. The rib height amounts to 55 cm along the entire rib length, while the rib width is variable. The rib width amounts to 50 cm at the spring level, and 38 cm at the crown [6].

After analysis of drawings, it was established that the rib shape can adequately be described by a parabola. It is defined by the rib axis equation.

$$z(x) = -\frac{h}{r^2}x^2 + h \quad [0{,}431] \tag{14}$$

The parabola is defined with two parameters h and r the value h defines the dome height, i.e. it represents the length between the origin and the crown of the parabola, while r is the radius of the octagon defining circle. The values of parameters h and r amount to 600,0 cm and 431,0 cm, respectively.

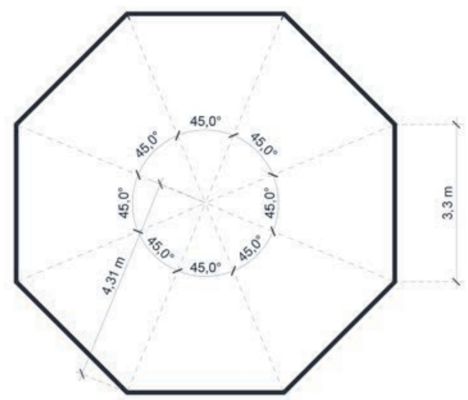

Figure 6. Disposition of rib axes

3.2. Ribs

After inspection of available documents, it was established that each rib is composed of ten segments of similar length, and so it was assumed that all segments are of equal length. The above assumption enables definition of conditions for the length and positioning of individual segments. The length and position of individual segments is defined by means of h, r, and r_1, and by the number of segments. The parameter r_1 defines the size of the central stone, i.e. the rib start coordinate. To define the length of individual segments, it is first of all necessary to calculate the total length of parabola in the zone from r_1 to r. The total length of parabola in the zone from r_1 to r can be calculated using the following expression:

$$d_l(h,r,r_1) = 0{,}5r\sqrt{\frac{4h^2}{r^2}+1} - 0{,}5r_1\sqrt{\frac{4h^2}{r^2}+1} - \frac{0{,}25}{\sqrt{\frac{h^2}{r^4}}}\sinh^{-1}\left(2r_1\sqrt{\frac{h^2}{r^4}}\right) + \frac{0{,}25}{\sqrt{\frac{h^2}{r^4}}}\sinh^{-1}\left(\frac{2h^2}{r^3\sqrt{\frac{h^2}{r^4}}}\right) \tag{15}$$

Equation 6 is derived on the basis of the known arch length expression. The length of individual segments is defined by dividing the arch length with the number of segments. If the segment length is inserted instead of the total arch length in Expression 6, then the value of r, defining the end of the segment, can be calculated. The value of r was determined numerically using the program language Python, and the code calculating final coordinates of individual rib segments was written. The calculation result is the list of coordinates that will be designated below as x_1.

The rib cross section is defined with seventeen characteristic points. Coordinates of characteristic points are determined from the reference point T_0 that is defined by the list of coordinates x_1, and by Expression 5. The remaining sixteen cross-section coordinates are defined using the pre-determined geometrical characteristics of the cross section and straight line perpendicular to the tangent of function 5 in point T_0.

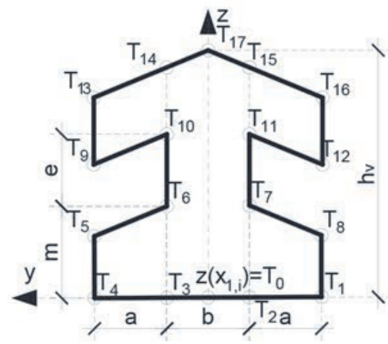

Figure 7. Approximation of cross-section

Cross-section parameters m, e, a, b and h_v change along the rib axis and must be calculated separately for each connection between two rib segments. To enable achievement of the desired cross-sectional shape, the rib segment is made of six four-sided prisms that behave as a single discrete element or as a rigid non-deformable body. The program defining the rib model was written. This program passes through two loops. One loop defines segments along the rib axis, and the other loop creates a new rib rotated for 45°.

Figure 8. Rib model

3.3. Central stone (keystone)

The function of the keystone is to link ribs into a single whole, i.e. to obtain a properly closed structure. The keystone is modelled in such a way that it links several standard discrete elements into a single whole that behaves as a single absolutely rigid discrete element.

A keystone segment defined with eight points and twelve triangular zones is presented in Figure 9. A complete keystone model (presented in Figure 10) is created by rotation of the segment shown in Figure 9. The rotation axis is situated in the origin of the coordinate system, i.e. it corresponds to the z axis.

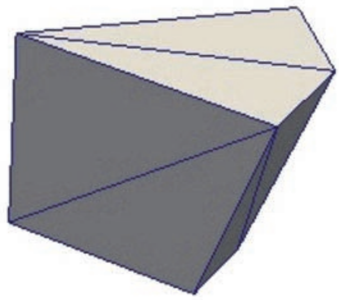

Figure 9. A keystone segment

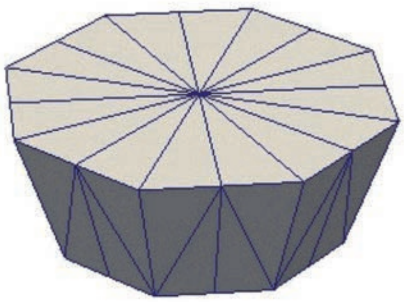

Figure 10. A keystone model

3.4. Roofing

The dome roofing is made of trapezoidal stone blocks. The roofing blocks fill the space between the ribs and lean onto the ribs. Ribs have grooves into which roofing elements are inserted. At the contact of two roofing elements there is an overlap, the top plate passes over the bottom one. Roofing elements are curved in keeping with the curvature of the dome, Figure 11.

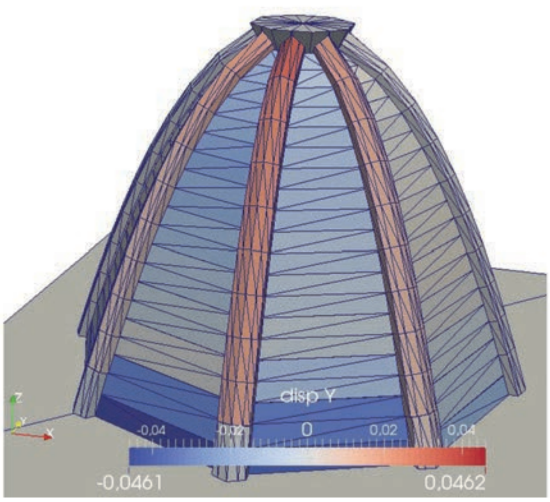

Figure 11. Discrete model of the dome of St. James Cathedral in Šibenik

It is very difficult to numerically define such a complex form of roofing elements. Therefore, model simplifications were introduced. Overlaps at the contact of two neighbouring roofing elements were neglected and the curvature was approximated with two areas. Individual roofing elements were defined through rib geometry. The geometry of one roofing element was defined in detail, and the remaining elements were obtained by means of a double loop. The first loop defines the elements along the rib, and the second one the elements between neighbouring ribs.

4. Dynamic response of the dome

Two dynamic analyses are presented in the paper. The real data analysis was conducted according to the accelerogram for El Centro [7], which was increased using factors 1.5, 2.0, 2.5, and 3.0 so as to define full failure of the dome. The second analysis was conducted by means of five artificially generated earthquake records.

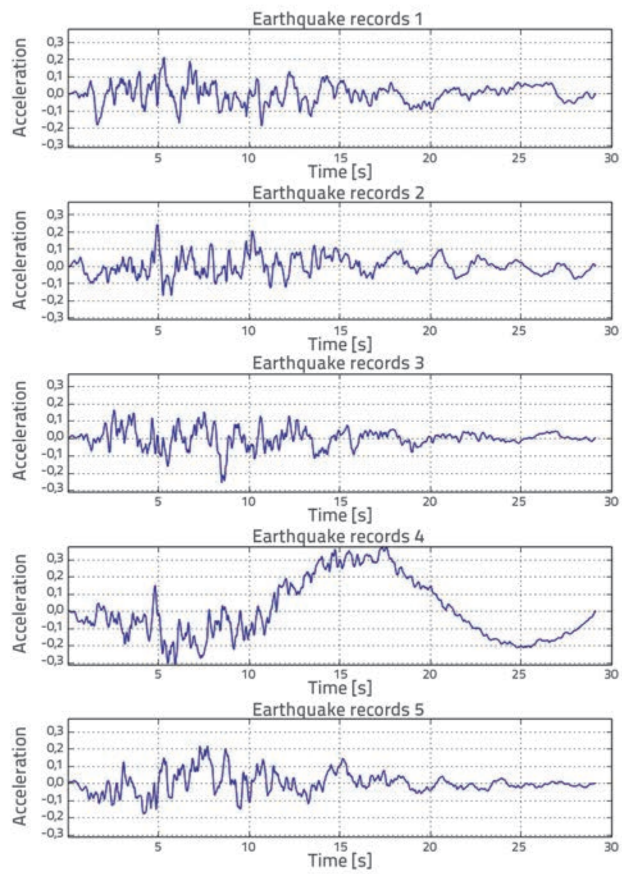

Figure 12. Artificially generated earthquake records

Earthquake records were generated using the Seismo Artif 2016 software [8, 9] The elastic spectrum was defined according to EC8 [10] parameters that correspond to the location of St. James Cathedral in Šibenik.

The ground acceleration a_{gS} amounting to 0,19 g, was taken from the *Map of earthquake-prone areas in the Republic of Croatia* [11] for the soil category A and the return period of 475 years. The

building/structure significance factor of 1,4 was selected. The assumed distance from the epicentre is 10 km, and the average shear wave velocity is $v_{S,30}$ = 940 m/s. The damping factor of 5% was assumed, and the assumed earthquake magnitude amounted to M_s = 7,5. Artificial seismic records were generated based on the elastic spectrum defined using the Seismo Artif 2016 software. The integration and correction, i.e. the baseline correction of the El Centro earthquake record and artificially generated records, was conducted using the Prisma software [12].
Two action types, force and velocity, were defined using the LMGC90 software. The integration and correction was made based on the known El Centro accelerations and artificially generated earthquake records, in order to obtain ground velocities or bases. The excitation was made in the x axis direction only, Figure 13.

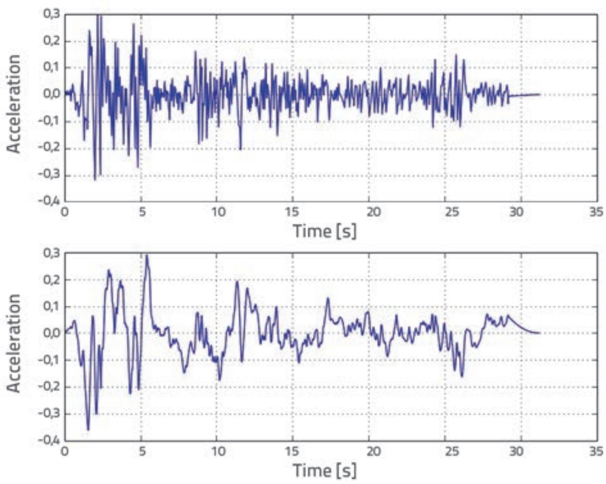

Figure 13. El Centro earthquake record

The iteration is made using the non-linear Gauss-Seidel method (NLGS). The system formed of two equations with two unknowns is assumed:

$$\begin{aligned} ax + by &= \lambda \\ cx + dy &= \delta \end{aligned} \tag{16}$$

It will be used to explain Gauss-Seidel methods. *a, b, c, d*, λ and δ and are constant values. Eq. (16) can be re-formulated as follows:

$$\begin{aligned} x_{n+1} &= \frac{\lambda - by_n}{a} \\ y_{n+1} &= \frac{\delta - cx_n}{d} \end{aligned} \tag{17}$$

The iteration procedure is conducted by assuming initial values of x_0 and y_0, which are inserted in Eq. (17). The new set of values is inserted in Eq. (16) and, if equations exhibit appropriate accuracy, the procedure is interrupted or values are re-inserted in Eq. (17). This iteration procedure is known as the Jacobi method. The Gauss-Seidel method is a modification of the Jacobi method: the same iteration pattern is used, except that new values are used within the same iteration, i.e. a soon as a new value is known - it is used in calculation of the next value. It can be seen from Expression 18 that the value of X_{n+1} is used in the calculation of the value y_{n+1}.

$$\begin{aligned} x_{n+1} &= \frac{\lambda - by_n}{a} \\ y_{n+1} &= \frac{\delta - cx_{n+1}}{d} \end{aligned} \tag{18}$$

The same principle can also be applied to the system of nonlinear equations [13].
The number of iterations in LMGC90 software is defined with two parameters gs_it_1 and gs_it_2 [3]. The first loop, known as the control loop, is defined by the value of gs_it_2. The control of accuracy is conducted in each step of the loop, i.e. it is determined whether the solution meets the accuracy criterion. If conditions of the required point are met, the iteration is interrupted. The second loop is the sub-loop of the first loop and is defined by the value of gs_it_1. Unlike the first loop, the second loop can not interrupt the iteration once the desired accuracy is attained because the accuracy control is not made in every step of the iteration. The calculation time is thus reduced. The selected iteration parameters are presented in Table 1.

Table 1. Parameters selected for iteration procedure

Tolerance	Θ	Time step value	gs_it_1	gs_it_2
$0{,}1666^{-3}$	0,5	0,002	2000	10

In his dissertation published in 2003, De Castro Oliveira determines the average coefficient of friction between stone blocks. The coefficient of friction to be used in this paper is set to μ = 0,62 [14]. An average weight of stone is 2350 kN/m³ [15]. The results are presented using the ParaView software [16] which monitors structural changes over time. After analysis of results for the earthquake record El Centro, taking into account the magnification factor 1, it was established that permanent deformations occur due to shear between individual blocks. Remaining dome displacements are shown in Figure 11. It can easily be seen that nonlinear displacement occurs between the first and the second rows of rib elements. Figure 14 shows a relative relationship between the first two rows of the rib forming stone blocks for various earthquake record magnification factors according to the El Centro accelerogram. It can be seen from Figure 14 that the dome response after 6 seconds is such that relative displacements between the studied stone blocks assume a constant value for magnification factors of 2, 2.5, and 3. Further displacements are caused by dome opening i.e. by an increase of distance between individual ribs. This phenomenon can be seen in Figure 15, which shows a relative relationship between the bases of two ribs that are situated opposite to one another.

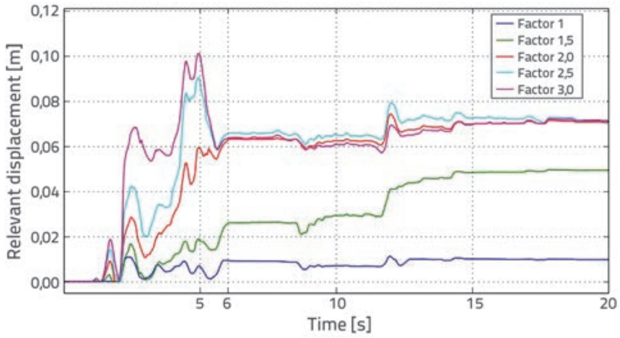

Figure 14. Relative displacements between the first two rows of rib-forming stone blocks for various earthquake-record magnification factors, according to El Centro accelerogram

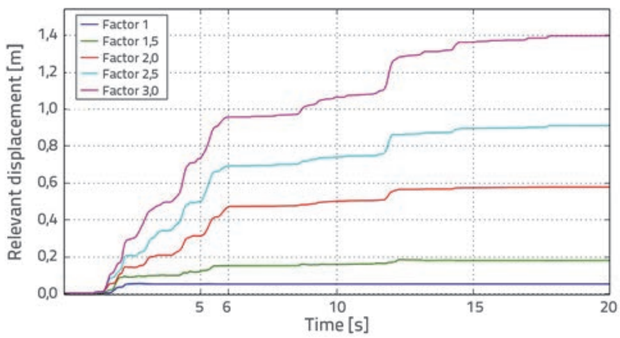

Figure 15. Correlation between two opposing ribs in their bases

The keystone push-out problem was also observed. In fact, a gradual push-out of the keystone occurs due to alternating change in direction of earthquake action. This may be due to the poorly defined geometry of the keystone and to poor definition of friction between blocks, although the possibility that this is the real dome behaviour can not be discarded. The keystone push-out phenomena are shown in Figure 16.

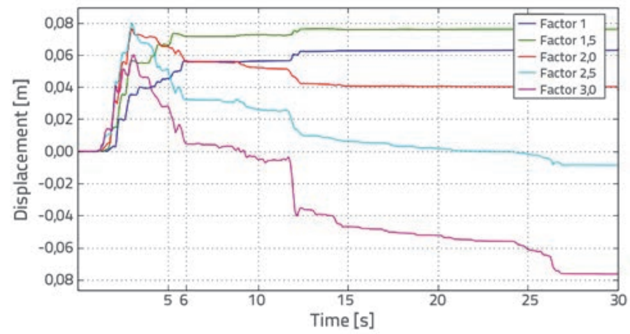

Figure 16. Dome keystone push-out for various earthquake record magnification factors, according to El Centro accelerogram

It can be seen from this figure that additional push-out after six seconds does not occur for factors 1 and 1.5. This interruption of keystone push-out is attributed to the reduction of acceleration i.e. to the ground acceleration in 6 seconds for the earthquake record according to the El Centro

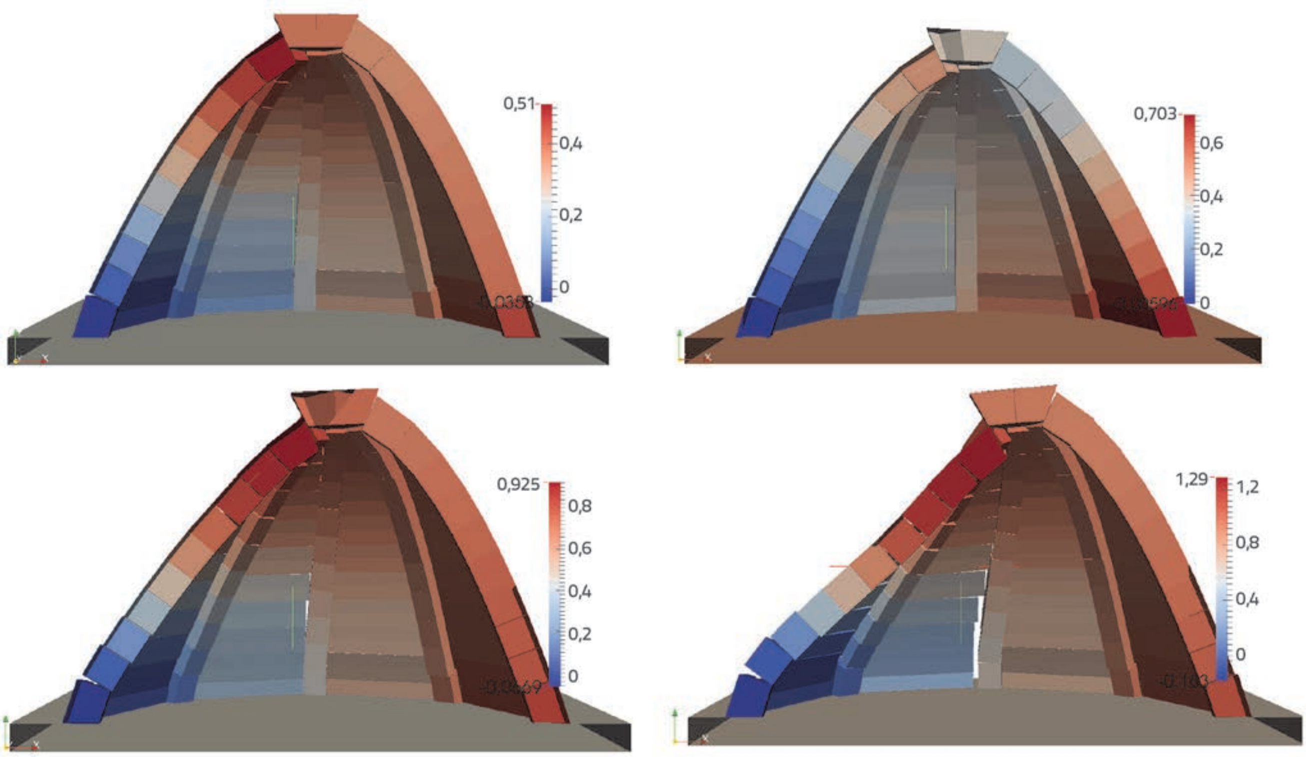

Figure 17. Dome response for El Centro earthquake action, magnified by three times

accelerogram, as shown in Figure 13. The dome keystone collapses (falls-through) after 6 seconds for factors 2, 2.5 and 3. This can be attributed to the rib separation phenomenon, as shown in Figure 16.

The interaction between individual blocks is shown in ParaViewer by means of dots, while the force value is designated by dot colour. It can be seen in Figure 18 that normal interaction forces are uniform along the ribs, and this situation remains unchanged throughout the earthquake action. Extreme values occur at the contact between the ribs and the support. Maximum value of the normal interaction force occurring in the dome model amounts to 43.2 kN. If it is assumed that the seating area is 50x50 mm, the stress at the contact amounts to 17,28 N/mm², which is less compared to the compressive strength of stone.

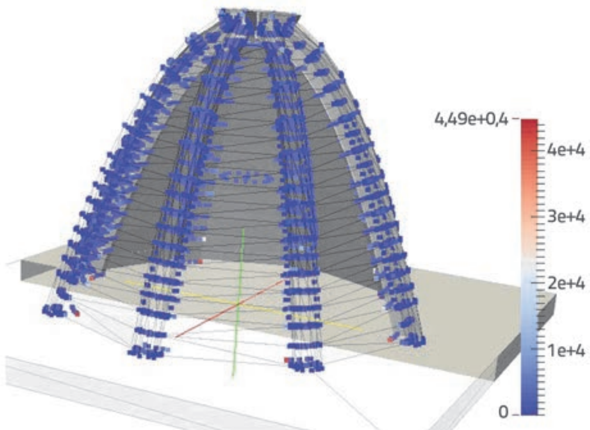

Figure 18. Normal interaction forces between stone blocks

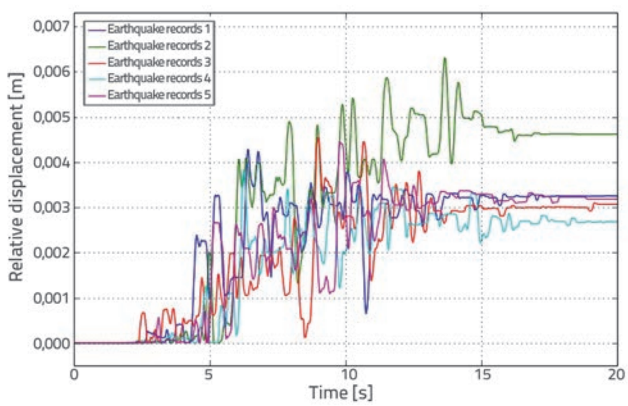

Figure 19. Relative displacements between the first two rows of rib-forming stone blocks for five artificially generated earthquake records

The dome response was determined for artificially generated earthquake records. The El Centro earthquake record analysis pointed to critical points with regard to dome response, relative displacements between the first and the second rows of rib-forming stone blocks, and keystone push-out. The results presented in Figures 19 and 20 point to uniform behaviour of all five artificially generated earthquake records.

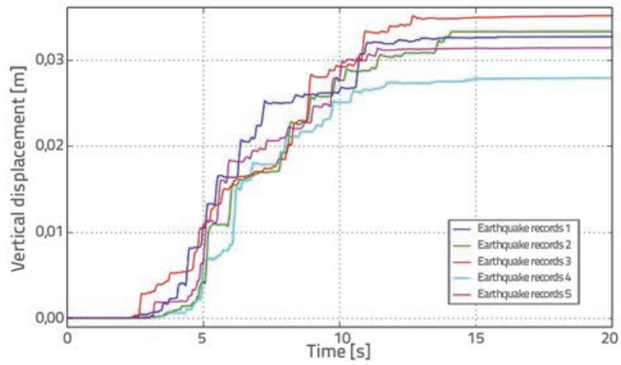

Figure 20. Dome keystone push-out for five artificially generated earthquake records

5. Conclusion

An approach to development of a discrete numerical model using the LMGC90 software based on the NSCD method is presented in the paper. The LMGC90 software does not have a graphical interface and so the model is described mathematically. The LMGC90 is based on an open source philosophy, which makes it a readily available program package.

Results obtained by dynamic analysis point to the problems of nonlinear behaviour of structures made of stone blocks. This nonlinearity is manifested in the shear or sliding between blocks, which is difficult to anticipate by means of the FEM. The model points to the keystone pushing-out problem, which may greatly affect stability of the structure, although additional investigations are needed in this respect.

Defining geometry by non-deformable discrete elements is a complex process. On the other hand, definition of material characteristics is quite simple. The stone weight and the coefficient of friction between individual blocks must be known. The research should be continued by expanding the model so as to comprise the entire cathedral, and by conducting experimental research with the purpose of obtaining good quality information about friction between individual discrete elements. In addition, development of model with deformable discrete elements might offer a better insight into the state of stress in individual blocks.

REFERENCES

[1] Smoljanović, H.: Seizmička analiza zidanih konstrukcija metodom konačno-diskretnih elemenata, doktorski rad, Sveučilište u Splitu, 2013.

[2] Hedman, S.: Smooth and non-smooth approaches to simulation of granular matter, magistarski rad, Umeå University, 2011.

[3] Dubios, F., Renouf, M.: Discrete Element Methods for the simulation of divided media, Laboratoire de Mécanique et Génie Civil, 2015.

[4] Hibbeler, R. C.: Engineering Mechanics: Dynamics, Prentice Hall, 2012.

[5] Acary, V., Jean, M.: Numerical simulation of monuments by the contact dynamics method, HAL (2009), pp. 69-78.

[6] Ćuzela, J.: Prilog obnovi kupole katedrale sv. Jakova u Šibeniku, Rad. Inst. povij. umjet. (1994), pp. 205–210.

[7] Vibrationdata, http://www.vibrationdata.com/elcentro.htm, pristupljeno: 11.2.2015.

[8] Seismo Artif 2016, http://www.seismosoft.com/, prstupljeno: 30.6.2016.

[9] Seismo Artif 2016, http://www.seismosoft.com/Public/EditorUpload/Flash/SeismoArtifv2.1_GettingStarted.swf, prstupljeno: 30.6.2016.

[10] Carvalho, E.: Eurocode 8 General rules and seismic actions, Dissemination of information workshop, Brussels, 2008.

[11] Karte potresnih područja Republike Hrvatske, http://seizkarta.gfz.hr/karta.php, pristupljeno 31.6.2016.

[12] Jeong, S., Lee, K., Jang, W.: PRISM for Earthquake Engineering A Program for seismic response analysis of SDOF system, Version 1.0.2, INHA University, 2011.

[13] Gutiérrez, J.M., Magreñán, A.A., Varona, J.L.: The "Gauss-Seidelization" of iterative methods for solving nonlinear equations in the complex plane, Applied Math. Comp., 218 (2011), pp. 2467–2479, http://dx.doi.org/10.1016/j.amc.2011.07.061

[14] De Casto Oliveira, D.V.: Experimental and numerical analysis of blocky masonry structures under cyclic loading, doktorski rad, Universidade do Minho, 2003.

[15] Crnković, B., Šarić, Lj.: Građenje prirodnim kamenom, Sveučilište u Zagrebu, 1992.

[16] ParaView, http://www.paraview.org/paraview-guide/, pristupljeno 30.6.2016.

DOI: 10.14256/JCE.1335.2015

Primljen / Received: 20.4.2015.
Ispravljen / Corrected: 19.6.2016.
Prihvaćen / Accepted: 20.7.2016.
Dostupno online / Available online: 10.10.2016.

Strength properties of coated E-glass fibres in concrete

Authors:

Prof. Sabapathy Yogeeswaran Kanag
SSN College of Engineering
Civil Engineering Department
sabkan@gmail.com

Yeshwant Kumar Anandan, BE
SSN College of Engineering
Civil Engineering Department
yeshwantkumaranandan@gmail.com

Prathulya Vaidyanath, BE
SSN College of Engineering
Civil Engineering Department
prathulyavaidyanath@gmail.com

Prashaanth Baskar, BE
SSN College of Engineering
Civil Engineering Department
prashaanthpb1794@gmail.com

Scientific paper - Preliminary note

Sabapathy Yogeeswaran Kanag, Yeshwant Kumar Anandan, Prathulya Vaidyanath, Prashaanth Baskar

Strength properties of coated E-glass fibres in concrete

Test results obtained by studying the influence of epoxy coated E-glass fibre composites on the compressive and splitting tensile strengths of concrete are reported in the paper. Three grades of concrete and varying fibre volume fractions (0.5 %, 1 %, 1.5 % and 2 %) were used as test variables. It was observed that the maximum compressive strength was attained for the fibre volume fraction of 1.5%, whereas the splitting tensile strength was found to increase with an increase in the fibre volume fraction. Based on the test results, a mathematical model was developed using regression analysis.

Ključne riječi:

coated glass fibres, fibre reinforced concrete, fibre volume fraction, compressive strength, splitting tensile strength

Prethodno priopćenje

Sabapathy Yogeeswaran Kanag, Yeshwant Kumar Anandan, Prathulya Vaidyanath, Prashaanth Baskar

Utjecaj obloženih E-staklenih vlakana na svojstva čvrstoće betona

U radu su prikazani rezultati ispitivanja o utjecaju E-staklenih vlakana obloženih epoksidom na tlačnu i vlačnu čvrstoću betona. Kao parametri ispitivanja su odabrana tri različita razreda betona s varirajućim volumnim udjelima vlakana (0,5 %, 1 %, 1,5 % i 2 %). Uočeno je da se najveća tlačna čvrstoća postiže pri volumnom udjelu vlakana od 1,5 %, a vlačna čvrstoća cijepanjem povećava se kako se povećava volumni udio vlakana. Na temelju rezultata ispitivanja razvijen je matematički model primjenom metode regresijske analize.

Ključne riječi:

obložena staklena vlakna, beton ojačan vlaknima, volumni udio vlakana, tlačna čvrstoća, vlačna čvrstoća cijepanjem

Vorherige Mitteilung

Sabapathy Yogeeswaran Kanag, Yeshwant Kumar Anandan, Prathulya Vaidyanath, Prashaanth Baskar

Einfluss beschichteter E-Glassfasern auf die Festigkeitseigenschaften von Beton

In dieser Arbeit werden Resultate von Untersuchungen zum Einfluss mit Epoxid beschichteter Glasfasern auf die Druck- und Zugfestigkeit von Beton dargestellt. Als Untersuchungsparameter wurden drei verschiedene Betonklassen mit verschiedenen Faservolumenanteilen (0,5 %, 1 %, 1,5 % und 2 %) gewählt. Es wurde festgestellt, dass die größte Druckfestigkeit bei einem Faservolumenanteil von 1,5% erzielt wird, während die Spaltzugfestigkeit mit dem Faservolumenanteil ansteigt. Aufgrund der experimentellen Resultate wurde aufgrund Methoden der Regressionsanalyse ein mathematisches Modell entwickelt.

Ključne riječi:

beschichtete Glasfasern, faserverstärker Beton, Faservolumenanteil, Druckfestigkeit, Spaltzugfestigkeit

1. Introduction

It has been well established that the use of fibres in concrete reduces the width of cracks developed due to external loads. Apart from reducing the crack width in concrete, the fibres also increase the ductility of concrete, improve the post-cracking behaviour of concrete, and resist high impact loads. Earlier researchers have reported that the behaviour of fibre reinforced concrete depends on factors such as the fibre shape, fibre geometry, aspect ratio, volume of fibres, curing method and curing time, use of superplasticisers, etc. (Trottier, J. F., and Banthia N., 1994 [1], Jianming Gao et al., 1997 [2], K. Ramesh et al., 2003 [3], A. Sivakumar and Manu Santhanam, 2007 [4]). It has also been demonstrated that the fibre distribution and orientation are important factors affecting properties of the fresh and hardened concrete, as proposed by Bensaid Boulekbache et al. [5].

The glass fibre reinforced concrete has increasingly been used in architectural and structural concrete members thanks to its anticorrosive properties, combined with high strength exceeding that of steel fibres. Junji Takagi [6] investigated the effect of randomly oriented glass fibres on the flexural strength, compressive strength, splitting tensile strength, and Young's modulus of concrete, and concluded that there was an increase in strength with an increase in fibre content. However, studies have shown that the use of uncoated E-glass fibres in concrete affects its durability due to high alkaline environment in concrete, and weakens the fibres, which in turn affects the overall strength of concrete. This setback due to durability was overcome by using the alkaline resistant (AR) glass fibres [7], which was found to reduce the propagation of shrinkage cracks [8] and improve the tensile and flexural strengths of concrete [9].

Although several research studies on the alkaline resistant glass-fibre reinforced concrete have so far been conducted, it appears that short coated E-glass fibres in concrete have not been investigated. It should be noted that the glass-fibre coating not only protects the fibres from alkaline environment but also improves its tensile strength significantly [10]. Although the durability of coated fibres is very essential, it is beyond the scope of this study. The durability of coated rigid fibres, considered both separately and with concrete, needs to be investigated, which could be the scope of some future research. Also, the cost-related study of coated fibres, and their comparison with other fibre types, are left to future investigators. This paper focuses on the investigation of properties of the Coated E-Glass Fibre Reinforced Concrete (CGFRC). The volume of fibres and grade of concrete were varied to evaluate the influence of these fibres in concrete under compression and tension. Since the addition of fibres influences the flow properties of concrete, flow table tests were carried out to determine its workability. The coatings of these fibres induce stiffness thereby preventing the balling of fibres, as observed in uncoated fibres. A fibre aspect ratio of 30 was maintained throughout this study. This aspect ratio was found to be lower than the optimum aspect ratio of steel fibres used in concrete by other researchers [11]. The low aspect ratio was considered necessary due to increase in its stiffness and low lateral strength. The objective of this paper is to establish the resistance of coated E-glass fibres in concrete to compressive and tensile loads. Using the test results, mathematical models were developed to express the strength of fibre reinforced concrete.

2. Materials

The ordinary Portland cement conforming to IS: 8112 [12] (equivalent to ASTM – Type-I cement standards), with a specific gravity of 3.15 g/cm^3, was used to prepare concrete. Fine and coarse aggregates with the specific gravity of 2.6 g/cm^3 and 2.7 g/cm^3, respectively, were used. The fine and coarse aggregates were well graded as per IS 383 [13]. E-glass fibre roving of 1200 Tex with an average filament diameter of 17 μm, with the density of 2.65 g/cm^3, was used to prepare coated fibres. The fibres were used without any pre-treatment. The epoxy resin containing a suitable hardener was used as a coating material to fabricate the fibres.

The coated E-glass fibres shown in Figure 1 were made at the laboratory. The E-glass fibre roving was coated with epoxy resin and the excess resin was removed through a narrow slit. The wet coated fibres were allowed to dry at room temperature for about 24 hours by holding them in tension, to avoid fibre wrinkles in coated fibres. Later on, the fibres were post-cured in oven for two hours. The dried fibres were then cut to the required lengths to attain the desired aspect ratio of 30. The coated glass fibre properties are presented in Table 1.

Figure 1. Coated E-Glass Fibres

Table 1. Properties of Coated Glass Fibres

Fibre shape	Straight
Fibre length [mm]	30
Fibre diameter [mm]	1
Aspect ratio	30
Elongation [mm]	4.273
Modulus [GPa]	55.737
Tensile strength [MPa]	1587.779

Three concrete grades were prepared to cast the test specimens. Their mix proportions are presented in Table 2. The cement, sand and coarse aggregate were initially mixed with water to prepare the fresh concrete. The coated fibres pre-mixed with cementitious paste were added in small quantities to the fresh concrete and mixed thoroughly. The pre-mixing was conducted to improve bonding properties of the coated fibres and concrete. The fibre mixed concrete was then cast in steel moulds and vibrated using a mechanical vibrator to reduce the air voids content and attain good compaction. The cast specimens were demoulded after 24 hours and cured in water for 28 days before testing. The specimens were completely dried before conducting the tests.

3. Experimental study

3.1. Testing of fibres

The tensile strength of coated glass fibres was determined as per testing standards ASTM D2343-03 [14] using the material testing machine as shown in Figure 2. Five tensile test specimens, each 250 mm in length, and 150 mm in gauge length, were prepared with their ends embedded in the fibre mat laminate. This special attachment was needed to prevent the crushing of fibres and to provide the necessary grip during tensile testing. The specimen was loaded under displacement control with the loading rate of 5 mm/min. The tensile strength and modulus of coated glass fibres were calculated as per expression given in the standard. The calculated values are presented in Table 1. The load and extension plot was obtained, as shown in Figure 3.

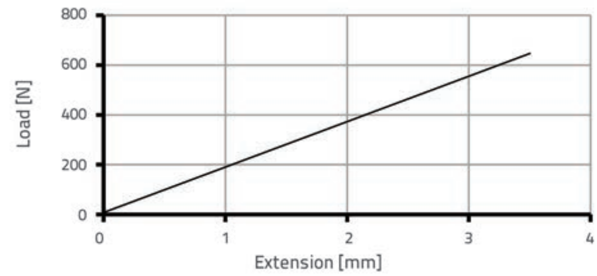

Figure 3. Graph depicting relation between load and extension

3.2. Testing methodology for concrete

Tests were conducted to examine workability of the coated E-glass fibre concrete by the flow table test method. The flow table test was conducted as per IS:1199:1959 [15]. Concrete cubes measuring 150 x150 x 150 mm were used as test specimens for compression tests. The compression tests were carried out as per IS 516 [16]. Three sets of cubes, each made of different concrete grade, in combination with varying percentages of fibres (0 %, 0.5 %, 1 %, 1.5 % and 2 %), totalling to 45 cubes, were cast and subjected to compressive strength testing. The compression testing machine 2000 kN in capacity was used to test the cube specimens. The loading rate was set to 14 MPa/min. Similarly, 45 cylindrical specimens measuring 150 x 300mm were cast and tested to obtain the splitting tensile strength. The split tensile test is a simple and reliable test for determining the tensile strength of concrete [17]. The splitting tensile strength tests were carried out as per IS 5816 [18].

The tested specimens presented in Figure 4 show that the core was intact in all fibre reinforced concrete cubes, while the peripheral concrete had split and fallen apart. This may be attributed to the greater anchorage of fibres in the core region, which are therefore more effective

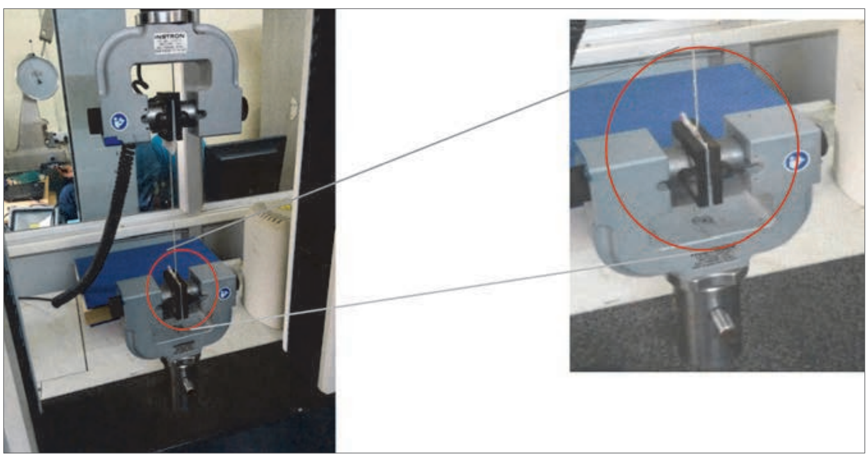

Figure 2. Tensile test setup and end griper

Table 2. Control Mix Proportions

Series no.	Cement content [kg/m³]	Water-cement ratio	Fine aggregate [kg/m³]	Coarse aggregate [kg/m³]	Water content [l/m³]
CGFRC-1	372	0.5	580	1177	186
CGFRC-2	413	0.45	552	1154	185
CGFRC-3	450	0.4	444	1265	180

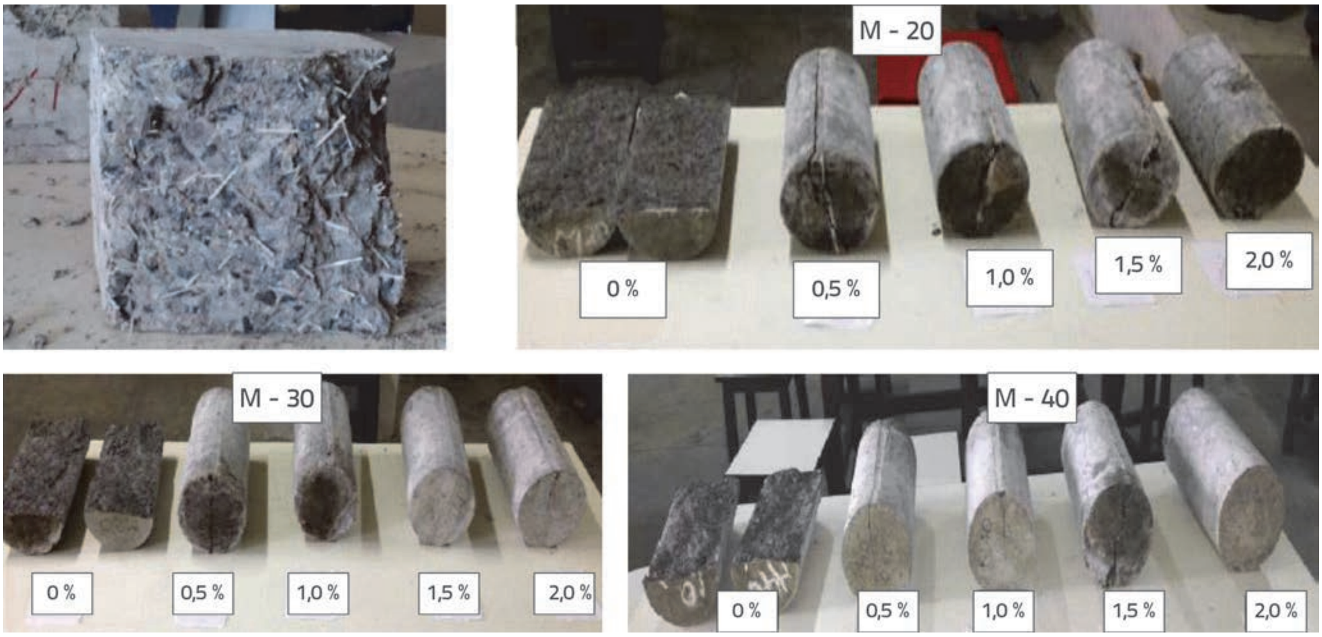

Figure 4. Fractured concrete cube and cylindrical specimens

in resisting crack formation compared to fibres present along the periphery. In case of cylindrical specimens, only the cylinder without fibres split into two halves, while the remaining cylinders - although cracked - did not split and fall apart, which shows that fibres are highly resistant to tension.

4. Test results and discussion

4.1. Fresh concrete test results

The influence of fibres on the workability of concrete is evaluated by means of flow test since the presence of fibres hinders flow properties of fresh concrete. The relative flow behaviour for various grades of concrete and different fibre volume fractions is depicted in Figure 5. It can be seen that flow decreases with an increase in the percentage of fibre volume fraction. The flow was reduced by less than 25 percent when the fibre volume fraction increased from 0 % to 2 %. The reason can be attributed to the straight shape of coated fibres and their short length, which can be advantageous as they cause minimum hindrance to the flow of concrete.

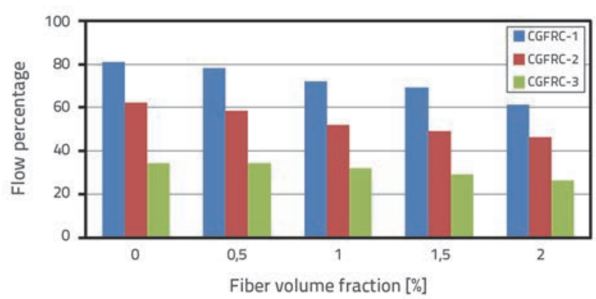

Figure 5. Flow properties of CGFRC

4.2. Hardened concrete test results

4.2.1. Compressive strength results

An average compressive strength of concrete was analysed for three different grades with varying percentages of fibre volume fraction. The corresponding results are presented in Table 3. When the tested specimens were cut open along the crack for investigation, the distribution of fibres was observed to be reasonably good, without any balling of fibres. This may be attributed to the short length of fibres and their straight and rigid shape. Also there was no indication of de-bonding of fibres from concrete. It was observed that the peak load was achieved for a fibre volume of 1.5 %. On further increase in fibre volume beyond 1.5 %, a sharp decline in compressive strength of concrete was registered for the addition of fibres of up to 2 %. This decrease in strength may be attributed to poor compaction of concrete due to the presence of a greater amount of fibres, as stated by earlier researchers in works related to steel fibre reinforced concrete [19]. The fibre coating increased the stiffness of fibres thereby preventing proper compaction of concrete.

4.2.2. Splitting tensile strength results

The peak load was registered for each test specimen to calculate the splitting tensile strength. The average splitting tensile strength of concrete is presented in Table 3. It was observed that the splitting tensile strength increased with an increase in the fibre volume fraction. Both the plain and fibre reinforced concrete specimens failed due to cracking at their respective ultimate loads. However, the splitting of cylinder into two separate halves was observed in the plain concrete

Table 3. Test results for compressive and tensile strength

Series	Fibre volume fraction [%]	Compressive strength		Splitting tensile strength	
		f_c [MPa] (average values)	Relative f_c [%]	f_{st} [MPa] (average values)	Relative f_{st} [%]
CGFRC-1	0	28	100	2.65	100
	0.5	31.11	111.11	3.15	118.67
	1.0	31.56	112.70	3.33	125.33
	1.5	33.78	120.63	3.43	129.07
	2.0	28.44	101.59	3.63	136.8
CGFRC-2	0	37.33	100	3.40	100
	0.5	41.33	110.71	3.57	105
	1.0	44.44	119.05	3.82	112.5
	1.5	45.78	122.62	4.08	120.21
	2.0	39.11	104.76	4.50	132.5
CGFRC-3	0	46.67	100	3.75	100
	0.5	46.22	99.05	3.85	102.64
	1.0	48.89	104.76	4.13	110.19
	1.5	50.67	108.57	4.27	113.96
	2.0	47.11	100.95	5.08	135.47

specimens only. This proves that coated E-glass fibres can effectively resist tension in concrete. It was established that the crack depth and width values were smaller in fibre reinforced specimens, which points to the effectiveness of coated fibres and their distribution. The increase in splitting tensile strength with an increasing volume of fibres was expected since the presence of fibres across the failure plane resists propagation of cracks more effectively.

Figure 6. Fibres in concrete across crack section

One tested specimen in each percentage variation of fibres was selected and was then cut open along the cracked failure surface for observation. It was registered that there was a uniform distribution of fibres in concrete. The number of fibres present across the crack was physically counted to determine the effective fibres resisting the splitting tensile force. Figure 6 shows fibres in concrete across the crack. As stated by earlier researchers, the orientation of rigid fibres also contributes to the capacity of fibres to resist propagation of cracks [20]. It was found that approximately 10 % to 20 % of the total fibres across the crack section were perpendicular to the loading plane, while all other fibres were oriented at different angles to the failure crack. On observation of the fibres, it was found that the fibres were not ruptured due to application of load, and that there was a good bond between the fibres and concrete.

5. Analysis of test results

The analysis of test results was carried out using the multiple regression analysis method to relate the test variables *i.e.* the grade of concrete and percentage of fibre volume to strength properties. A relationship was established to relate the influence of fibres on compressive strength (f_c) and splitting tensile strength (f_{st}) of concrete. The proposed general prediction model s given as follows:

$$f_{CGFRC} = A\left(f_c^{'}\right)^{\alpha} + B\,V_f + C\,V_f^2 \tag{1}$$

where:

f_c' - 28-day compressive strength of concrete
V_f - volume fraction of fibres
A, B, C - regression coefficients
α - amounts to 0.5 and 1.0 for the splitting tensile strength and compressive strength, respectively.

The first term represents the effect of characteristic strength of concrete, while subsequent terms are dependent on the volume fraction of fibres present in concrete. The model proposed in this paper is similar to the one proposed by Song et al. [21] except for the changes in the coefficients, representing coated E-glass fibres instead of steel fibres.

$$f_c = 0.98 \cdot f_c^{'} + 10.325 \cdot V_f - 4.526 \cdot V_f^2 \qquad (2)$$

$$f_{st} = 0.546 \cdot \sqrt{f_c^{'}} + 0.276 \cdot V_f + 0.123 \cdot V_f^2 \qquad (3)$$

The coefficient of determination (COD) was found to be 0.91 for both proposed equations (Eqns. (2) and (3)). It was observed that the compressive strength of concrete decreased with the addition of 2% of fibres. In Eqn. (2), it was found that the coefficient of V_f^2 was significant due to non-linear behaviour of the compressive strength of concrete with the addition of fibres. The splitting tensile strength of concrete was found to vary linearly with the addition of fibres. The coefficient of V_f^2 was very low due to linearity of test results.

It is known that the strength of CGFRC is also dependent on various factors such as the fibre shape, fibre length and aspect ratio, orientation of fibres, embedded length, and concrete properties. Since no literature is available on research about the coated E-glass fibres in concrete, further research is needed to validate the proposed equations with additional experimental data. The relationship between predicted values and experimental values is presented in Table 4. This table shows that predicted values are convincingly close to experimental values. The correlation between the experimental values and strength model values (from Eqns. (2) and (3)) can be seen in Figures 7 & 8. The closeness of experimental values and predicted values is described by the linear trend presented in Figures 7 and 8.

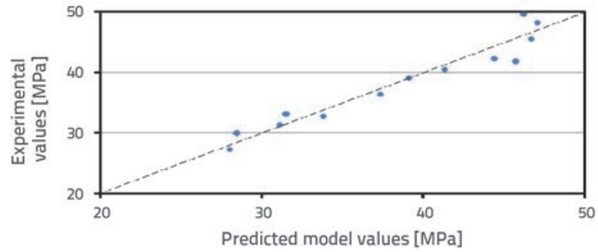

Figure 7. Relation between experimental and model values for compressive strength

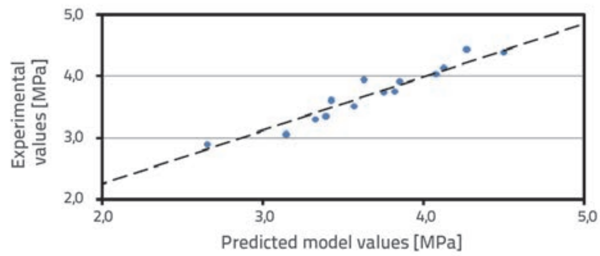

Figure 8. Relation between experimental and model values for splitting tensile strength

Table 4. Comparison of predicted values and experimental values

Series	Fibre volume fraction [%]	Compressive strength			Splitting tensile strength		
		Experimental $(f_c)_{exp}$	Predicted $(f_c)_{pre}$	$(f_c)_{pre}/(f_c)_{exp}$	Experimental $(f_{st})_{exp}$	Predicted $(f_{st})_{pre}$	$(f_{st})_{pre}/(f_{st})_{exp}$
CGFRC-1	0	28	27.44	0.98	2.65	2.89	1.08
	0.5	31.11	31.47	1.01	3.15	3.06	0.97
	1.0	31.56	33.24	1.05	3.33	3.29	0.99
	1.5	33.78	32.74	0.97	3.43	3.58	1.05
	2.0	28.44	29.98	1.05	3.63	3.94	1.08
CGFRC-2	0	37.33	36.59	0.98	3.40	3.34	0.98
	0.5	41.33	40.62	0.98	3.57	3.51	0.98
	1.0	44.44	42.39	0.95	3.82	3.74	0.98
	1.5	45.78	41.89	0.92	4.08	4.03	0.99
	2.0	39.11	39.13	1.00	4.50	4.39	0.97
CGFRC-3	0	46.67	45.73	0.98	3.75	3.73	1.00
	0.5	46.22	49.76	1.08	3.85	3.90	1.01
	1.0	48.89	51.53	1.05	4.13	4.13	1.00
	1.5	50.67	51.04	1.01	4.27	4.43	1.04
	2.0	47.11	48.28	1.02	5.08	4.78	0.94

6. Conclusion

The objective of this study was to evaluate strength properties of concrete reinforced with coated E-glass fibres. The following conclusions were drawn after the testing and analysis of results:

- As expected, the flow of concrete was found to be affected by the addition of fibres. Yet, it did not prove to be a great obstruction to the flow of concrete due to straight shape of fibres. The measured concrete flow properties indicate that the flow gradually decreased by only 25 percent for an increase in fibre content ranging from 0 % to 2 %.
- It was found that the compressive strength of concrete increased with an increase in fibre content. However, the addition of fibres beyond 1.5 % had a retarding effect on compressive strength. The increase in strength for the fibre volume fraction of up to 1.5 % was found to be in the range of 10 % to 20 % of the control-mix concrete strength.
- The splitting tensile strength showed a linear variation with respect to an increase in the volume fraction of fibres. The strength improved significantly with an increase of about 35% compared to the control mix concrete, for the 2 % fibre volume fraction. These fibres were found to be effective in resisting propagation of tensile cracks.
- The proposed empirical models, formulated by multiple regression analysis of experimental test data to predict strength properties of fibre reinforced concrete, were found to be close to test results. However, further research is needed to validate the proposed equations.

REFERENCES

[1] Trottier, J.F., Banthia, N.: Toughness characterization steel fibers reinforced concrete, *Journal of Materials in Civil Engineering*, 6 (1994) 4, pp. 264-289.

[2] Gao, J., Sun, W., Morino, K.: Mechanical properties of steel fiber-reinforced, high-strength, lightweight Concrete, *Cement and Concrete Composites*, 19 (1997) 4, pp. 307-313.

[3] Ramesh, K., Seshu, D.R., Prabhakar, M.: Constitutive Behavior of Confined Fiber Reinforced Concrete under axial compression, *Cement and Concrete Composites*, 25 (2003) 3, pp. 343-350.

[4] Sivakumar, A., Santhanam, M.: Mechanical properties of high strength concrete reinforced with metallic and non-metallic fibres, *Cement and Concrete Composites*, 29 (2007) 7, pp. 575-581.

[5] Boulekbache, B., Hamrat, M., Chemrouk, M., Amziane, S.: Flowability of fibre-reinforced concrete and its effect on the mechanical properties of the material, *Construction and Building Materials*, 24 (2010) 9, pp. 1664-1671.

[6] Takagi, J.: Some Properties of glass fiber reinforced concrete, *Fiber Reinforced Concrete, ACI SP-44, Detroit, Michigan*, pp. 93-111, 1974.

[7] Brandt, A.M.: Fibre reinforced cement-based (FRC) composites after over 40 years of development in uilding and civil engineering, *Composite Structures*, 86 (2008) 1-3, pp. 3-9,.

[8] Barluenga, G., Hernández-Olivares, F.: Cracking control of concretes modified with short AR-glass fibers at early age. Experimental results on standard concrete and SCC, *Cement and Concrete Research* 37 (2007) 12, pp. 1624–1638.

[9] Ali, M.A., Majumdar, A.J., Singh, B.: Properties of glass fiber reinforced cement-the effect of fiber length and content, *Journal of Materials Science*, 10 (1975) 10, pp. 1732–1740.

[10] Biswas, A.K., Cherif, C., Hund, R.D., Shayed, M.A., Hossain, M.: Influence of Coatings on Tensile Properties of Glass Fiber, *Materials Science (MEDŽIAGOTYRA)*, 20 (2014) 1, pp. 50-54,.

[11] Yazici, S., Inan, G., Tabak, V.: Effect of aspect ratio and volume fraction of steel fiber on mechanical properties of SFRC, *Construction and Building Materials*, 21 (2007) 6, pp. 1250-1253,.

[12] IS: 8112(1989). Specification for 43 Grade Ordinary Portland Cement, Second Revision, Reprint 2013, Bureau of Indian Standards, New Delhi.

[13] IS: 383(1970). Specification for Coarse and Fine Aggregate from Natural Sources For Concrete, Second Revision, Reprint 2002, Bureau of Indian Standards, New Delhi.

[14] ASTM D 2343, "Standard Test Method for Tensile Properties of Glass Fiber Strands, Yarns, and Rovings Used in Reinforced Plastics", ASTM Standards, 2003.

[15] IS: 1199(1959). Methods of Sampling and Analysis of Concrete, Reprint 2004, Bureau of Indian Standards, New Delhi.

[16] IS: 516(1959). Method of Tests for Strength of Concrete, Amendment No. 2, Reprint 1993, Bureau of Indian Standards, New Delhi.

[17] Rocco, C., Guinea, G.V., Planas, J., Elices, M.: Review of the splitting-test standards from a fracture mechanics point of view, *Cement and Concrete Research*, 31 (2001) 1, pp. 73-82.

[18] IS: 5816(1999), Splitting Tensile Strength of Concrete-Method of Test, First Revision, Reprint 1999, Bureau of Indian Standards, New Delhi.

[19] Mohammadi, Y., Singh, S.P., Kaushik, S.K.: Properties of steel fibrous concrete containing mixed fibres in fresh and hardened state, *Construction and Building Materials*, 22 (2008) 9, pp. 956-965.

[20] Folgar, F.: Orientation Behavior of Fibers in Concentrated Suspensions, *Journal of Reinforced Plastics and Composites*, 3 (2000) 2, pp. 98-119.

[21] Song, P.S., Hwang, S.: Mechanical Properties of high-strength steel fiber-reinforced concrete, *Construction and Building Materials*, 18 (2004) 9, pp. 669-673.

Primljen / Received: 15.2.2015.
Ispravljen / Corrected: 12.1.2016.
Prihvaćen / Accepted: 8.2.2016.
Dostupno online / Available online: 10.10.2016.

Impact of speed limit method on motorway safety

Authors:

Mostafa Adresi, PhD
University of Tarbiat Modares, Tehran
Faculty of Civil Engineering
mostafa.adressi@modares.ac.ir

Ali Mohammad Baghalishahi, MSc. CE
University of Science and Technology, Tehran
Faculty of Civil Engineering
ali.baghalishahi@yahoo.com

Maryam Zeini, Ph.D student
Tarbiat Modares University
Department of Civil and Environmental Engineering
maryam.zeini@gmail.com

Abolfazl Khishdari, PhD student
Yazd University, Yazd
Department of Civil Engineering
abolfazl_khishdari@yahoo.com

Scientific paper - Preliminary report

Mostafa Adresi, Ali Mohammad Baghalishahi, Maryam Zeini, Abolfazl Khishdari

Impact of speed limit method on motorway safety

Results obtained during the study of various speed limit methods, including uniform, differential, and lane-based methods, are presented in this paper. The results show that the LBSL strategy is by 20 % better than other methods when safety is considered, while its traffic performance is by almost 16 % lower compared to other methods. The results also show that traffic performance decreases approximately by 19 %, but safety increases roughly by 20 %, if the speed limit is reduced from 130 km/h to 100 km/h.

Ključne riječi:
motorway safety, road network, performance, simulation, VISSIM, SSAM

Prethodno priopćenje

Mostafa Adresi, Ali Mohammad Baghalishahi, Maryam Zeini, Abolfazl Khishdari

Utjecaj primjene metode ograničenja brzine na sigurnost autocesta

U radu su prikazani rezultati ispitivanja primjene različitih metoda ograničenja brzine: jednolike, diferencijalne i metode pojedinačnog prometnog traka. Rezultati pokazuju da metoda LBSL ima 20 % bolje rezultate od ostalih metoda s obzirom na kriterij sigurnosti, no za kriterij prometne učinkovitosti rezultati su 16 % slabiji od rezultata ostalih metoda. Štoviše, rezultati pokazuju da su zbog smanjenja dopuštene brzine sa 130 km/h na 100 km/h, prometni pokazatelji lošiji za 19 %, no sigurnost autoceste je povećana 20 %.

Ključne riječi:
sigurnost autocesta, cestovna mreža, učinkovitost, simulacija, VISSIM, SSAM

Vorherige Mitteilung

Mostafa Adresi, Ali Mohammad Baghalishahi, Maryam Zeini, Abolfazl Khishdari

Einfluss von Methoden der Geschwindigkeitsbegrenzung auf die Sicherheit von Autobahnen

In dieser Arbeit werden die Resultate von Untersuchungen zur Anwendung verschiedener Methoden der Geschwindigkeitsbegrenzung dargestellt: einheitlicher und differentieller Methoden, sowie Methoden einzelner Fahrbahnen. Die Resultate zeigen, dass LBSL Methoden eine 20 % bessere Auswirkung im Vergleich zu anderen Methoden bezüglich Sicherheitskriterien haben, aber hinsichtlich Kriterien der Verkehrseffizienz 16 % schlechter abschneiden. Darüber hinaus zeigen die Resultate, dass durch ein Abmindern der Höchstgeschwindigkeit von 130 km/h auf 100 km/h die Verkehrsparameter 19 % schlechter werden, die Sicherheit der Autobahn aber um 20 % ansteigt.

Ključne riječi:
Sicherheit von Autobahnen, Straßennetz, Effizienz, Simulation, VISSIM, SSAM

1. Introduction

The terms road safety and road network performance play a crucial role in each and every kind of road. The assurance of transportation safety has become even more important with an increase in road facilities such as freeways, and with rapid development in transportation technologies. Due to high cost of accidents, speed limits and related strategies have become important topics, particularly when regarded as factors affecting safety. A number of researchers, such as Evans [1] and Elvik [2], claim that speed is the single most contributing factor affecting the frequency and severity of highway accidents. Amir H. Ghods et al (2012) have defined two main speed limit strategies including the uniform speed limit (USL) and differential speed limit (DSL), based on the size, weight, and manoeuvrability characteristics of cars and trucks. [3]. In the USL strategy, all vehicles regardless of their type (light and heavy), have the same speed limit, whereas in the DSL strategy, different vehicles have different speed limits. Naturally, the speed limit for heavy vehicles is lower than that for light vehicles (Figure 1).

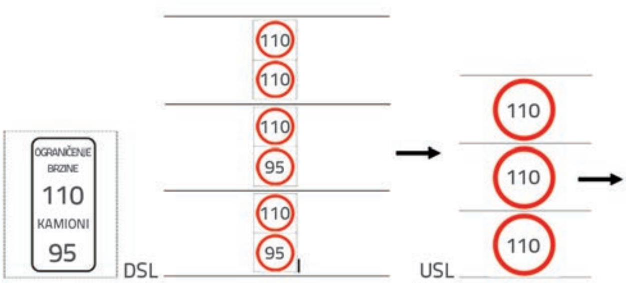

Figure 1. Vehicle-based speed limit strategies such as (DSL, USL). (speed limits expressed in km/h)

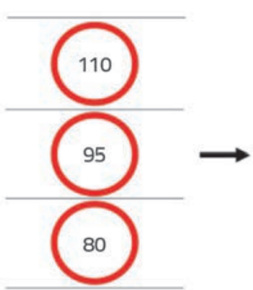

Figure 2. Lane based speed limit (LBSL), expressed in km/h

The DSL normally sets the maximum speeds for trucks in such a way that they are by about 10–15 km/h lower than the speed limits for cars in the same conditions. For instance, in Michigan the posted speed limit for trucks is by 16 km/h (10 mph, mph = miles per hour) lower than that applied for cars (95 versus 110 km/h, respectively) on rural interstate highways [4]. Thus, these speed limit strategies were categorized as vehicle-based (VB) strategies. Another speed limit strategy, totally different and known as the lane-based speed limit (LBSL), is practiced in some countries, like Iran. In LBSL, the speed limit is different at different lanes rather than for different vehicles. As a matter of fact, each lane has its own speed limit which increases from the right-side lane to the left-side one, and is equal for all vehicles, regardless of their type (light and heavy) (Figure 2).

Some studies focus on traffic performance versus safety effects of the speed limit strategies (USL & DSL). Freedman and Williams have studied traffic performance when the DSL approach was implemented. They analysed speed data collected from 54 sites in 11 North-eastern States of the USA, and determined the effects of DSL on the mean and 85th percentile speeds [5]. Their studies revealed results that are similar to those obtained by Harkey and Mera, who established that there is no significant difference between the passenger car and truck mean speeds and 85th percentile speeds when comparing USLs and DSLs [6, 7].

In safety impacts based studies, Harkey and Mera have found no significant differences between car speed variances at the USL and DSL implementation sections [7]. However, Council et al. have established that rear-end collisions between cars and trucks increase severity of crashes, at a high speed freeway with the DSL strategy [8]. An evaluation conducted by the Idaho Department of Transportation shows that changing the strategy from the USL to DSL does not bring about an increase in crashes [9]. However, there is some evidence showing that the DSL can cause an increase in some types of crashes while reducing others [6].

A study conducted by Garber and Gadiraju shows that crash rates, with an increase in posted speed limit for trucks to up to 105 km/h (65 mph), in the adjacent states of Virginia (DSL implementation site) and West Virginia (USL implementation site), do not result in a significant increase in fatal injuries and overall accident rates. In most transportation agencies, the DSL control strategies tend to be discretionary, inherently depending on agreement among various drivers taking part in the traffic stream (cars as well as trucks) [10]. Solomon found the U-shaped relationship between the crash involvement rate and the amount of deviation from average speed. An increase in speed variance may lead to an increase in the number of accidents, especially accidents involving (noncompliant) cars and (compliant) trucks [11].

The safety results of differential speed limits among cars and trucks have not been akin in previous studies. Some studies found no difference between the USL and DSL [7, 9, 10], while other studies found that one or the other policy is better [5, 8]. Most of these studies related to the impact of DSL on road safety have been adopted from statistical before-and-after approaches. One of major deficiencies of the statistical approach lies in the limitations allocated to the analysis because of the available data [3]. Thus the use of microscopic traffic simulation platforms in conjunction with surrogate safety measures would provide an alternative approach for safety implication evaluation of uniform and differential speed limits [3]. Saccomanno et al. [12] discussed advantages of this approach in their study of

the DSL and maximum speed limit (MSL) (differential speed controls with truck speed limiters) strategies applied to freeway segments.
In this study, the safety and traffic performance impacts of the LBSL and VB (including USL and DSL) strategies are analysed for freeways, under similar laboratory circumstances, using the VISSIM traffic simulation software package. This study claims to be of prime importance, because no study has previously been made on the comparison between these two kinds of speed limits strategies (VB, LBSL).

2. Simulation model for freeway

The effect of individual-vehicle interactions is the result of a complex process that can only be captured using simulation, and cannot be explained by a simple analytic process [3]. Thus a microscopic traffic simulation was conducted in this study using the VISSIM software. Each vehicle's behaviour in the simulated network was analysed sporadically, while they all relied on a simulated network environment. The response of each vehicle was considered as a result of interactions between many users and vehicles present in the network. Results were significantly affected by details used in the model [13]. Any changes in the car following lane changing and lateral spacing models can significantly affect the traffic and safety outputs of the simulation model. Shaykh al-slami et al (2011) and Safarzadeh et al (2010) described the VISSIM models and their underlying mathematical expressions and calibration results [14, 15]. Four individual traffic performance criteria and five individual safety criteria were considered in this study, in order to evaluate traffic performance and safety. The traffic performance criteria were evaluated in two positions. The first one was located in the middle of the basic section (first part), and the second one was located in the middle of the weaving section. These sections are marked with red coloured circle signs in Figure 3. Traffic performance criteria were: speed difference between various lanes in two sections, lane utilization in two sections, travel time per kilometre, and average speed in the network.

Figure 3. Case study freeway segments

Vehicle trajectories, extracted from VISSIM simulation models results, were used for traffic safety evaluation, which was based on traffic conflict analysis. Traffic conflict analysis is a safety analysis method that uses non-crash data. It is based on observations of individual vehicle movements, and on identification of situations that can result in critical incidents. Critical incidents are serious incidents that may result in a crash. They are characterized by sudden braking, sudden change of lane, or steering off the road [16]. Parker and Zegeer defined a traffic conflict as an event involving the interactions of at least two vehicles where at least one takes evasive actions to avoid an imminent collision. The danger was caused by a leading vehicle that reduces speed abruptly or changes lane to cut the following vehicle. They elaborated this definition in which a conflict occurred when the vehicles were on a collision course i.e., vehicles attempted to occupy the same space at the same time [17]. The advantage of using the conflict analysis on crashes is the possibility of examining even the near-crash events that are not available in the crash report information. These events occur more frequently than crashes and their prior information is the same as that of crashes [18].
To evaluate a comprehensive scrutiny, other criteria such as (PET, MaxS, DeltaS, DeltaV and MaxDeltaV) were considered in addition to the Time-to-Collision (TTC), which is defined as the ratio of relative speed of vehicles to their relative positions (Equation 1),.

$$TTC = \frac{X_i - X_{i+1} - L_i}{V_{i+1} - V_i} \tag{1}$$

Here, X_i and X_{i+1} are positions of two successive vehicles and V_i and V_{i+1} are their velocities; and L_i is the length of the first vehicle. PET is the time difference between the first vehicle's last occupied position and the second vehicle's arrival to the same position. A value of 0 indicates an actual collision [14]. MaxS is the maximum speed of any vehicle throughout the conflict. DeltaS is defined as the magnitude of the difference in vehicle velocities (or trajectories), DeltaS = | v1 - v2 |. MaxDeltaV is the maximum DeltaV value of any vehicle in the conflict [19].

3. Simulation variables

A case study simulation was carried out for a six-kilometre segment of a multi-lane freeway, as illustrated in Figure 3. The first kilometre was considered as the warm-up zone and was not included in the simulation results. The simulation time was taken to be 70 minutes, including a 10-min warm-up interval. On an average, 10 runs were carried out for each speed control strategy (USL, DSL, and LBSL). In the simulation, the input traffic flow varied from 3750 to 9000 vph (vph - vehicle per hour) and the trucks participated with 10 to 15 percent in the traffic. In the USL strategy, all vehicles had the same speed limit regardless of their types and the lane of crossing, whereas in the DSL strategy the car and truck maximum posted speed differences were set to 15 km/h. As the Iranian traffic organization regulated the corresponding differential speed in the LBSL strategy, the maximum posted speed differences between vehicles (cars & trucks) in each lane amounted to 15 km/h in this strategy. Thus in the LBSL strategy simulation, if in simulation the number of lanes is 3 and the maximum posted speed limit is 100 km/h, the posted speed limit for each of the individual lanes from the left lane to the right line will be 100, 85, and 60 km/h, respectively. It should be noted that the maximum posted speed

Table 1. Studied parameters and scenarios

Symbol	Explanation	Unit	Values	Variants
L	Distance between on- ramp and off-ramp	[m]	650 i 850	2
N	Number of lanes in basic freeway	-	3 i 4	2
V1	Input volume in basic freeway	[veh/h per each lane]	750, 1250 i 1750	3
V2	Input volume in on-ramp	[veh/h]	1500 i 2000	2
T	Heavy vehicle percentage	[%]	10 i 15	2
Sc	Speed limit scenarios	-	USL, DSL i LBSL	3
SL	Maximum posted speed limits	[km/h]	100, 110, 120 i 130	4
			Number of the whole scenarios	576

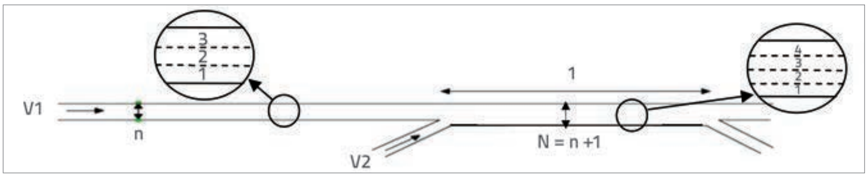

Figure 4. Parameters that are entered in model

weaving section, L = 650 m. Four and five lanes were considered for the research model. Lane 1 is labelled for the last lane situated at the right-side section of the freeway for the corresponding direction.

limits assumed in simulation models have been obeyed by 85 percent of drivers. As shown in Figure 4, the number of lanes is geometrically different in the basic and weaving freeway sections. There is one extra lane in the weaving section that is related to the basic freeway section.

In this study, some important parameters were chosen for the analysis, and various values were assigned to each parameter. A total of 576 scenarios were considered in this study. The figures for analysis resulted from multiplication of variants shown in the last column of Table 1. Some of these are illustrated in Figure 4.

4. Research model

The goal of this study was to compare different impacts of speed limit scenarios such as USL,DSL and LBSL at maximum speeds limits (such as 100, 110, 120, and 130 km/h) on the network performance and safety. Probable differences between speed limit scenarios were thus examined. According to this, one criterion out of nine (4 traffic performance & 5 safety) was selected as target, as illustrated in graph form in figures 5 to 12. The difference between strategies was studied by comparing variations in each graph based on the corresponding criterion. Finally, the statistical Analysis Of Variance (ANOVA) was used for quantitative verification of results.

4.1. Lane Utilization for area between on-ramp and off-ramp

The lane utilization after devising different strategies with varying number of lanes between on-ramp and off-ramp is compared in Figure 5. The constrained flow does not occur when the length between these two is as far as the critical length, L = 850 m. However, the constrained flow does occur in

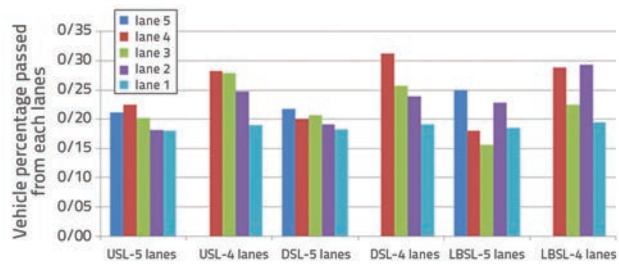

Figure 5. Lane utilization for area between on-ramp and off-ramp (In this graph, L = 650 m, V_1 = 1750 veh/h, V_2 = 2000 veh/h, T = 15 %)

It can be inferred from Figure 5 that the lane occupation decreased from the last lane to lane 1. The difference in usage between the first and the last lane in 4-lane section roads was even greater compared to 5-lane roads. An extraordinary use of the second lane was also observed in the LBSL strategy. The speed arrangement in the LBSL approach, which was different from other approaches, justified this extraordinary use in the second lane. It means that some of the drivers who tend to enter or exit the freeway, are more inclined to use a lane with a higher speed limit to move faster. Results show that the LBSL creates more lane changes in this area, and may bring about deterioration of safety conditions. Also, the LBSL strategy leads to the creeping movement of vehicles in the second lane, which was a boundary of change for vehicles moving from outer lanes toward the first lane and vice versa. This by itself can cause an increase in the proportion of the second lane use, which means that the percentage of crossing vehicles in this lane is higher compared to other lanes.

4.2. Lane Utilization in basic freeway segment

The percentage of use of each lane after implementation of various strategies in the basic freeway section with three or four lanes is compared in Figure 6. Here, lane 1 is labelled for the last lane situated at right-side section of the freeway for the corresponding direction.

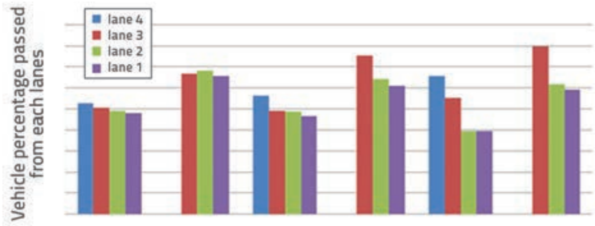

Figure 6. Lane utilization in basic freeway section (In this graph, L = 650 m, V_1 = 1750 veh/h per lane, V_2 = 2000 veh/h, T = 15 %)

According to Figure 6, the USL to LBSL Strategies, which were implemented for the three-lane or four-lane basic freeway sections, show that the lane usage increased from the first lane (lane 1) toward the last lane. Two reasons should be given to explain this trend. The first one is that drivers tend to do and finish their travel as soon as possible (car following model combined to lane changing model find the opportunity for each vehicles independently to pass the other vehicles to ascertain it). As shown in Figure 7 (from USL to LBSL), the second reason is that the speed differences from the first lane (lane 1) to the last one naturally increase because the drivers tend to move to the fastest lane (last lane). Also it can be derived that the LBSL strategy increases congestion in the high-speed lanes (i.e. lane 3 in a 3-lane freeway, and lane 4 in a 4-lane freeway) of the basic freeway section, and also that the overtaking potential declines with an increase in the possibility of overtaking from the right side of each vehicle. Hence, it was expected that the number of lane changes in the LBSL strategy is greater compared to the other two strategies. The amount of this measure was not related to the changes in length between the entrance and exit ramps, the number of lanes, and the percentage of heavy vehicles, but was related to speed limit scenarios. It can be claimed that the USL and DSL strategies were not different considering the percentage of traffic passing via the basic freeway section, while these strategies both differed from the LBSL strategy.

4.3. Speed difference between various lanes in basic freeway section and area between on-ramp and off-ramp

Speed differences between each of the individual lanes, after implementation of various speed limit strategies, are compared in Figures 7 and 8. Thus, the maximum number of speed differences between all vehicles that used a particular lane is shown in this graph.

After analysis of figures, it was established that speed variances between various lanes in the basic section, and also between the on-ramp and off-ramp segments, were identical in the USL and DSL scenarios, but were completely different from LBSL scenario; here, the speed variance was much higher compared to other scenarios. In the basic section, speed variances were lower compared to the one between the on-ramp and off-ramp. It can be concluded that the strategy with more unity produces more speed driving but the speed differences between each lane are lower, and so the USL has the best traffic performance and mobility, while the LBSL is characterized by greater disturbance in the traffic flow.

Speed differences between the on-ramp and off-ramp sections are compared in Figure 7, whereas the same factor for the basic freeway section is compared in Figure 8. Horizontal axes are V_1+V_2 in Figures 7 to 12.

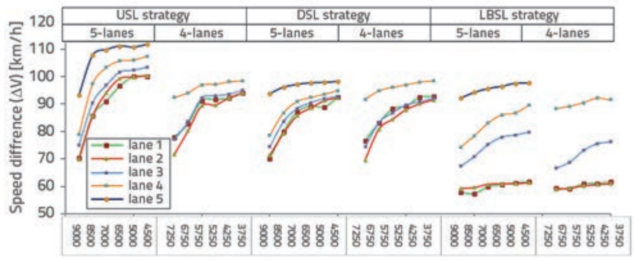

Figure 7. Speed difference between various lanes in the area between on-ramp and off-ramp (in this graph, L = 650 m, M.S.L = 120 km/h, T = 15 %)

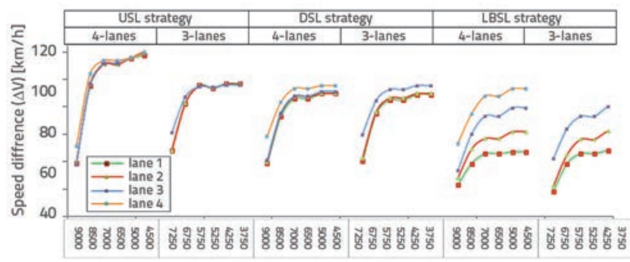

Figure 8. Speed difference between various lanes at basic freeway section (in this graph, L = 650 m, T = 15 %)

4.4. Average speed in the network

Figure 9 shows variation in the network average speed for different strategies and for various numbers of maximum posted speed limit, which is labeled as M.S.L. (maximum speed limit).

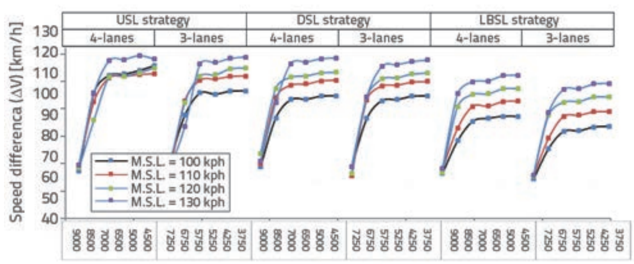

Figure 9. Average speed in network (In this graph, L = 650 m, M.S.L = 120 km/h, T = 15 %, M.S.L. maximum speed limit)

The results show that the USL and DSL are the same, but the LBSL scenario has the weakest performance with about 16 percent. Also, it is clear that, after decreasing lane numbers from 4 to 3, the performance becomes even worse. Furthermore, it can be seen that the traffic flow is more fluent and that the average speed increases with variation of some parameters such as the distance between two ramps (from 650 m to 850 m), truck percentage (20% to 1%0), and speed limit (100 km/h to 130 km/h),.

4.5. Travel time per one kilometre

The variation in travel time for each individual strategy, with different posted speed limit numbers, is presented in Figure 1.

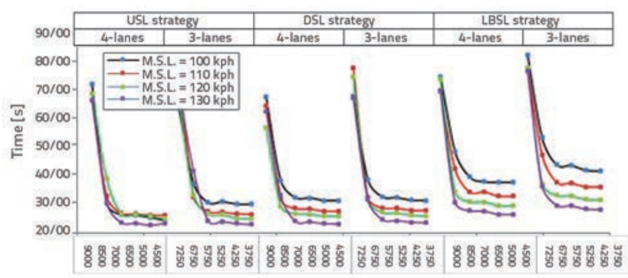

Figure 10. Travel time per one kilometre (in this graph, L = 650 m, T = 15 %)

It can be seen that the USL and DSL scenarios are similar, as confirmed by statistical analysis. Furthermore, it was revealed that the LBSL scenario has the weakest performance, due to its lowest average speed. Also, the travel time reduces with an increase in maximum speed limits. As shown in Figures 9 and 10, the DSL strategy has some similarities with the USL, but the difference between the USL and LBSL is greater compared to that between the DSL and USL strategies. Consequently, the graph analysis shows that the USL and DSL strategies are approximately the same, but that they completely differ from the LBSL. It can therefore be concluded that the LBSL has the lowest traffic performance compared to all other strategies.

4.6. TTC and PET safety criteria

Safety criteria variations after implementation of different strategies are compared in Figure 11. In top series, charts are allocated to the time-to-collision (TTC) whereas in bottom series, charts are allocated to the post-encroachment-time (PET).

Unexpectedly, Graph trends and statistical analysis indicate that the LBSL strategy does not reduce the level of safety. The chart analysis and analytical calculations show that the LBSL strategy is more desirable than the other two strategies in terms of safety and performance. The LBSL strategy is more convincing than other strategies for about 15 % with respect to the TTC, and for about 24% with regard to the PET. This result was justified by a lower average speed of the entire network in the LBSL strategy, compared to other strategies. As a result, it can be expected that the LBSL strategy will have a better safety effect compared to the other two strategies. The analysis of variance shows that individual strategies are completely independent. Also, the one-way ANOVA shows that the USL and DSL strategies have the same safety effects, and that they do not greatly differ. This also confirms the results obtained in previous studies. In addition, the one-way ANOVA confirms that an increase of the maximum speed limit from 100km/h to 130 km/h, causes a decrease in the average TTC value by about 12 %, and PET by roughly 21 %. As shown by the above mentioned lane utilization parameter, the LBSL strategy creates a greater lane changing opportunity and, as this strategy increases vehicles portion in the high-speed lane (last lane) compared to other lanes, it causes a decrease in overtaking opportunity and increases the chance of illegal overtaking, which may lead to

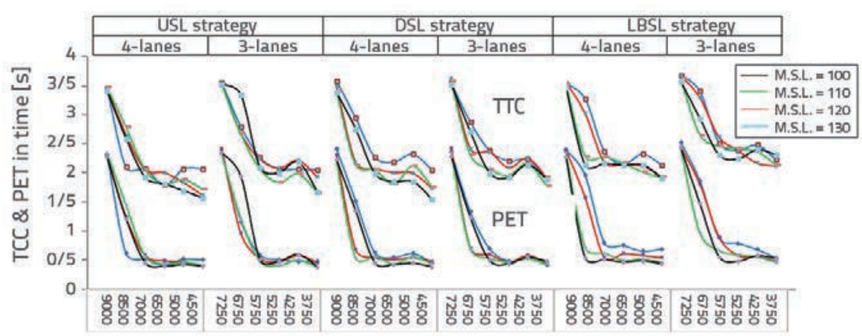

Figure 11. Safety criteria TTC and PET (in this graph, L = 650 m, M.S.L = 120 km/h, T = 15 %)

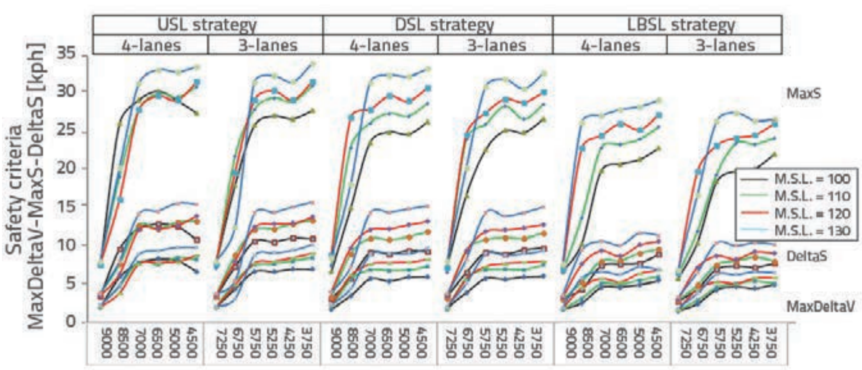

Figure 12. Safety criteria: MaxDeltaV – MaxS - DeltaS (in this graph, L = 650 m, M.S.L = 120 km/h, T = 15 %, M.S.L. maximum speed limit)

Table 2. One-way and two-way ANOVA results

Criteria							Title	ANOVA analysis
Safety					Traffic performance			
MaxDeltaV	DeltaS	MaxS	PET	TTC	Travel time	Average speed		
0.000	0.000	0.000	0.004	0.000	0.000	0.000	Speed limit Scenarios P-Value	Two-way
IN.	IN.	IN.	IN.	IN.	IN.	IN.*	Interpretation	
0.000	0.000	0.000	.016	0.000	0.000	0.000	Maximum speed limits P-Value	
IN.	IN.	IN.	IN.	IN.	IN.	IN.	Interpretation	
0.692	0.582	0.930	0.849	0.998	0.502	0.746	Interaction P-Value	
No Interaction**	No Interaction**	No Interaction**	No Interaction**	No Interaction**	No Interaction**	No Interaction**	Interpretation	
6.477	10.463	24.222	0.774	2.298	38.12	98.92***	DSL-value	One-way for scenarios
6.829	10.985	24.828	0.781	2.270	38.02	100.08	USL-value	
4.797	7.760	19.956	0.956	2.600	44.81	84.41	LBSL- value	
4.992	8.046	19.920	0.969	2.567	44.87	83.97	100 km/h - value	One-way for maximum speed limits
5.825	9.414	22.437	0.844	2.399	40.85	92.62	110 km/h - value	
6.296	10.147	23.999	0.772	2.329	38.97	97.22	120 km/h - value	
7.024	11.337	25.651	0.764	2.270	36.57	104.06	130 km/h - value	

IN. = Independent

* Independent is used in both one-way and two-way analysis of variance when both parameters have no effect on each other (at least one of them is different).

** **: If speed limit scenarios such as the DSL, USL and LBSL and speed limits such as 100, 110, 120 and 130 km/h do not have any effect on each other, two-way analysis of variance is not necessary and the investigation of each case, such as speed limit scenarios and maximum speed limits, should be analysed independently. So, the one-way analysis of variance is adequate.

*** Best scenarios are underlined.

a higher accident hazard. It could therefore be expected that the LBSL strategy is characterized by the lowest safety level. But, as the safety criteria show, this strategy actually has the best safety conditions. It may be due to a lower speed (lower traffic performance) rather than to a higher lane changing and illegal overtaking in the traffic stream. Thus, safety conditions are much more sensitive to speed reduction compared to other parameters such as lane changing and illegal overtaking.

4.7. Different speed safety criteria variations

Variations of different speed safety criteria, including the maximum speed variation (MaxDeltaV), maximum speed (MaxS), and speed difference (DeltaS), as obtained based on various strategies, are shown in Figure 12. Top series charts are for the MaxS evaluation, middle charts are for the DeltaS evaluation, while low charts are for the MaxDeltaV evaluation.

It can be observed that the LBSL strategy had a lower (about 27 %) maximum speed variation (MaxDeltaV) compared to the other two strategies. On the other hand, speed variations would supply the mean collision acceleration. Thus, the lower the possible maximum acceleration, the lower the severity of the collision. As a result, in the total network, a decrease in maximum speed variance improved safety and driver convenience considerably. It was also found that, as the LBSL strategy was implemented, it had the lowest (about 19 %) maximum speed (MaxS) compared to other strategies. Since the maximum speed decreased in collision situations, the system was improved in terms of safety and hence collision severity was reduced remarkably. In addition, it was established that the LBSL strategy had a lower speed variation rate (about 27 %) as related to the other strategies. However, as speed variations in the system lowered, a greater homogeneity was achieved, and the safety was improved. Finally, when considering the three criteria MaxDeltaV-MaxS-DeltaS on graphs and in the scope of statistical analysis, it was found that the LBSL strategy is better in terms of safety compared to the other two strategies. The analysis of variance indicated that different strategies were independent from one another, and that there was no interaction. Also, the one-way ANOVA related to these parameters (MaxDeltaV-MaxS-DeltaS) made it clear that the USL and DSL strategies were the same in terms of safety but that they also presented slight differences. In addition, the one-way ANOVA test shows that the safety improves remarkably (roughly 30 %) for three criteria i.e. MaxDeltaV-MaxS-DeltaSon, if the maximum speed limit is reduced.

5. ANOVA test results

The analysis of variance (ANOVA) is used in order to analyse the differences between group means in order to identify whether the means of several groups are probably equal or not. So, it generalizes the t-test to more than two groups.

ANOVA is a particular form of statistical hypothesis testing heavily used in the analysis of experimental data. A statistically significant result, when a probability (p-value) is less than a threshold (significance level), justifies rejection of the null hypothesis. In this research, the null hypotheses of all the speed limit scenarios, and all the maximum speed limits, are the same [20].

In the analytical process, the interaction between two main cases such as the speed limit scenarios and maximum speed limits, is first clarified using the two-way ANOVA test. As the results show (Table 2), speed limit scenarios and maximum speed limits have no effect on each other, and they are independent. So, the one-way analysis of variance is considered adequate. Also, the two way ANOVA analysis shows that all seven criteria are independent of speed limit scenarios and maximum speed limits, because of speed limit scenarios, P-Value < 0.05, and also maximum speed limits, P–Value < 0.05, in which the significant level is 0.05 (α = 0.05) [20]. It means that, in all seven criteria, at least one of the maximum speed limits or speed limit scenarios is statistically different. For example, as shown in Table 2: "one-way for scenarios", there is no significant difference between the USL and DSL scenarios in case of all seven criteria, but the two greatly differ from the LBSL scenario as the P-Value is at the less than significant level.

As can be seen in results shown in "one-way for scenarios", the average of the "average speed" criterion in both USL and DSL statistically presents no significant change, but there is a great difference compared to the LBSL. It is obvious that the traffic performance increases with an increase in average speed in different circumstances.

6. Conclusion

Various strategies currently applied as the speed limit strategies for freeway traffic control in Iran and other countries are examined in this study. Strategies currently applied in Iran are compared with other strategies in terms of safety and freeway network performance. The VISSIM is used to compare the impact of these strategies and scenarios under a range of traffic and geometric conditions. The SSAM is also used for further in depth safety analysis. The results are compared through graphical tools and also through more quantitative statistical tools such as ANOVA. Based on the analysis, a comparison of the strategies is made in terms of safety and network performance.

The results indicate that the LBSL (lane based speed limit) strategy is less adequate in terms of performance criteria (average speed of the entire network and average travel time) when compared to the other two strategies (DSL and USL). Simulation results show that the LBSL strategy has a lower traffic performance (by about 16 %) than the other two strategies (DSL and USL). However, in terms of safety, it is preferable to the other strategies (by about 20 %). Results also indicate that the speed difference and the lane changing potential are higher in the LBSL compared to the other strategies. Nevertheless, it was established that the average speed in the LBSL strategy with the same speed limit is lower compared to the other two strategies. In terms of safety, the LBSL strategy ranks better than the other two strategies. The comparison of the effects of the USL and DSL strategies on the average speed shows that the changes in these types of strategies have a marginal effect on the average speed. This means that the differences in speed between the light and heavy vehicles do not have a significant effect on the average network speed. Considering both performance and safety, the USL and DSL strategies do not have a significant priority over one another; and it can be concluded that the main distinction is between the LBSL and VB strategies. Furthermore, results show that traffic performance decreases by approximately 19 %, whereas safety increases by approximately 20 %, with the reduction in speed limit strategies from 130 km/h to 100 km/h.

REFERENCES

[1] Evans, L.: Traffic safety and the driver. Van Nostrand Reinhold Company, First edition, Van Nostrand Reinhold Company, New York, 1991.

[2] Elvik, R.: Speed and road safety: Synthesis of evidence from evaluation studies, Transportation Research Record:Journal of the Transportation Research Board, pp. 59-69, 2006.

[3] Ghods, A., Saccomanno, F., Guido, G.: Effect of Car/Truck Differential Speed Limits on Two-Lane Highways Safety Operation using Microscopic Simulation, Procedia - Social and Behavioral Sciences, 53 (2001), pp. 834 – 841

[4] GHSA. State speed limit laws. In Governors Highway Safety Association, http://www.ghsa.org/html/stateinfo/laws/speedlimit_laws.html, 15.07.2012

[5] Freedman, M., Williams, A. F.: Speeds Associated with 55 mph and 65 mph Speed Limits in Northeastern States, ITE Journal, 2 (1992), pp. 17-21

[6] US Department of Transportation, The Safety Impacts of Differential Speed Limits on Rural Interstate Highways, Federal Highway Administration, Publication No. FHWA-HRT-04-156, Washington DC, 2004.

[7] Harkey D.L., Mera, R.: Safety Impacts of Different Speed Limits on Cars and Trucks, U.S. Department of Transportation, Federal Highway Administration, Publication No. FHWA-RD-93-161, Washington DC.1994

[8] Duncan, C.S., Khattak, A.J., Council, F.M.: Applying the Ordered Probit Model to Injury Severity in Truck-Passenger Car Rear-End Collisions, Transportation Research Record: Journal of Transportation Research Board , No. 1635, pp. 63-71, 1998.

[9] Idaho Transportation Department Planning Division, Evaluation of the Impacts of Reducing Truck Speeds on Interstate Highways in Idaho, - Phase III, Final Report, National Institute for Advanced Transportation Technology, University of Idaho, 2000.

[10] Garber, N.J., Gadiraju, R.: Impact of Differential Speed Limits on Highway Speeds and Accidents, Transportation Research Record: Journal of Transportation Research Board, 58 p., 1991.

[11] United States. Bureau of Public Roads, Accidents on main rural highways related to speed, driver, and vehicle, For sale by the Superintendent of Documents, US Govt. Print. Off, 1964.

[12] Saccomanno, F.F., Duong, D., Cunto, F., Hellinga, B., Philp, C., Thiffault, P.: Safety implications of mandated truck speed limiters on freeways, Transportation Research Record: Journal of the Transportation Research Board, Vol. 2096, pp. 65-75, 2009.

[13] VISSIM 5.10 user manual, PTV, http://www.ptvamerica.com, 10.AG.2008.

[14] Shaykh Al-Slami, A., Baghalishahi, A.M., Gahrpoor, A.A.: Investigation of impacts of truck lane restriction strategies on freeway traffic performance with simulation, Journal of transportation research institute, pp. 377-388, 2011.

[15] Safarzadeh, M., Adressi, M., Baghalishahi, A.M.: Investigation of car-following models in traffic simulation using VISSIM simulation software, journal of Police-Rahvar, Iran, 2010.

[16] Muchuruza, V.F.: Simulation of traffic crashes using cell based micro-simulation, The Florida State University FAMU-FSU College of engineering, A Dissertation submitted to the Department of Civil and Environmental Engineering in partial fulfillment of the requirements for the degree of Doctor of Philosophy, 2006.

[17] Parker, M.R., Zegeer, Jr., Zegeer, C.V.: Traffic Conflict Techniques for Safety and Operations: Engineers Guide, Report FHWA-IP-88-026, FHWA, U. S. Department of Transportation, Washington, D.C, 1989.

[18] Van der Horst, A.R.A.: A Time-Based Analysis of Road User Behavior in Normal and Critical Encounters, TNO Institute for Perception, Soesterberg, Netherlands, 1990.

[19] Joshi, L., Joshi, R.: FHWA-HRT-08-050, Surrogate Safety Assessment Model (SSAM): Software User Manual, 2008.

[20] Gelman, A.: Variance, analysis of, in book: The new Palgrave dictionary of economics (eds.: Durlauf, N.S., Blume, E.L.), Basingstoke, Hampshire New York: Palgrave Macmillan. (2008). ISBN 978-0-333-78676-5, http://dx.doi.org/10.1057/9780230226203.1787

Primljen / Received: 24.2.2016.
Ispravljen / Corrected: 29.8.2016.
Prihvaćen / Accepted: 15.9.2016.
Dostupno online / Available online: 10.10.2016.

A review of the Gavrilović method (erosion potential method) application

Authors:

Nevena DragičevićMCE
University of Rijeka
Faculty of Civil Engineering
nevena.dragicevic@uniri.hr

Assist.Prof. Barbara Karleuša, PhD. CE
University of Rijeka
Faculty of Civil Engineering
barbara.karleusa@uniri.hr

Prof. Nevenka Ožanić, PhD. CE
University of Rijeka
Faculty of Civil Engineering
nevenka.ozanic@uniri.hr

Subject review

Nevena Dragičević, Barbara Karleuša, Nevenka Ožanić

A review of the Gavrilović method (Erosion Potential Method) application

A detailed review of application of the Gavrilović method (Erosion Potential Method) and its modifications, with a focus on the potential surface erosion, is presented in the paper, together with the guidelines and recommendations for future analysis and research as needed for physical planning and urban development. The Gavrilović method results are based on the source of information, expert experience, accuracy, and level of detail of the model input and output data. For further analysis, the authors propose investigation of additional sources of erosion materials, such as construction plots in expanding urban areas.

Ključne riječi:
Gavrilović method, Erosion Potential Method, erosion sediment production, transported sediment, erosion intensity

Pregledni rad

Nevena Dragičević, Barbara Karleuša, Nevenka Ožanić

Pregled primjene Gavrilovićeve metode (metoda potencijala erozije)

U ovome radu dan je detaljan pregled primjene Gavrilovićeve metode i njezinih modifikacija, s fokusom na potencijalnu površinsku eroziju, kao i smjernice te preporuke za buduće analize i istraživanja neophodna za prostorno planiranje i urbani razvoj. Rezultati Gavrilovićeve metode uvjetovani su izvorom informacija, iskustvom stručnjaka, točnošću i razinom detalja ulaza i izlaza iz modela. Za buduće analize autori predlažu da se u obzir uzmu dodatni izvori erozijskog nanosa poput gradilišta u područjima urbanog razvoja.

Ključne riječi:
Gavrilovićeva metoda, metoda potencijala erozije, produkcija erozijskog nanosa, transportirani nanos, intenzitet erozije

Übersichtsarbeit

Nevena Dragičević, Barbara Karleuša, Nevenka Ožanić

Überblick zur Anwendung der Methode nach Gavrilović (Erosionspotenzial-Methode)

In dieser Arbeit wird ein detaillierter Überblick zur Anwendung der Methode nach Gavrilović und ihrer Modifikationen, mit Fokus auf die potentielle Oberflächenerosion gegeben. Ebenso werden Richtlinien und Empfehlungen für zukünftige, bei der Raumplanung und Stadtentwicklung notwendige Analysen und Untersuchungen dargestellt. Resultate der Analysen nach Gavrilović sind durch die Informationsquelle, die Erfahrung von Spezialisten, die Genauigkeit und die Detailstufe von Modelleingaben und –ausgaben bedingt. Für zukünftige Analysen schlagen die Autoren vor, zusätzliche Quellen von Erosionsmaterial, wie z. B. aus Baustellen in Gebieten städtischer Entwicklung, zu berücksichtigen.

Ključne riječi:
Methode nach Gavrilović, Erosionspotenzial-Methode, Entstehung von Erosionsmaterial, transportierte Ablagerungen, Erosionsintensität

1. Introduction

As indicated in the proposed Directive for the Protection of Soil, and the Amending Directive from 2004 [1], a significant increase in soil degradation processes has been registered in recent centuries. There are eight main processes causing soil degradation in European countries, among which erosion is considered to be the main and the most widespread [1]. According to Morgan [2], the occurrence of erosion processes, as well as their distribution and timing, are closely related to anthropogenic factors such as local, social, economic, and political conditions. It is well known that erosion processes can be triggered by heavy rainstorm events. The impact of flash floods on the erosion and sediment transport processes is considered to be quite significant. Until today, prediction activities remain difficult due to complexity of their nature [3]. The soil erosion, flooding, and channel management are considered to be interconnected environmental problems, especially at the catchment level where intensive precipitation can cause widespread gullies, mass movements, and flooding [4]. The erosion sediment production assessment, which begins at the parcel size and then broadens to the catchment level, is considered to be the basic component of an appropriate erosion management. This information is essential for decision makers when choosing future erosion mitigation and protection measures [5], and also to stakeholders involved in spatial planning and urban development. The erosion and flash flood prevention and mitigation measures accentuate the importance of building appropriate hydraulic structures (e.g. retention structures), and implementing various protection works (e.g. afforestation, removal of sediments from riverbeds) and other measures (e.g. defining an appropriate land use, informing interest groups and local population, ...) in affected areas and areas of interest [6].

Various models are currently being applied in the area of water erosion risk and sediment yield assessment. They can be classified as empirical or regression models, conceptual models, and physics-based models. In addition, they can be classified as qualitative, quantitative and semi-quantitative models [2, 7]. The Pacific Southwest Inter-Agency Committee (PSIAC), The Modified Pacific Southwest Inter-Agency Committee (MPSIAC), the Factorial Scoring Model (FSM), the Vegetation-Surface Material-Drainage Density Model (VSD), the Gavrilović Model (Erosion Potential Method - EPM), Erosion Hazard Units (EHU), CORINE erosion risk maps, the Coleman & Scatena Scoring Model (CSSM), the Fleming & Kadhimi Scoring Model (FKSM), the Wallingford Scoring Model (WSM), and Revised Universal Soil Loss Equation (RUSLE), are all semi-quantitative models whose basic description and comparison are given by De Vente [7] and Eisazadeh et al. [8]. In this paper, the authors provide a detailed overview of implementation of the Gavrilović method for the erosion risk and sediment assessment, as well as conclusions and suggestions for future development and improvement of the method and its application.

2. Gavrilović method (Erosion Potential Method)

The Gavrilović model, also known as the Erosion Potential Model (EPM), was developed by Slobodan Gavrilović based on erosion field research in the Morava River catchment area in Serbia in the 1960`s [9]. The method itself is based on the Method for the

Table 1. Equations and description of Gavrilović method parameters [7, 9]

Equation	No.	Symbol	Description
$W_a = T \cdot P_a \cdot \pi \sqrt{Z^3} \cdot F$	(1)	W_a	Total annual volume of detached soil [m³/year]
		T	Temperature coefficient [-]
		P_a	Average annual precipitation [mm]
$T = \sqrt{\frac{T_0}{10} + 0{,}1}$	(2)	Z	Erosion coefficient [-]
		F	Study area [km²]
		T_0	Average annual temperature [°C]
$Z = Y \cdot X_a \cdot \left(\phi + \sqrt{J_a}\right)$	(3)	Y	Soil erodibility coefficient [-]
		X_a	Soil protection coefficient [-]
$\xi = \frac{\sqrt{O \cdot z}}{\left(l_p + 10\right)} \cdot D_d$	(4)	φ	Coefficient of type and extent of erosion [-]
		J_a	Average slope of the study area [%]
		ξ	Sediment delivery ratio [-]
$D_{d,original} = \frac{1}{0{,}25} = 4$	(5)#	O	Perimeter of the watershed [km]
		z	Mean difference in elevation of the watershed [km]
$D_{d,modified} = \frac{l_p + l_a}{F} = \frac{L}{F}$	(6)##	D_d	Drainage density [km/km²]
		l_p	Length of the principal waterway [km]
		l_a	Cumulated length of secondary waterways [km]
$G_y = \xi \cdot W_a$	(7)	L	Cumulated length of the principal and secondary waterways [km]
		G_y	Actual sediment yield [m³/year]

Originally set as a constant value, continues to be applied in various research
Modification of the method made by Lazarević [12], applied today in various studies.

Quantitative Classification of Erosion (MQCE), formally developed in 1954. During his research, Gavrilović discovered the possibility for further developing the MQCE method, which was used for defining the intensity of erosion. Extensions of this method were directed towards quantification of erosion processes by assessing the sediment transported downstream that reaches the control profiles [10]. Today, the method encompasses erosion mapping, sediment quantity estimation, and torrent classification, and has been extensively applied since 1968 for solving erosion and torrent-related problems in the Balkan countries [11]. It is currently being applied worldwide, from Croatia, Serbia, Slovenia, Italy, the Republic of Macedonia, Bosnia and Herzegovina, Montenegro, Iran to Chile (references are given in Table 4). Several distinct erosion processes can be assessed using the Gavrilović method, such as the surface erosion, downward erosion, or lateral erosion. In this paper the emphasis is placed on the application and modifications of the Gavrilović method for the assessment of potential surface erosion and suspended sediment and bed load in river network transported downstream.

The most often calculated outputs of the method (equations 1-8, Table 1) are:

- the total annual volume of detached soil Wa (equation 1, Table 1)
- the erosion coefficient Z (equation 3, Table 1)
- the actual sediment yield Gy (equation 7, Table 1).

According to De Vente [7], this method can be characterised as a semi-quantitative method because it is based on a combination of descriptive and quantitative procedures. However, compared to other semi-quantitative methods named in the introduction, this method is the most quantitative because it uses descriptive evaluation for three parameters only: soil erodibility, soil protection and extent of erosion in the catchment. All other parameters are quantitative catchment descriptors.

3. Modifications to Gavrilović method

One of the first upgrades to the method was proposed by Lazarević [13], who noted in his work the need to adjust the assigned values so as to take into account the coefficient describing the type and extent of erosion φ, the soil protection coefficient X_a and the soil erodibility coefficient Y. These three parameters, along with the slope angle, form the erosion coefficient Z. The purpose of this modification was to transform the definition of the erosion coefficient from its original meaning as soil erodibility to the today`s version as erosion intensity. Lazarević also modified the erosion intensity classification table represented by the erosion coefficient Z [13].

Tošić and Dragićević [12] proposed a new methodology for determining the erosion coefficient Z adapted for the use in GIS environments. It is based on the empirical methodology proposed by Gavrilović, and on its extensions by Lazarević. The very essence of their work involves the use of a PDA (Personal Digital Assistant) device with an integrated GPS receiver. The use of the device was combined with an appropriate software, namely ArcPad, to merge the GPS with the GIS. The aim was to directly determine an on-site coefficient for the type and extent of erosion (φ), and to transform the data accordingly to the erosion parcel condition. Yet another modification was proposed by Globevnik et al. [14] who suggested values for the soil protection coefficient based on the land cover classification CORINE (Table 2). Later on, Fanetti and Vezzoli [15] suggested a change in the categorisation of the soil protection coefficient X_a based on different land use categories (Table 2). They were the first to consider urban areas as areas of potential erosion, thus assigning them a value greater than zero. They included several stages of urbanisation as well as various vegetation types, from growing cultures to pastures and forests.

Table 2. Suggested modifications for evaluation of soil protection coefficient X_a

By Globevnik et al. [14]	
Land cover classification	X_a
Artificial surfaces, Inland water	0
Broad-leaved forest, Mixed forest	0,05
Heterogeneous agricultural areas	0,4
Transitional woodland shrub	0,5
Pastures, Natural grassland	0,6
Permanent crops	0,7
Arable land	0,9
Bare rocks, Areas under erosion	0,95
By Fanetti and Vezzoli [15]	
Land use categories	X_a
Scattered urbanisation	0,05
Rare urbanisation, Copse broad-leaved wood	0,1
Discontinuous urbanisation	0,15
Continuous urbanisation	0,18
Dense urbanisation, Copse broad-leaved and coniferous wood	0,2
Coniferous wood	0,4
Meadow and pasture with isolated arboreous elements	0,5
Meadow and pasture	0,6

Fanetti and Vezzoli [15] also proposed a different categorisation for the coefficient of type and extent of erosion φ and the soil erodibility coefficient Y (Table 3), which they applied to the Greggio River catchment in Italy. For the Greggio River catchment in Italy, they divided the parameter that describes the average slope of the study area J_a into five categories: 0-10 %, 10-20 %, 20-40 %, 40-60 % and 60-80 %, but omitted suggestion for the assessment of slopes steeper than 80 %.

Table 3. Suggested modifications by Fanetti and Vezzoli [15] for evaluation of Gavrilović method parameters

Soil type	*Y*
Limestone: moderate erosion resistance	0.8
Alluvial deposit: little erosion resistance	1.3
Glacial deposit: very little erosion resistance	1.6
Average slope angle	J_a
0 – 10 %	0.05
10 – 20 %	0.15
20 – 40 %	0.3
40 – 60 %	0.5
60 – 80 %	0.7

4. Review of Gavrilović method application

This paper summarises application of the Gavrilović method (original one and modified version) based on the analysis of more than fifty different papers from relevant scientific bases that were available to the authors. The erosion risk/intensity, and sediment production and transportation, were estimated for more than fifty different catchments worldwide (Table 4).
The most commonly calculated method output (82 % of the catchments) is the total annual volume of soil W_a. The value varies from 50 m³/km²/year for Rokava, Slovenia, [14, 18, 19] to 12,252 m³/km²/year for Khiav Chav, Iran [35, 38]. The actual sediment yield, or sediment transported downstream, given for 38 % of the catchments, ranges from 37 m³/km²/year to 2495 m³/km²/year.
A small number of analysed case studies (14 % of the analysed catchments) only provide an assessment of the erosion coefficient *Z*, thus giving insight the into erosion severity/intensity for certain catchments, while not providing information about the expected sediment production [40].
Depending on characteristics of a catchment area, drainage density in particular, final results for the actual sediment yield can vary from quite small to the values similar to those estimated for the total annual volume of soil, or yearly amount of sediment available for detachment. In no case should the values obtained for the actual sediment yield result in values that are larger than those calculated for the total annual volume of soil [21]. One of the reasons for this outcome lies in the use of a different formula for the sediment delivery ratio that includes the drainage density parameter. In the original form of the Gavrilović method, a constant value of 4 was used instead of the drainage density formula. Later on, the model was modified, and the drainage density was taken to be the ratio between the primary and secondary river length and the contributing/catchment area. Results such as those for the Upper Sezar River can be obtained using the constant value instead of the length/area ratio. Overall, 37 % of catchment results showing the actual sediment yield are based on a constant value of the drainage density coefficient.

4.1. Gavrilović method, GIS and remote-sensing data

According to Thieken et al. and Vogt et al. [61, 62], the reliability of final GIS based results is strongly correlated with the accuracy and level of detail of input data (topographic, land-use, and soil-data sources). Newer technologies, namely areal and satellite remote-sensing data, can be used to provide a substantially greater level of detail, and therefore simplify the erosion assessment procedure in the area of interest [15]. These technologies provide an improvement by enabling defragmentation of catchments to arbitrary cell sizes. For example, Bagherzadeh et al. [16, 17] subdivided a catchment into eight homogeneous terrain units based on a visual interpretation of satellite images and field observations. Additionally, Globevnik et al. [14] and Milevski et al. [22] analysed applicability of the Gavrilović method in combination with a GIS technique. Their results demonstrated the decrease in predicted values for sediment production caused by erosion processes if calculated using parameters as a spatial variant, which is in contrast with the results obtained using the traditional/automatic method/catchment-oriented soil erosion map.
GIS is used in 66 % out of the total of fifty-one (51) analysed catchments. In other papers, the use of GIS is not clear or GIS is not used at all, and 42 % use a remote sensing technology for the land cover parameter determination.

4.2. Land use/cover change and erosion mitigation measures

Since their development, GIS technologies have enabled analysis of land use/cover maps in greater spatial detail, while remote sensing technologies have facilitated generation of new and varied data sources for the same parameter.
Solaimani et al. [24, 25] analysed the effect of applying the change in land use as an erosion mitigation and land management measure, and showed that the output of the model predicts an 89.24 % decrease in erosion sediment yield. Although the authors did not analyse the sensitivity of outputs obtained by the Gavrilović method, this paper is the first one that refers to a significant oscillation in the predicted erosion sediment quantities that depends on the change in the soil protection coefficient representing the land use component in the Gavrilović model.
Zorn and Komac [27, 28] noted in their research a 37 % decrease in predicted values for the annual volume of detached soil as a result of applying a different land use map (from the Ministry of Agriculture, Forestry and Food of the Republic of Slovenia) for the year 2000 compared to the one from the year before (1999-cadastral data).
In another application of the Gavrilović method in Iran [29], an attempt was made to define relations between the slope

Table 4. Overview of application of Gavrilović method

Literature	Analyzed basin	Country	Size [km^2]	Calculated output, W_a [m^3/km^2]	G_y [m^3/km^2]	Z **
[16,17]	Kardeh	Iran	555	266	N/A	
[14,18,19]	Rokava	Slovenia	91/20,4	50	N/A	
[14,20]	Jukani	Croatia	26,7	1070	399,47	
[14]	Raša	Croatia	205	1270	N/A	
[21]	Upper Sezar River	Iran	344,91	15299,84	15483,13	
[22,23]	Upper part of Bregalnica	Republic of Macedonia	1124,7	925	N/A	
[24,25]	Neka	Iran	N/a	144465,1; 15542,9	N/A	
[26]	Musone	Italy	374	700,5	N/A	
[26]	Esino	Italy	1223	621,4	N/A	
[27,28]	Upper Soča	Slovenia	591,5	8047-9670	N/A	
[15]	Greggio	Italy	6,1	640	465	
[12]	Republic of Srpska	Bosnia and Herzegovina	N/a	N/A	N/A	N/A
[29]	Jam and Riz	Iran	909,19	2327,4	N/A	
[10]	Ekbatan Dam	Iran	218	942,29	810,37	
[30]	Afzar	Iran	800	556	N/A	
[31]	Karoon	Iran	27694,8	8374,78	1507,4	
[32]	Plots in Serbia	Serbia	N/a	N/A	N/A	N/A
[33]	Amrovan	Iran	1023	5,1027	N/A	
[33]	Atary	Iran	6,27	7,171	N/A	
[33]	Ali Abad	Iran	1,29	5,401	N/A	
[33]	Ebrahim Abad	Iran	5,07	1,248	N/A	
[33]	Royan	Iran	5,39	7,296	N/A	
[34]	N/A	N/A	N/A	N/A	N/A	
[35,36]	Khiav chay	Iran	800	2237,49 (1968); 12252,44 (2007)	N/A	
[37]	Ramian	Iran	240	N/A	N/A	+
[38]	Vranjsko-banjska	Serbia	150	2936 (1956); 1050 (2007)	2123 (1956); 759,50 (2007)	
[39]	Kalimanska	Serbia	16,04	3775 (1927); 533,17 (2010)	2494,45 (1927); 350,7 (2010)	
[40]	Ghara-aghch	Iran	89,62	N/A	N/A	+
[41]	Kasilian	Iran	68	N/A	N/A	+
[42]	Imamzade Abdullah Baghmalak	Iran	105	370,08-3481,25	418,19	
[43]	Jelašnica	Serbia	30,04	910,82	397,12	
[44]	Prescudin	Italy	16	N/A	N/A	+
[45]	Manastirica	Serbia	29,93	813,8	425,6	
[46]	Kamišna	Serbia	26,94	741,4	375,9	
[46]	Rujevac	Serbia	0,89	259,2	60,36	
[46]	Vasovića	Serbia	2,52	502,6	125,67	
[48]	Rasina	Serbia	N/A	N/A	N/A	+
[49]	Ukrina	Bosnia and Herzegovina	1498,48	632,3 (1980); 551,3 (2010)	306,06 (1980); 247,47 (2010)	
[50]	Celje reservoir	Serbia	609,15	1189 (1960); 586 (2008)	540(1960); 266 (2008)	
[51]	Eastern Srbija	Serbia	17060,15	N/A	N/A	+
[52]	Abrami	Croatia	N/A	20-28	N/A	
[53]	Požarevac	Serbia	N/A	100-3000	N/A	
[54]	Rovacki	Montenegro	11,7	404,17	117,19	
[55]	Djuricka	Montenegro	69,5	1663,2	645	
[56]	Polimlje	Montenegro	2200	331,78	N/A	
[56]	Navotinski	Montenegro	8,4	123,79	37	
[57]	Boljanska	Montenegro	27,5	1072,15	315	
[58]	Dubračina	Croatia	43,5	250-682	-	
[5]	Bermejo	Chile	N/A	100*	N/A	
[5]	Pilcomayo	Chile	N/A	108*	N/A	
[59]	Tartano	Italy	47	965,34	1126,19	+
[60]	Dragonja	Slovenia	91	292,44 (1971); 119,30 (1994)	-	+

*In the following units: Mt/catchment/year, ** Only calculated method output derived from the analysis gradient and land use in order to reduce erosion in the Jam and Riz basins. The authors predicted an up to 58.3 % decrease in erosion for the entire catchment (from 2327.4 $m^3/km^2/year$ to 970.4 $m^3/km^2/year$) if adequate land-use management measures are implemented. In their research, they discovered that the areas used for irrigation farming are not situated in the most appropriate catchment zones. The results showing the decrease in sediment production derive from changing these areas to range lands and consequently decreasing the area used for irrigated farming.

The impact of four different biological activities (agro-foresting, tree plantation, seeding, and sowing) and 16 different vegetation management scenarios in the Ramian catchments in Iran is analysed by Sadoddin et al. [37]. One of the objectives was a cost-benefit analysis that demonstrated the economic and social impact upon soil erosion for a time period of 80 years.

Dragičević et al. [51] were the first to analyse uncertainties in the magnitude and spatial distribution of annual sediment production predictions in the Dubračina catchment, Croatia, where several alternative land cover/use inputs were applied. They used three different land cover/use data sets: a CORINE land cover map, a Spatial Plan, and a Landsat 8 scene, and demonstrated the Gavrilović method sensitivity to different land cover/use inputs.

Ristić et al. [39] analysed the effect of the change of hydrological conditions by restoring the catchment upon erosion and flood processes to define effective erosion mitigation and protection measures. They compared the outputs from the Kalimanska River catchment in Serbia for two time periods: 1967, before the restoration works, and 2010, after implementation of mitigation measures. The model showed a decrease in predicted volume of detached soil, and in erosion sediment transport via the river network.

In another paper, Ristić et al. [43] predicted a 44.1 % decrease in annual sediment production of eroded material if a specific combination of biotechnical, technical and administrative measures were to be implemented in the Jalešnica catchment in Serbia. During their research, they noticed that the land use is closely related to erosion processes, and that it is the key to erosion mitigation and protection. Although technical structures in the riverbed are often applied as the erosion and torrent flood mitigation measures, they are not highly effective if used as the only measure in the catchment. The same analysis was conducted for the Manastirica and Kamišna catchments in Serbia [45].

The 40-year change in erosion sediment production caused by the impact of anti-erosion measures applied at the Celije reservoir in Serbia was analysed by Milovanović et al. [50]. They concluded that the implemented anti-erosion works, which included technical, biotechnical and biological activities, lead to a 49 % decrease in erosion sediment production and transported sediment yields in 40 years.

Two other research activities showing results obtained by analysing the change in sediment production from past to present time were conducted at the Dragonja catchment (time change from 1971 to 1994) [14, 60] and the Botonega catchment (time change 1989 to 2000) [14]. Both studies revealed a decrease in erosion sediment production due to abandonment of agricultural lands, followed by vegetation change in these areas to bush and forest lands. These changes were simultaneously backed by implementation of erosion control measures such as weirs, dams, special vegetation protection, bank stabilisation, etc., all of which has contributed to a substantial decrease in annual erosion sediment production.

4.3. Other applications of Gavrilović method

Lakicevic and Srdjevic [48] analysed connection between social-economic conditions and erosion processes in small catchments in Serbia, while Tošić et al. [49] analysed anthropogenic effects (demographic changes) on erosion processes in form of changes in population over time. Both papers concluded that human emigration leading to abandonment of agricultural land leads to a decrease in the intensity of erosion processes and sediment production in that area.

Barmaki et al. [35, 36] registered a 41 % increase in drainage density from 1968 to 2007 due to rill erosion and an increase in agricultural practices caused by population increase in the Khiav Chay catchment, Iran.

Kazimierski et al. [5] analysed the impact of climate change parameters on the sediment yield production and, based on the Gavrilović method, they developed a methodology for estimating future sediment yield production for the Upper Plata Catchment in Chile, Bolivia. These authors generated projections for sediment yield production for the period until the year 2100 based on changes in temperature and precipitation, without considering potential changes in land cover/use. The significant difference between the observed and predicted erosion sediment yield values was associated with inaccurate interpretation of the observed data and deficiencies in the Regional Climate Models. Their analysis did not indicate either a significant change in annual sediment production over time, or a relatively small contribution of temperature in comparison to precipitation to the final sediment predictions.

Bemporad et al. [44] used the Gavrilović method for calculating annual and monthly sediment production. In these calculations, temperature and rainfall were the only time-varied (monthly) parameters. For estimating the erosion sediment transport, they used the hydrological water discharge model and the equation for sediment continuity and motion by Hrissanthou (not Gavrilović). The values (only annual) were verified through a one-time field observation after a flood in 1992 that filled the newly built retention dam.

4.4. Comparison of Gavrilović method with other erosion assessment methods

The results obtained using the Gavrilović method have been compared with the PSIAC, MPSIAC and RUSLE methods based on all papers available to the authors.

Tangestani [30] compared the Gavrilović and PSIAC model outputs and established that the PSIAC model is more reliable for determining the areas of very high erosion potential. A visual field overview with GPS confirmed a good estimation for areas of moderate and heavy erosion with the Gavrilović method, and a poorer accuracy for areas with slight erosion potential. Another comparison with the PSIAC method [16, 17] showed the same pattern for the predicted sediment yield by both methods, with a correlation coefficient of 0.95, which confirmed applicability of both methods for semi-arid and arid catchments. Ghobadi et al. [42] compared the Gavrilović method with PSIAC and MPSIAC and concluded that the Gavrilović method is not suitable for weather conditions in Iran, and that it provides much less accurate annual sediment production assessments compared to the MPSIAC method. In their assessments, they also used a simplified formula for the sediment delivery ratio.

Petraš et al. [52] compared results obtained using the RUSLE and Gavrilović methods with on-site observations and concluded that the RUSLE method is more compatible with the on-site data measurements for the Abrami test field.

In comparison with some other procedures, the Gavrilović method does not explore the physics of erosion processes and is therefore advantageous for areas where minimum data are available, or where there is a lack of previous erosion research. As such, the method can provide not only the amount of sediment production and sediment transport, but also the erosion intensity as a preliminary result, and indications or areas of potential erosion threats.

4.5. Field measurement and Gavrilović method verification

Out of all analysed catchments, verification of results is presented in papers for fifteen (15) catchments only (Table 5). In these papers, different verification methods are applied, depending on available equipment and accessibility of the terrain. Measurements of sediment yield on erosion plots were conducted at the Rokava (Dragonja) River basin in Slovenia [18, 19], Abrami [52] and Jukani (Butonega), Croatia [14, 20]. At the Bregalnica basin, Republic of Macedonia [19, 20], a very good correspondence was obtained between the results obtained using the Gavrilović method and on-site measurements. Haghizadeh et al. [21] and Tangestani [30] used a comparison of model output results with field observations and a GLASGOD (Global Assessment of Soil Degradation) map as a verification method.

Bagherzadeh et al. [16, 17] verified model outputs by a field survey using GPS and a visual comparison of areas characterised as areas with moderate and heavy annual sediment yields.

Amini et al. [10] applied the Gavrilović method to the Ekbatan Dam drainage basin in Iran and concluded that sediment yield can be overestimated by this method because it lacks the grain size distribution structure, humus concentration, slope morphology, and runoff parameters that affect erosion processes, all of which are usually included in physical models, which is not the case for empirical models such as Gavrilović.

Kouhpeima et al. [33] analysed five different catchments in Iran and used comparison results to measure sediment deposits in the reservoir as a verification method. The same method was also used in the Prescudin catchment, Italy, [44] and it showed minimum deviation between predicted and measured sediment yield values. Nuclear probes for suspended-load measurements were used at the Esino and Musone river basin in Italy [26]. The measurements exhibited some deviations in comparison with the overall sediment yield production estimated with the Gavrilović method but, overall, a good order-of-magnitude correspondence was obtained concerning yearly sediment yield. It was concluded that further measurements are necessary because the Gavrilović model considers total sediment load, whereas the measurements conducted take into account suspended load only. Other verification methods include the use of a PDA device and on-site observations [49], and certain verification methods remain unspecified in papers [41, 42] but provide poor overall ratings for the Gavrilović method, which is said to overestimate sediment yield [41].

Table 5. Analysed catchments categorised by size

Catchment categorisation by size [63]		No. of analysed catchments	No. of catchments with verification of results
Unclasified	< 10 km^2	8	0
Small	10 – 100 km^2	14	4
Mid-size	>100 – 1000 km^2	13	5
Large	>1000 – 10 000 km^2	5	3
Very large	> 10 000 km^2	2	0
Unknown size		9	3
	Summarised	51	15

5. Discussion and conclusion

A detailed review of practical application of the Gavrilović method is presented in the paper. The most commonly calculated results using the model are the total annual volume of soil and the erosion coefficient. The actual sediment yield is calculated for no more than 38 % of analysed catchments. Although several modifications of the model have been used over the years, different variations of the model continue to be applied. These variations concern assessment of actual sediment yield involved in transportation. The analyses exhibit better results and correspondence with on-site measurements when a modified formula is used for the sediment delivery ratio. A modified sediment delivery ratio uses drainage density as a ratio between the primary and secondary river length and the catchment area. If the simplified (original) formula is used and the ratio is replaced with a constant, the values obtained using the model can exceed the predicted values for the total annual volume of soil or the overall yearly amount of detached soil. Therefore, the authors conclude that the use of the formula for drainage density is recommended for all future analyses as a means to avoid incorrect results indicating larger values for the actual sediment yield compared to those of the total annual volume of soil. However, none of the analysed papers includes an explanation as to why a given formula, original or modified, is preferred to any other. Additionally, these papers do not provide a comparison that could be used to roughly estimate the error/difference between the calculated and measured values if both formulas are used.

The evolution of the Gavrilović model began with the development of GIS technologies. However, this method has not as yet fully benefited from all possibilities offered by GIS. For example, the actual sediment yield or sediment involved in transportation is calculated within the method for the entire catchment/sub-catchment and refers to the value representing sediment transport, measured at the tow of the catchment. Today, GIS technologies enable assessment of each cell within the catchment and, as such, they can provide an estimation of the material transported in each cell representing the river. This approach can to some extent simplify the process of choosing the best location for field measurements in less accessible catchments, and provide multiple options as adequate positions for field measurements. Thus, the verification of the method in terms of the assessed parameter for actual sediment yield can also be simplified and conducted on any part/length of the river, which can potentially lead to more frequent calculations of this parameter. To achieve this, the analysis must be narrowed down from the catchment and sub-catchment assessment to the cell resolution, and later gradually broadened to the catchment size. Unfortunately, this procedure will continue to depend upon resolution of the available input data.

Lazarević, Globevnik, Fanetti and Vezzoli significantly improved the method using changes in the assessment of descriptive parameters within the model. It is important to note that certain catchment areas are currently affected by substantial changes in type, extent and density of vegetation cover and by expansion of urban areas. Therefore, if this is considered, the land use/cover parameter can be considered as an extremely important parameter that will affect the final estimated values, as shown in a number of previously mentioned papers [24, 25, 27, 28, 29, 58, 60]. The changes in land use will not only affect the changes in the soil protection coefficient but subsequently the coefficient of type and extent of erosion, whose contribution to Gavrilović method and sediment production should not be neglected.

For such areas with intensive urban changes, the parameter for urban areas (Table 6) is recommended in future analyses. It is often forgotten in erosion analysis that agricultural areas and areas with low or no vegetation cover are not the only source of eroded material in a catchment. Therefore, all catchments are unique and complex in their own way, and additional sources of erosion material should be considered, such as construction areas in expanding urban regions. These areas, although short lived, have a substantial impact on the yearly amount of erosion sediment production and should be considered when planning future activities in the catchment. Another source of erosion material that is rarely considered are residential areas with small green plots used mainly for agriculture. In larger towns, such areas are not considered to be significant; however, in towns and villages where such residential areas are often represented, this can be considered a problem and an additional source of erosion material that is often forgotten and simply classified as urban/rural area. Therefore, a new categorisation for the soil protection coefficient for urban/rural areas, including undeveloped areas designated for urban development in the near future, is suggested in Table 6. Such a categorisation would change the model output information concerning erosion intensity and the total amount of erosion material.

Table 6. Proposed assessment of soil protection coefficient for urban areas X_a

Descriptive evaluation	Numerical evaluation X_a
Dense urban areas with no or little green areas	0,05
Scattered urban/rural residential areas with green plots used mainly for agriculture	0,3
Scattered urban/rural residential areas with green plots used mainly for agriculture using agronomic, soil management or mechanical anti-erosion measures	0,1
Construction areas	0,9

Land use/cover parameters greatly influence final results of the model, and lead to predictions of decreased erosion production if appropriate land use management is applied. Dragičević et al. [58] highlighted the problem through generation of different results by simply using a different land use/cover input source. It can therefore be concluded that reliability of final results is strongly correlated with the data source, experience of the expert in charge of map production, and the accuracy and level of detail of input data. The expert conducting erosion analysis should also consider different data sets/maps available for the same parameter, compare their differences and, based on field surveys and local population information exchange, choose the best option for future analysis, as shown in [27, 28, 58]. In the future, it could be interesting to analyse the interconnection between the Gavrilović model outputs from small catchments and its geology, which would lead to possible further modifications of the model.

It should be noted that the verification aspect of the analysis is omitted in most of the analysed papers, which leads to a shortage of information concerning the adaptability and applicability of the Gavrilović method to different areas varying primarily in terms of geology and hydrology. The lack of these data has also hindered possible extensions of the method because these data have yet to be provided. Additionally, it is noted in several papers that a strong correlation exists between the knowledge and experience of the erosion expert and the deviation of predicted and measured sediment yield. Not one of the papers containing verification actually addresses sensitivity of the model and the uncertainty of overall results regarding the source of input data. The verification of the models should be conducted with greater frequency so as to obtain a better correspondence between on-site measured values for sediment production and those obtained with the model.

Acknowledgements

The research for development and publication of this paper was co-financed through grants awarded by the University of Rijeka (Grant No. 13.05.1.3.08., entitled: Development of New Methodologies in Water and Soil Management in Karstic, Sensitive and Protected Areas, and Grant No. 13.05.1.03. entitled: "Water Resources Hydrology and Floods and Mud Flow Risks Identification in the Karstic Area"). A part of the research related to this paper was conducted in the scope of the bilateral Croatian-Japanese project "Risk Identification and Land Use Planning for Disaster Mitigation of Landslides and Floods in Croatia" and research project "Hydrology of Sensitive Water Resources in Karst" (114-0982709-2549) co-financed by the Ministry of Science, Education and Sport of the Republic of Croatia.

REFERENCES

[1] EC (European Commision), 2004 EC (European Commision), Proposal for Directive of the European Parliament and of the Council Establishing a Framework for the Protection of Soil and Amending Directive 2004/35/EC, COM(2006) 232 final.

[2] Morgan, R.P.C.: Soil Erosion & Conservation. Blackwell, Oxford, 2005.

[3] Vanmaercke, M., Zenebe, A., Poesen, J., Nyssen, J., Verstraeten, G., Deckers, J.: Sediment dynamics and the role of flash floods in sediment export from medium-sized catchments: a case study from the semi-arid tropical highlands in northern Ethiopia. Journal of Soil Sediments, 10 (2010), pp. 611-627, http://dx.doi.org/10.1007/s11368-010-0203-9

[4] Poesen, J., Hooke, J.M.: Erosion, flooding and channel management in Mediterranean environments of southern Europe. Progress in Physical Geography, 21 (1997), pp. 157-199, http://dx.doi.org/10.1177/030913339702100201

[5] Kayimierski, L.D., Irigoyen, M., Re, M., Menendey, A.N., Spalletti, P., Brea, J.D.: Impact of climate change on sediment yield from the upper Plata basin. International Journal of River Basin Management, 11 (2013) 4, pp. 1-11, http://dx.doi.org/10.1080/15715124.2013.828066

[6] Dragičević, N., Karleuša, B., Ožanić, N.: GIS based monitoring database for Dubračina river catchment area as a tool for mitigation and prevention of flash flood and erosion. In: Proceedings of the thirteenth International Symposium on Water Management and Hydraulic Engineering, Bratislava, Sovakia, pp. 553-565, 2013.

[7] De Vente, J., Poesen, J.: Predicting soil erosion and sediment yield at the basin scale: scale issues and semi-quantitative models. Earth-Science Reviews ,71 (2005) 1-2, pp. 95-125, http://dx.doi.org/10.1002/esp.1305

[8] Eisazadeh, L., Sokouti, R., Homaee, M., Pazira, E.: Comparison of empirical models to estimate soil erosion and sediment yield in micro catchments. Eurasian Journal of Soil Science, 1 (2012), pp. 28-33.

[9] Gavrilović, S.: Inženjering o bujičnim tokovima i eroziji. Izgradnja, special issue, pp 1-292, 1972.

[10] Amini, S., Rafiei, B., Khodabakhsh, S., Heydari, M.: Estimation of erosion and sediment yield of Ekbatan Dam drainage basin with EPM, using GIS. Iranian Journal of Earth Sciences, 2 (2010), pp. 173-180.

[11] Gavrilovic, Z., Stefanovic, M., Milovanovic, I., Cotric, .J., Milojevic, M.: Torrent classification - base of rational management of erosive regions. In: IOP Conference Series: Earth and Environmental Science 4 (1), pp. 1-8, 2008.

[12] Tosic, R., Dragicevic, S.: Methodology update for determination of the erosion coefficient. Glasnik Srpskog Geografskog Društva, 92 (2012) 1, pp. 11-26.

[13] Lazarević, R.: Novi postupak za određivanje koeficijenta erozije (Z). EROZIJA – stručno-informativni bilten, 13 (1985), pp. 53-61.

[14] Globevnik, L., Holjevic, D., Petkovsek, G., Rubinic, J.: Applicability of the Gavrilovic method in erosion calculation using spatial data manipulation techniques, erosion prediction in Ungauged Basins: integrating methods and techniques. In: Proceedings of Symposium HS01, Sapporo, 279 (2003), pp. 224-233.

[15] Fanetti, D., Vezzoli, L.: Sediment input and evolution of lacustrine deltas: the Breggia and Greggio rivers case study (lake Como, Italy). Quaternary International, 173–174 (2007), pp. 113-124, http://dx.doi.org/10.1016/j.quaint.2007.02.008

[16] Bagherzadeh, A., Daneshvae, M.R.M.: Sediment yield assessment by EPM and PSIAC models using GIS data in semi-arid region. Frontiers of Earth Science, 5 (2011) 2, pp. 207-216, http://dx.doi.org/10.1007/s11707-011-0168-z

[17] Bagherzadeh, A., Daneshvae, M.R.M.: Estimating and mapping sediment production at Kardeh Watershed by using GIS. In: The 1st International Applied Geological Congress. Mashad Branch, Iran, pp 1440-1446, 2010.

[18] Zorn, M., Komac, B.: The importance of measuring erosion processes on the example of Slovenia. Hrvatski Geografski Glasnik, 73 (2011) 2, pp. 19-34.

[19] Petkovšek, G.: Kvantifikacija in Modeliranje Erozije Tal z aplikacijo na Povodju Dragonje. Dissertation, University of Ljubljana, Slovenia, 2002.

[20] Petraš, J., Holjević, D., Plišić, I.: Possibilities to Estimate Soil Erosion Intensity and Sediment Transport by GIS Technology Application. In: Proceedings of conference of the 1st International Yellow River Forum on River Basin Management. Zhengzhou, China, 2, pp. 421-431, 2003.

[21] Haghizadeh, A., Teang Shui, L., Godarzi, E.: Forecasting sediment with erosion potential method with emphasis on Land use changes at basin, electronic. Journal of Geotechnical Engineering, 14 (2009), pp. 1-12.

[22] Milevski, I., Blinkov, I., Trendafilov, A.: Soil erosion processes and modelling in the upper Bregalnica catchment. In: Proceedings of the conference of the Danubial countries on the hydrological forecasting and hydrological bases of water management (XXIV). Bled, Slovenia, pp 1-10, 2008.

[23] Blinkov, I., Bojcovski, B., Trendafilov, B., Trendafilov, A., Mincev, I.: Effects of forest fires on erosion processes. In: Proceedings of First Serbian Forestry Congress – Future with Forests. Belgrade, Serbia, pp 902-915, 2010.

[24] Solaimani, K., Modallaldoust, S., Lotfi, S.: Investigation of land use changes on soil erosion process using geographical information system. International Journal of Environmental Science and Technology, 6 (2009) 3, pp. 415-424.

[25] Solaimani, K., Modallaldoust, S., Lotfi, S.: Soil erosion prediction based on land use changes (A case in Neka wathershed). American Journal of Agricultural and Biological Sciences, 4 (2009) 2, pp. 97-104.

[26] Tazioli, A.: Evaluation of erosion in equipped basins: preliminary results of a comparison between the Gavrilovic model and direct measurements of sediment transport. Environmental Geology, 56 (2009) 5, pp. 825-831, http://dx.doi.org/10.1007/s00254-007-1183-y

[27] Zorn, M., Komac, B.: Response of soil erosion to land use change with particular reference to the last 200 years (Julian Alps, Western Slovenia. Revista de Geomorfologie, 11 (2009), pp. 39-47.

[28] Zorn, M., Komac, B., Gabrovec, M.: Influence of land use changes on erosion in the Slovenian Alps. In: Proceedings of the IGU-LUCC Central Europe Conference, Man in the Landscape Across Frontiers, pp. 221-234, 2007.

[29] Soliamani, K.S., Modallaldoust, S.M.: The effect of land suitability to reduce erosion risks, using GIS (case study, Boushehr Province, Iran). Journal of Applied Sciences, 8 (2008) 8, pp. 1495-1502.

[30] Tangestani, M.H.: Comparison of EPM and PSIAC models in GIS for erosion and sediment yield assessment in a semi-arid environment: Afzar catchment, Fars Province, Iran. Journal of Asian Earth Sciences, 27 (5), pp. 585-597, http://dx.doi.org/10.1016/j.jseaes.2005.06.002

[31] Deilami, B.R., Sheikhi, M.L.A., Al-Saffar, M.R.A., Barati, V.: Estimation of erosion and sedimentation in Karoon Basin using EPM with in geographic information system. Engineering science and technology: An International Journal, 2 (2012) 5, pp. 2250-3498.

[32] Gavrilovic, Z., Milojevic, M., Jurisic, S.: Rain generators – important equipment in the field of erosion science. In: Proceeding of 1st Serbian Forestry Congress: Future with Forests, pp. 916–929, 2013.

[33] Kouhpeima, A., Hashemi, S.A.A., Feiznia, S. A study on the efficiency of erosion potential model (EPM) using reservoir sediments. Elixir Pollution, 38 (2011), pp. 4135–4139.

[34] Ghazavi, R., Vali, A., Maghami, Y., Abdi, J., Sharafi, S.: Comparison of EPM, MPSIAC and PESIAC models for estimating sediment and erosion by using GIS (case study: Ghaleh – Ghaph Catchment, Golestan Province). Geography and Development, 10 (2012) 27, pp. 30-32.

[35] Barmaki, M., Pazira, E., Hedayat, N.: Investigation of relationships among the environmental factors and water erosion changes using EPM model and GIS. International Research Journal of Applied and Basic Sciences, 3 (2012) 5, pp. 945-949.

[36] Barmaki, M., Pazira, E., Esmali, A.: Relationships among environmental factors influencing soil erosion using GIS. Eurasian Journal of Soil Science, 1 (2012), pp. 40-44.

[37] Sadoddin, A., Sheikh, V., Mostafazade, R., Halili, M.G.: Multiple-criteria decision making for integrated watershed management in the Ramian watershed Golestan, Iran. In: Proceedings of International Congress on Environmental Modelling and Software Integrating Sciences and Information Technology for Environmental Assessment and Decision Making, 4th Biennial Meeting of iEMSs, pp. 662-669, 2008.

[38] Konstadinov, S., Zlatic, M., Dragovic, N., Todosijevic, M.: Unknown soil erosion and the possibility of its control in the watershed of the water reservoir "Prvonek". In: Proceedings of the 15th International Congress of ISCO 18-23, http://tucson.ars.ag.gov/isco/isco15/GL.html. Accessed 10 June 2015, 2008.

[39] Ristic, R., Konstadinov, S., Radic, B., Trivan, G., Nikic, Z.: Torrential floods in Serbia – man made and natural hazards. In: Conference Proceedings of 12th Congress INTERPRAEVENT, pp. 771-779, 2012.

[40] Amiri, F., Shariff, A.R.B.M., Tabatabaie, T.: Monitoring land suitability for mixed livestock grazing using Geographic Information System (GIS), Application of Geographic Information Systems, InTech, pp. 241-266, 2012, http://dx.doi.org/10.5772/47939

[41] Abadi, L.Z., Ahmadi, H.: Comparison of EPM and geomorphology methods for erosion and sediment yield assessment in Kasilian Watershed, Mazandaran Province, Iran. DESERT, 16 (2011), pp. 103-109.

[42] Ghobadi, Y., Pirasteh, S., Pradhan, B., Ahmad, N.B., Shafri, H.Z.B.M., Sayyad, Gh.A., Kabiri, K.: Determine of correlation coefficient between EPM and MPSIAC models and generation of erosion maps by GIS techniques in Baghmalek watershed, Khuzestan, Iran. In: Proceedings of the 5th Symposium on Advances in Science and Technology SAStech, Mashhad, Iran. pp 1-12, 2011.

[43] Ristic, R., Radic, B., Vasiljevic, N., Nikic, Z.: Land use change for flood protection- a prospective study for the restoration of the river Jelasnica watershed. Bulletin of the Faculty of Forestry, Serbia, 103 (2011), pp. 115-130.

[44] Bemporad, G.A., Alterach, J., Amighetti, F.F., Peviani, M., Saccardo, I.: A distributed approach for sediment yield evaluation in Alpine regions. Journal of Hydrology, 197 (1997) 1–4, pp. 370-392, http://dx.doi.org/10.5772/47939

[45] Ristic, R., Radic, B., Nikic, Z., Trivan, G., Vasiljević, N., Dragićević, S., Živković, N., Radosavljević, Z.: Erosion control and protection from torrential floods in Serbia-spatial aspets. Spatium International Review, 25 (2011) pp. 1-6, http://dx.doi.org/10.2298/SPAT1125001R

[46] Sekularac, G., Djuric, M., Stojiljkovic, D., Milic, V., Kulina, M., Jaksic, T.: Soil erosion of Rujevac small basin (west Serbia) In: Proceedings of the Third International scientific Symposium "Agroszm Jahorina 2012", Jahorina, Bosina and Herzegovina, pp. 441-444, 2012.

[47] Sekularac, G., Stojiljkovic, D., Jelic, M.: Combined effect of soil erosion agents within a small catchment. In: Proceedings of 46th Croatian and 6th International Szmposium on Agriculture, Opatia, Croatia, pp. 161-164, 2011.

[48] Lakicevic, M., Srdjevic, B.: Soil erosion in hilly-mountainous region of south Serbia. In: Proceedings of COST FO0603: Modelling Forest Ecoszstems concepts, Data and Application, Vienna, pp. 75-78, 2011.

[49] Tosic, R., Dragicevic, S., Zlatic, M., Todosijevic, M., Kostadinov, S.: The impact of socio-demographic changes on land use and soil erosion (case study: Ukrina River catchment). Geographical Reviews, 46 (2012), pp. 69-78.

[50] Milovanovic, I., Cotric, J., Stefanovic, M.: Analysis of the impact of applied antierosion works on reducing siltation in the reservoir "Celije". Forum Geografic S.C.G.P.M., pp. 849-855., 2011.

[51] Dragicevic, S., Novkovic, I., Carevic, I., Zivkovic, N.: Geohazard assessment in the Eastern Serbia. Forum Geografic, 10 (2011) 1, pp. 10-19.

[52] Petraš, J., Holjević, D., Patrčević, V.: Mjerenje produkcije erozijskog nanosa na istraživačkom poligonu "Abrami" u Istri. In: Book of Proceeding of Hidrološka mjerenja i obrada podataka, Croatia, pp. 191-206, 2008.

[53] Gavrilović, Z., Stefanović, M., Brajković, M., Isaković, D.: Identifikacija erozionih područja. Upravljanje vodnim resursima Srbije, 1 (2001), pp. 191-208.

[54] Spalevic, V., Mahoney, W., Djurovic, N., Üzen, N., Curovic, M.: Calculation of soil erosion intensity and maximum outflow from the Rovacki River Basin, Montenegro, Podgorica. Agriculture & Forestry, 58 (2012) 3, pp. 7-21.

[55] Spalevic, V., Djurovic, N., Mijovic, S., Vukelic-Sutoska, M., Curovic, M.: Soil erosion intensity and runoff on the Djuricka River Basin (north of Montenegro). Malaysian Journal of Soil Science, 17 (2013), pp. 49-68.

[56] Spalevic, V., Šimunić, I., Vukelić-Šutoska, M., Üzen, N, Čurović, M.: Prediction of the soil erosion intensity from the River Basin Navotinski, Polimlje (northeast Montenegro). Agriculture & Forestry, 59 (2013) 2, pp. 9-20.

[57] Spalević, V., Nyssen, J., Curovic, M., Lenaerts, T., Kerckhof, A., Annys, K., Van Den Branden, J., Frankl, A.: The impact of land use on soil erosion in the River Basin Boljanska Rijeka in Montenegro. In: Proceedings of the IV International Symposium Agrosym 2013, pp. 54-63., 2013.

[58] Dragičević, N., Whyatt, D., Davies, G., Karleuša, B., Ožanić, N.: Erosion model sensitivity to Land cover inputs: case study of the Dubračina catchment, Croatia. In: Proceedings of the GIS Research UK 22nd Annual Conference GISRUK 2014, Glasgow. pp 340 -348, 2014.

[59] Ballio, F., Brambilla, D., Giorgetti, E., Longoni, L., Papini, M., Radice, A.: Evaluation of sediment yield from valley slopes: a case study. In:Proceedings of the conference of the Monitoring, Simulation, Prevention and Remediation of Dense and Debris Flows III, Milano, Italy, 67 (2010), pp. 149-160.

[60] Globevnik, L., Sovinc, A., Fazarinc, R.: Land degradation and environmental changes in the Slovenian submediterranean (The Dragonja River Catchment). Geoökodynamik XIX (1998), pp. 281-291.

[61] Thieken, A.H., Lücke, A., Diekkrüger, B., Richter, O.: Scaling input data by GIS for hydrological modelling. Hydrological Processes, 13 (1999) 4, pp. 611-630, http://dx.doi.org/10.1002/(SICI)1099-1085(199903)13:4<611::AID-HYP758>3.0.CO;2-6

[62] Vogt, J.V., Colombo, R., Bertolo, F.: Deriving drainage networks and catchment boundaries: a new methodology combining digital elevation data and environmental characteristics. Geomorphology, 53 (2003) 3-4, pp. 281-298, http://dx.doi.org/10.1016/S0169-555X(02)00319-7

[63] EC (European Commision), 2000 EC (European Commision), Directive of the European Parliament and of the Council of 23 October 2000 establishing a framework for Community action in the field of water policy 2000/60/EC.

DOI: 10.14256/JCE.1689.2016
Građevinar 9/2016

Primljen / Received: 8.6.2016.
Ispravljen / Corrected: 15.9.2016.
Prihvaćen / Accepted: 21.9.2016.
Dostupno online / Available online: 10.10.2016.

Management and strategic efficiency of construction companies

Authors:

Dr.sc. **Mladen Bandić**, dipl.ing.građ.
Tehničko veleučilište Zagreb
mbandic1@tvz.hr

Dr.sc. **Mirko Orešković**, dipl.ing.građ.
Investinženjering GI grupa
mirko.oreskovic@gin.hr

Professional paper

Mladen Bandić, Mirko Orešković

Management and strategic efficiency of construction companies

Over the past two decades, Croatian construction companies have been undergoing intensive dynamic changes caused by political and economic influences on the construction market: privatisation of state-owned companies, opening of Croatian market, vigorous post-war reconstruction activities, intensive construction of motorways, etc. Such turbulent changes have influenced construction companies in a variety of ways. A number of Croatian companies that used to be dominant have disappeared from the market. Some companies have transformed their management and construction processes. The Balanced Scorecard model for shaping and implementing business strategies of construction companies is presented in the paper.

Ključne riječi:
strategy of construction company, balanced scorecard, success indicators, strategic initiative

Stručni rad

Mladen Bandić, Mirko Orešković

Menadžment i učinkovitost strategije graditeljske tvrtke

Hrvatske graditeljske tvrtke zadnjih 20-ak godina prolaze kroz intenzivne dinamične promjene uvjetovane političkim i ekonomskim utjecajima na graditeljskome tržištu kao što su proces privatizacije državnih tvrtki, otvaranje hrvatskog tržišta, intenzivna obnova u ratu porušenih objekata ili intenzivna izgradnja autocesta. Takve turbulentne promjene utjecale su na graditeljske tvrtke na različite načine. Neke, prije Domovinskog velike hrvatske tvrtke nestale su s tržišta, a neke su transformirale menadžment i provedbu procesa građenja. U radu je prikazan Balanced Scorecard, model pristupa oblikovanju i provedbi poslovne strategije graditeljske tvrtke.

Ključne riječi:
strategija graditeljske tvrtke, Balanced Scorecard, mjerila uspjeha, strateška inicijativa

Fachbericht

Mladen Bandić, Mirko Orešković

Management und Effizienz bei Strategien für Bauunternehmen

Kroatische Bauunternehmen durchgehen in den letzten 20 Jahren intensive dynamische Veränderungen, die auf politische und ökonomische Einflüsse im Bauwesen zurückzuführen sind, wie z.B. den Prozess der Privatisierung staatlicher Unternehmen, die Öffnung des kroatischen Marktes, die Wiederherstellung im Krieg zerstörter Objekte oder den intensiven Ausbau von Autobahnen. Diese turbulenten Veränderungen haben Bauunternehmen auf verschiedene Weise beeinflusst. Einige große kroatische Unternehmen sind vom Markt verschwunden, einige haben sich dem Management und der Bauausführung zugewandt. In dieser Arbeit wird die Balanced Scorecard als Modell zur Entwicklung und Umsetzung von Geschäftsstrategien für Bauunternehmen dargestellt.

Ključne riječi:
Strategien für Bauunternehmen, Balanced Scorecard, Erfolgsmassstäbe, Strategieinitiative

1. Introduction

After the turbulent and sometimes painful period of transition from the 1990s to the present day, Croatian construction companies have been trying to find a way to adjust to intensive changes in their business environments, and have in the process adopted various new strategic management methods and procedures. Some construction companies have successfully transformed into modern construction companies highly competitive on construction market in the country and abroad. These companies have learned and applied, sometimes intuitively, modern business management methods and business strategies.

The aim of the paper is to present areas of strategic management of construction companies, as a basis for further systemic study in this field, in accordance with the needs for developing management practices currently applied in construction industry. An approach to the change of business strategies in construction companies, to the way of setting development objectives, and to the role and significance of design management in construction companies, is presented.

The BSC (balanced scorecard) model is presented in the paper [1]. The BSC model is a balanced scorecard or an indicator of success of a business strategy. The indicator of success is used for measuring the effects and results of strategic initiatives, as well as the results obtained by implementing an overall strategy of a company. The BSC model serves as a communication tool, a system for measuring success of strategic initiatives, and a system for strategic management of companies. The company strategy is observed through four distinct points of view, i.e. through four strategic perspectives of companies. Strategic perspectives of companies:

- financial perspective,
- investors / clients,
- internal processes, and
- development of employee knowledge.

Presentation of company strategy, as viewed from four above-mentioned strategic perspectives, to all participants in the company provides a clear image of the strategy, and thus enables its implementation and success. In addition to the Balanced Scorecard model, the following strategic tools are also presented:

- **PEST** (influence of Political, Economic, Societal and Technological environment),
- **Five competitive forces:** 1. Barriers to entry – at the access of competing companies to a new market, 2. Threat of substitution, 3. Buyer power, 4. Supplier power, and 5. Competitive rivalry – threat posed by existing competition.
- **SWOT** analyses capacity of companies S (strength), W (weaknesses), O (opportunities), and T (threats).

2. Strategy of construction companies

"The essence of formulating strategy is relating a company to its environment" [2]. The company environment is dominated by investors, buyers, suppliers, competing companies, political and administrative bodies, and many other factors of significance to company profit.

Various authors have formulated their distinct definitions of business strategy.

Porter [2] defines the strategy as "integrated set of strategic initiatives that ensure the company's superior and long-term competitive position in the marketplace".

Leagaard et al. [3] define the strategy as "a logical set of activities, goals, means, and scenarios for implementation and achievement of results". It is further stated that "a construction company competes with its "competitors" and that the company survival depends on the capacity of its management to adjust and create management options in accordance with external influences and conditions. The area of business competition covers regional, national, and international segments of the market and, at the operational level, the strongest weapon resides in the capabilities of employees and in financial basis, and also in the capacity to cooperate at all company levels".

In the paper entitled "Implementation management models in construction companies" [4], the authors present the Balanced Scorecard model or BSC and the Excellence Model EFQM, and their use in construction companies in the country and worldwide. The BSC model is presented from the standpoint of estimating implementation of company strategy, while the EFQM is presented from the perspective of estimating success of overall operation of construction companies. The paper also provides an overview of application of these models in Croatia, with guidelines for implementation.

In conclusions of the paper "it is presented that only a small number of construction companies in Croatia uses modern implementation management models (33 %), which greatly differs from international practice (77.4 %)... and further on "Construction companies should start introducing modern implementation management systems so that they can adjust as much as possible to the increasingly present acceleration and tension in the marketplace. In this way they could compare their results with those of the competition and hence adjust their strategic goals toward realisation of an overall success of their business activities".

The strategic analysis of the Croatian construction industry at the economic branch (sector) level is presented in the paper "Strategic Analysis of Croatian Construction Industry" [5]. The analysis was conducted using the PEST model and the Porter's five competitive forces.

In the period from 2008 to 2014, participation of Croatian construction industry in national GDP fell from 7.3 % in 2008 to 4.1 % in 2014. Statistical indicators and influences by PEST model categories, and influence factors of Porter's five competitive forces, are presented.

The long-lasting crisis and reduced activity in Croatian construction industry requires companies to adopt new procedures and planning strategies that will ensure their survival and development.

Definition of the terms "building" and "construction" [7]:
The **building project** is a part of investment project (enterprise), a part of economic program (complex or aggregated project), through which realisation of material, spatial and manufacturing conditions are planned for the one-time or continuous realisation of an objective (or objectives) of an investment project over a project lifetime.
The result of a building project is a (new or modified) structure having the following characteristics:
- one-time realisation
- defined location
- long life span
- numerous participants from various professions (architects, builders, survey engineers, building-installations experts, etc.)
- realisation based on order – contract

The role of construction project, being one of significant subprojects within a building project, is to materialise "in-situ" previous phases of the building project, during which phases the future significant consumption of material resources is planned.
The **construction project** (the investor's construction project) is the undertaking by which the investor's expectations are to be realised through realisation of construction works on a structure that has to meet requirements and expectations of the investor, while taking into account legislative and material limitations of the location.
The realisation project (the contractor's construction project) is the contractor's project by which the latter tries to convince the investor - by planning the realisation of works within the required, accepted or offered time, and by calculating the expected cost of specified works - that the best offer for the investor is the one presenting optimum conditions for the investor and, during realisation of works, attempts are made to realise the maximum of contractor's expectations through the use of appropriate technological procedures involving an optimum use of the contractor-owned technological and material resources.

The purpose and aim of this paper is to assist national business entities to adopt modern methods for creating company strategies, and it can also inspire further research in the development and implementation of strategies to be used by domestic companies.
The authors' interest is concentrated on construction projects, with an unambiguous relationship toward such projects. To facilitate understanding of the authors' position, the definitions of a building project and construction project are presented as follows.
The **PEST** is used for the analysis and estimation of the influences exerted by Political, Economic, Societal and Technological environment. The PEST analysis results point to the type and intensity of negative and positive influences the environment exerts on company operations, and they represent the basis for initiating strategic initiatives aimed at achieving better company position on the marketplace.

"Five competitive forces", the Porter's model of analysing influences starts from the analysis of:
1. Barriers to entry – at the entry of competitive companies to a new market,
2. Threat of substitution
3. Buyer's negotiating power
4. Supplier's negotiating power, and
5. Competitive rivalry – threat posed by existing competition.

The result of this analysis points to the short-term and long-term business potential of a company.

The **SWOT** analyses the company's strength S, weaknesses W, opportunities O, and threats T.
The SWOT analysis is carried out by iterative processing of influences exerted on the company by external environment on the one side, and capabilities of the company's internal functions on the other.
The company's weaknesses are recognised in the parts of the company that perform their activities with substandard efficiency. The efficiency of these parts of the company must be improved. Opportunities are trends, influences, events and ideas that the company, or a part of the company, can make use of on the marketplace. Threats are possible events or influences beyond the control of the company, for which plans for elimination of unfavourable influences are made.
The analysis of Threats and Opportunities is conducted by analysis of the company's business environment and, at that, the following elements are analysed: positions and possible business moves of the investors and buyers, price limitations, occurrence of new technologies, market uncertainties, legislation, etc. The company's Strength and Weaknesses are determined by internal analysis of the company and, at that, with the focus on: company's productivity, internal cost structure, products and services, technical equipment, employee competencies, business culture of the company, etc.
The analysis of external and internal influences is significant for creating a realistic image of the company's business environment and for projecting future operations of the company.
Croatian construction companies are exposed to strong pressures of the competition on the open market environment. The company competitive edge can be increased by developing the company in accordance with the international market requirements.

2.1. Balanced scorecard (BSC)

Based on the use of four strategic perspectives, the Balanced Scorecard (BSC) is a tool for presenting the company strategy, the system for measuring implementation of the strategy, and the basis of the strategic management system.

Table 1. Balanced scorecard perspectives

Perspective	Strategic initiative	Objectives	Criteria/ implementation indicators	Implementation
Financial	A B C	1, 2, 3 4 5, 6	α, β, χ δ, ε ϕ	
Investors/clients	D E	7 8, 9, 10	η λ	
Internal processes	F G H	11, 12 13 14, 15	μ π	
Learning and employee development	I	16	σ	

A, B, C, .. - strategic initiatives; 1, 2, 3........n - objectives of strategic initiatives;
α, β, γ....... - indicators of implementation of a strategic initiative

The presentation of company strategies in four perspectives was developed by Kaplan and Norton in 1980s, after extensive research of strategies used by American companies which mostly shaped and monitored effects based on financial indicators. In addition to financial perspective, Kaplan and Norton also proposed non-financial perspectives: investors/clients, internal processes and development of employee knowledge [1]. They established that company assets are increasingly becoming non-material: knowledge, information, organisation, management, project management in particular. Strategic initiatives are strategic development projects selected by strategic company management, which is accompanied by continuous measurement of success gained in project implementation.

Strategic initiatives are determined by objectives, several of which can be defined for each strategic initiative. The implementation of each initiative is measured using appropriate criteria or success indicators.

The implementation of strategic initiatives is the result of multiproject management, which is conducted using appropriate project management tools in all phases of the project.

Four BSC perspectives are presented in the following Table 1:

Financial perspective

presents implementation of a company strategy, which is also presented by initiatives and implementation indicators in other perspectives (investors/clients, internal processes, learning and employee development) through the company's financial results. These are the indicators of past events, and they typically include profitability, income growth, and use of (material) assets.

Investors/clients

The investors/clients perspective presents strategic initiatives and results obtained by measuring implementation of company initiatives in establishing connections with investors/clients, understanding of needs, and fulfilment of expectations of investors/clients.

Internal processes of companies

This perspective presents key business processes in the realisation of which the company must make excellent results in creating added values for investors/clients. Due to turbulent changes in construction market and changes in the expectations of investors/clients, companies are obliged to periodically identify completely new internal processes. This can concern the use of information technology (BIM, GIS, business process management, etc.) in internal processes of companies. The Building Information Modelling (BIM) represents the information-based modelling of structures. It is based on the computer software that processes the geometry of space, spatial relationships, analysis of views in space, geographical information, quantities and properties of construction elements with all relevant details. BIM can be used for simulation of the entire life span of a structure, from the planning, design, construction, to the use of the structure. BIM can be fed with data collected via sensors during the life of the structure so as to enable analysis and optimisation of maintenance activities for the said structure. The "Integrated Project Delivery at Autodesk.Inc." Harvard Business School, Case Study 2011. GIS is a geographic information system that collects, analyses and presents information about geographical location of the structure.

In construction, cooperation with supplies is a significant set of internal processes, as this cooperation is vital for an efficient fulfilment of contractor's contractual obligations.

Learning and employee development

Results obtained by the initiative and measurement of employee development and learning success constitute the foundation and are the instigators of strategic initiatives for other three perspectives as well.

Companies strategically strive toward improvement of employee skills (human capital), information systems (information technology capital), and organisational structure as needed for successful implementation (organisational capital). A strategic initiative is a project (or several projects) and is implemented through harmonisation and distribution of available resources, with simultaneous optimum implementation of several projects. Strategic balanced-scorecard (BSC) initiatives are implemented according to objectives set in advance using the multiproject management principle and, at that, selected implementation criteria - success indicators - are used to measure success during implementation and results obtained by implementation of strategic initiatives.

2.2. Objectives of strategic initiatives

Objectives of strategic initiatives are presented within four BSC perspectives. Examples of such objectives and possible implementation criteria/indicators are shown in the following table (Table 2).

Table 2. PSC objectives and implementation criteria

Perspective	Objectives of strategic initiatives	Implementation criteria/indicators
Financial	Increase in revenues Cost reduction	HRK / year Plan / realisation HRK / year
Investors / clients	Development of business partnerships Increase in market share information about current and possible future investors / clients	New investors / year % of share in construction market New investors / clients / year Processing potential investors
Internal processes	Use of IT in company operations Project management	Current use of IT applications in the company (software, hardware) Business information (BI) processing system Project success: deadlines, costs, quality
Professional advancement of employees	Development of employee skills and knowledge Knowledge management	Existing / new competences of employees Employee excellence

Well shaped strategic objectives and strategic initiatives – projects have the following properties, i.e. they have to be:
- **neutral:** with regard to selection of solutions during project implementation
- **measurable:** with regard to implementation indicators – monitoring results and measurement results gained during implementation of projects serve for making management decisions
- **realistic, achievable:** only realistic objectives can in fact be achieved
- **motivating:** project team members accept project objectives as their own objectives
- **demanding:** represent challenge for the project team
- **specific:** aimed at good-quality monitoring of project implementation [6].

These properties of properly shaped objectives can be achieved using appropriate project development tools.

2.3. Objectives matrix

One of practical tools for the definition of objectives is the so called Objectives Matrix, as shown in the following table 3. The following questions are put for every objective when defining the strategic initiative objectives: **What? Why? Who?**, and the **method for measuring initiative implementation success** is defined.

Table 3. Objectives matrix

1. PURPOSE AND MEANING Why?	2. RESULT What?
OBJECTIVE	
4. CRITERION OF SUCCESS Results measurement method	3. STAKEHOLDER Who?

When individual objectives have been defined, the process continues by defining implementation priorities and the connection between individual objectives or initiatives. A special attention must be paid to mutually-dependent objectives (e.g. cost reduction – investment in development).

In the opinion of the authors, the objectives matrix is a highly efficient tool for the development of strategic objectives, initiatives and projects in construction companies.

2.4. Business processes and construction projects

According to PMBOK Guide 3rd edition, business processes are a set of interconnected activities and decisions by which materials, semi-manufactured products, energy, and information, are processed in the scope of a system / process, and are thus converted into the final product (output) and/or services of higher value that a buyer is willing to purchase on the marketplace. These business processes in a construction company can be presented (for a fictitious company) as follows:

Management processes:
- Strategic planning and implementation
- Planning and controlling costs and revenues of a company
- Business risks management
- Project management
- Business processes and decision making.

Basic business processes –support to management processes:
- Planning
- Implementation of business plans,
- Monitoring implementation of business plans,
- Implementation documents
- Preparations for construction work
- Construction
- Maintenance
- Marketing
- Procurement
- Machines and mechanical plant – operation, maintenance.

Accessory business processes – as support to management:
- Human resources: selection, positioning and development
- Finances and personnel services
- Information management: business documentation and acquired knowledge

As a part of total company management processes, project management can be divided into project management for construction projects, i.e. for the realization of contracts and orders placed by investors/clients, and project management for internal strategic development projects, i.e. for the realisation of strategic objectives. To enable better planning and control during implementation of construction projects, optimum use of resources and efficient realisation of objectives, the life span of a project can be divided into groups of project activities, i.e project phases, which are implemented by means of business processes. The authors propose a general division of the construction project life span, as shown in Figure 1 [7].

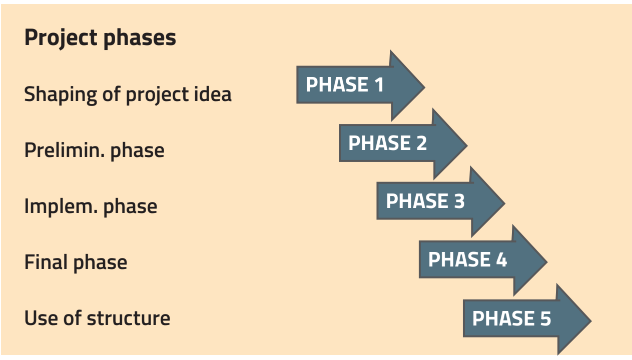

Figure 1. Phases within life span of a construction project

Depending on project circumstances, investors/clients and project managers will decide on the way in which they will divide phases within the life span of the project.
Successful implementation of project management practices on internal and external projects of a company is highly significant for companies that are nowadays exposed to influences of the open and turbulent construction market.

2.5. Strategic initiatives of construction companies

Based on BSC objectives and criteria as shown in Table 2, various strategic initiatives are implemented by companies. Some of these initiatives are presented in Table 4 below. During initial opening-up of Croatian market, this market was accessed a number of powerful international construction companies (such as Bechtel, Bouygues, Astaldi, Strabag, etc.). These companies had some considerable advantages over domestic companies: easier access to low-price capital, modern construction technology, experienced managers. Using their comparative advantages - knowledge of local and regional market and a high-quality employee base - as supported by agile implementation of innovative strategies, domestic companies can change their business strategies by:
- establishing good links with other domestic companies
- strengthening their presence on domestic and regional market
- internal development
- gaining access to international segments of construction market.

In addition tp the above-mentioned strategic initiatives, companies can also make use of other initiatives, depending on business conditions and trends of change in business environment.

3. Strategy implementation in construction companies

The strategy of a construction company, presented through four BSC perspectives, enables the company management to adjust business processes, and directs all organisational units of the company toward adoption of a single strategy. The company's strategic management team defines the way in which changes

Table 4. Some strategic initiatives implemented by construction companies

Perspective	Strategic initiative	Objective of the initiative	Implementation criteria / indicators
Financial	Agreeing on long-term cooperation with suppliers	Lower purchase price	Comparison of unit rates
	Long-term contracts with subcontractors	Lower subcontractor prices Lower project risks Better use of capacities	Comparison of supplier prices Comparison of realisation costs
Investors/ Clients	Conditions for entering into PPP contracts – investment co-financing	Diversification	Growth of contract value (%/year)
	Exploring market for potential new investments		
Internal processes	Planning and controlling deadlines and capacities for realisation of works	Better use of resources Completion within schedule	Comparison: planned / realised Use of capacities and resources
	Improvement of project management practices – based on excellence criteria	Better project implementation results	Criteria for estimating maturity in project management [8]
	Improving organisation of construction practices	Better results as to realisation of works	Deadlines, costs, quality by type of work
Learning and development of employees	Enhancement of employee knowledge in the use of new technologies in construction industry: IT, BIM, IoT	Increasing company's competitive edge on international market	Employee excellence

IoT (Internet of Things) is digital connection of objects equipped with digital devices, such as GPS (geographic positioning system), sensors, and/or other electronic units installed in construction machines, vehicles, etc.

(results of strategic initiatives) will influence adjustment of other organisational units.

3.1. Strategies applied by company's organisational units

Once the company strategy has been defined at the highest level, individual parts of the strategy are transferred (cascaded) and adjusted for adoption by lower organisational units, down to each and every employee. Each employee must be informed about the company strategy at his/her particular level, and is required to continuously adjust his/her business activities to this strategy.

The strategy is transferred to individual departments in form of BSE, which is adjusted to the level and role of each particular organisational unit. The implementation of strategy by each organisational unit is also measured through realisation of implementation process – by monitoring implementation indicators.

3.2. Success in strategy implementation

The implementation of the long-term strategy adopted by the company and its organisational units requires the same level of attention as is necessary during definition of the strategy [9] presented through four strategic perspectives and strategic initiatives.

The company management provides required assets and defines priorities for the realisation of strategic initiatives. To ensure successful implementation of strategic initiatives, the company defines performance incentives as a means to motivate its employees.

Due to big and rapid changes of conditions on the global, European and regional markets, the business management team guided by the company management must consider, on several occasions within each year, the company success indicators i.e. the success in implementation of necessary adjustments to the change in conditions in which the company operates.

Based on fulfilment of results of the current strategy, the company management decides on the changes and adjustments of the strategy immediately after influences have been observed, rather than once a year based on the last-year's historic financial indicators.

4. Conclusion

The long-term business strategy and its implementation is the precondition and final result of harmonisation of business processes in a company. The success of a strategy depends on good realisation of strategic initiatives, which involves realisation of all initiatives rather than only some of them, and on mutual harmonisation of these initiatives. The company is negatively affected in case of a lack of strategic harmonisation.

In addition to creative shaping and implementation of a successful strategy, there is also a permanent obligation of achieving excellence in the field of activity of the construction company, which is defined by influences of its external environment:

Clients:
- preparation of documents;
- organisation of tendering activities;
- contract award criteria (the most favourable financial offer);
- response to Contractor's requests;
- reaction to project changes and/or disturbances.

Contractors:
- organisation;
- technology;
- equipment;
- conditions for participation in a tendering activity;
- forming requests toward the Client;
- reaction to project changes and/or disturbances.

The adjustment of companies to the influences of external environment in which they operate is controlled by means of the BSC, which is a tool for shaping and managing implementation of company strategies.

The authors expect that the paper will contribute to further study in the field of implementation and development of construction management practices.

REFERENCES

[1] Kaplan, R., Norton, D.: The Balanced Scorecard: Measures that drive performance, Harvard Business Review, 70 (1992) 1, pp. 71-79.

[2] Porter, M.E.: What is Strategy?, Harvard Business Review, 74 (1996) 6, pp. 61-78.

[3] Lægaard, M., Vest, J.: Strategy in winning companies (in Danish), Jyllands postens forlag (2006)

[4] Vukomanović, M., Radujković, M., Burcar Dunović, I.: Modeli upravljanja izvršenjem u građevinskim poduzećima, GRAĐEVINAR, 60 (2008) 9, pp. 771-778.

[5] Katavić, M., Lovrenčić Butković, L., Džunić, M.: Strategic Analysis of Croatian Construction Industry, OTMC Conferrence, Croatian Assotiation for Construction Management - CAPM, Primošten, 2015.

[6] Bandić, M., Orešković, M., Izetbegović, J.: Razvoj ciljeva projekata u graditeljstvu, Međunarodni znanstveno-stručni skup Menadžment, Zagreb 2014. pp. 5-13.

[7] Bandić, M., Orešković, M.: Projektni menadžment u graditeljstvu, Hrvatska sveučilišna naklada, Tehničko veleučilište Zagreb, 2015.

[8] Kerzner, H.: Project Management Maturity model. 2, Hoboken, New Jersey: John Wiley & Sons, 2005.

[9] Reeves, M., Haanaes, K., Sinha, J.: Your Strategy needs Strategy, Boston Consulting Group, Amazon, 2015.

Primljen / Received: 31.7.2015.
Ispravljen / Corrected: 18.6.2016.
Prihvaćen / Accepted: 6.9.2016.
Dostupno online / Available online: 10.10.2016.

Repair of Krk Bridge

Authors:

Boris Huzjan, PhD. CE
Hrvatske autoceste, održavanje i naplata cestarine, HAC-ONC
boris.huzjan@hac-onc.hr

Nina Ostojić, MCE
Autocesta Rijeka Zagreb
nina.ostojic@arz.hr

Professional paper

Boris Huzjan, Nina Ostojić

Repair of Krk Bridge

The construction chronology of both arches of the Krk Bridge is described, and specific features of the site on which the bridge was built are given. The influence of the arches on the reinforced concrete structure of the bridge is explained. A general overview of analyses conducted on the small and large arches of the bridge is given, and the proposed repair and protection solutions are presented. The results of the last chloride penetration analysis, and the report submitted after final repair, are described in great detail.

Ključne riječi:
Krk Bridge, chloride penetration, analyses, repairs, protection

Stručni rad

Boris Huzjan, Nina Ostojić

Sanacije Krčkog mosta

U radu je opisana kronologija gradnje oba luka Krčkog mosta, specifičnosti lokacije na kojoj je most izgrađen te njihov utjecaj na armiranobetonsku konstrukciju mosta. Dan je pregled ispitivanja koja su obavljena na malom i velikom luku mosta kao i ponuđena rješenja sanacije i zaštite. Detaljno su prikazani rezultati zadnjih ispitivanja prodora klorida te izvješće nakon obavljene konačne sanacije.

Ključne riječi:
Krčki most, prodor klorida, ispitivanja, sanacije, zaštita

Fachbericht

Boris Huzjan, Nina Ostojić

Sanierung der Brücke Krk

In dieser Arbeit werden die Chronologie der Erbauung beider Bogenkonstruktionen der Brücke Krk, die Besonderheiten des Standorts der Brücke, sowie ihre Einflüsse auf die Stahlbetonkonstruktion beschrieben. Es wird eine Übersicht der Untersuchungen gegeben, die am kleinen und am großen Bogen der Brücke durchgeführt wurden, sowie ein Vorschlag zu Sanierungs- und Schutzmaßnahmen dargelegt. Resultate der letzten Untersuchungen bezüglich Durchdringung von Chloriden und der Bericht zur durchgeführten abschließenden Sanierung werden detailliert dargestellt.

Ključne riječi:
Brücke Krk, Durchdringen von Chloriden, Untersuchung, Sanierung, Schutz

1. Introduction

Although the construction of the Krk Bridge ended 36 years ago, this bridge still has the world's largest traditional reinforced concrete arch span. Considering the aggressive maritime environment and errors made during the design and construction of this bridge, the structure suffered damage over time namely due to chloride penetration, i.e. deterioration of the protective layer and reinforcement corrosion.

The idea about connecting the Krk Island with the mainland was first formulated after the World War One, in the late 1918, but it is only four decades later that serious activities were initiated in order to enable practical realisation of this idea. Three proposals were made in the study presented in 1964: tunnel under the sea, concrete girder bridge with concrete piers across St. Mark Island, and a steel girder bridge on concrete piers between Krk Island and Jadranovo. Various proposals were considered and, in 1971, the design prepared by *Industrijski projektni zavod* (Institute for Industrial Design) was accepted. The route was set and preliminary works started but the realization was unfortunately interrupted. The tendering procedure was repeated in 1975. Out of several alternatives offered by the tenderers, which can be classified into four groups (suspended structures, cable-stayed systems, girder systems, and arch systems), the client accepted the one presented by the design office Mostogradnja from Belgrade [1], while the following joint venture was selected for realisation of the works: Mostogradnja (superstructure) and Hidroelektra (foundations and pavement structure) [2]. The bridge construction works started in July 1976 and lasted until July 1980.

The bridge connects mainland with Krk Island and passes across St. Mark Island. The bridge crosses two sea channels: "Calm Channel" and "Agitated Channel". The total length of the bridge is 1,309.50 m not including aboutments, as can be seen in Figure 1 [3].

What makes this bridge so special is the fact that, by its construction, the world record has been achieved in the reinforced-concrete span length, i.e. the span of the former largest arch was exceeded by as much as 85.0 m. Credits for such outstanding design solution go to Mr. Ilija Stojadinović, designer of this and many other known bridges, and to Dr. Stanko Šraom, who skilfully realised this impressive project [4].

The pressing need for implementation of this project can *inter alia* be seen in the fact that as many as 27.2 million vehicles used the bridge during the first 20 years of its operation. An annual average daily traffic measured in 2015 at the Krk Bridge toll station amounted to 10,512 vehicles, while the annual summer daily traffic amounted to 20,804 vehicles [5]. The Adriatic petroleum pipeline, drinking water pipeline, and pipeline for the INA's industrial plants, were incorporated into the bridge structure.

2. Description of bridge structure and presentation of construction process

The bridge measures 11.40 m in total width, which includes pavement 7,50 m in width, footways 2 x 1.30 m in width, and side strips 2 x 0,65 m in width. The span traversing the „Calm Channel" is 390 m long, while the span over the „Agitated Channel" is 244 m long. In transverse direction, the deck slab leans onto three prestressed "I" girders resting on head beams of piers (Figure 2). Foundations of the big arch are realized in form of a branching at 19.0 m below the sea level. Horizontal legs of foundations transfer the horizontal arch pressure directly onto the rock above the sea, while the vertical component of the force is transferred via inclined struts onto the foundations. The arches can be accessed via approach viaducts.

Considering that the project was considered to be highly demanding at that time, it was also necessary to make some modifications, improvements, and fine adjustments to the design ant construction technology. Some changes to the construction practices used at that were also introduced:

1. Installation of ties - instead of emerging from one point, ties now come from different points creating, together with piers and a part of the realized arch, a truss structure at all phases of construction work.
2. Piers as a part of the cantilever arch construction method - piers were concreted in parallel with arch construction, and they formed vertical trusses in the load-bearing cantilever system.
3. Anchoring - prestressed cables were installed in the rocky terrain to hold the concrete block and, in that way, the rock mass was included in the bearing part of the system.
4. Arch concreting in phases - the central box was realised in the first phase along the entire length of the arch, and then the side boxes were realised. (Figure 3)
5. Steel trusses in crown - bracing with hydraulic jacks was conducted over two trusses that were mounted in crown immediately before connection of arch cantilevers [1].

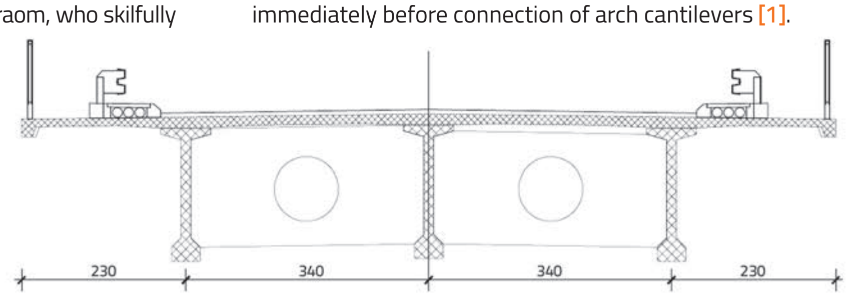

Figure 2. Cross-section of pavement structure [2]

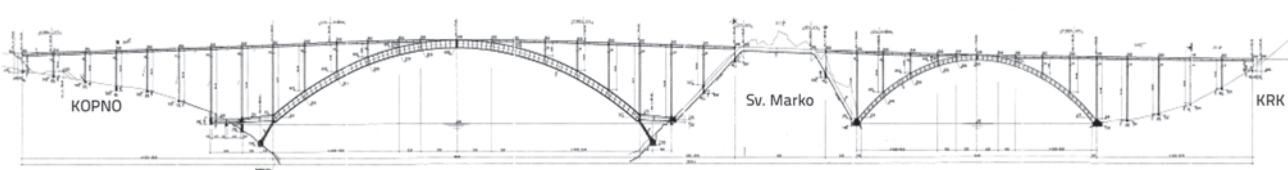

Figure 1. Layout of Krk Bridge [3]

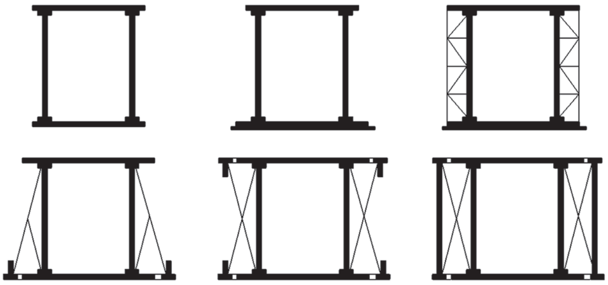

Figure 3. Arch cross-section construction phases for big span of Krk Bridge [1]

The bridge piers situated above the arches on Krk are spaced at the following intervals: 25x33 m + 6x28 m + 2x23 m + 2x19 m, and they were realised as shown in Figure 4., i.e. as double T sections using sliding formwork [2].

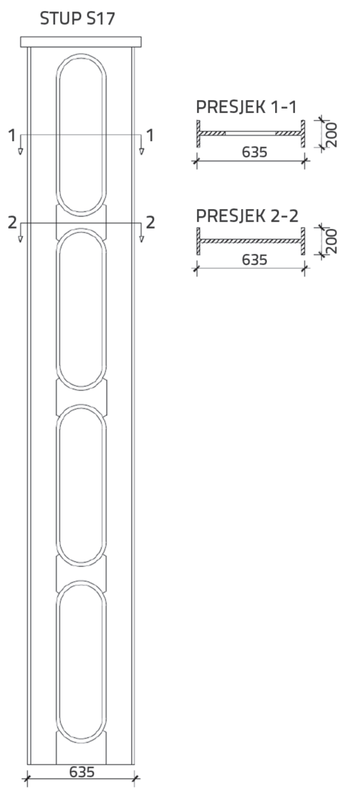

Figure 4. Cross section of pier S17 [2]

Concrete grades for bridge structure were defined in accordance with the *Byelaw for concrete and reinforced concrete* passed in 1971, i.e. MB50 was used for bridge arches and main girders of the pavement structure, MB45 was used for the big arch bracings, MB40 for the envelope and ribs of the big-arch inclined struts, and for cross girders and deck slab, while MB35 was used for piers [2].

Load testing was conducted according to then valid Byelaw, and the bridge was subjected to load using 18 trucks 540 tons in total weight that were positioned along the bridge in such a way to obtain extreme bending moment values with the corresponding longitudinal forces in typical arch sections. The largest measured arch deflection to arch span ratio amounted to w/l = 1/8260 [2].

Dynamic testing was conducted on the big arch by causing vertical excitation using a vehicle passing over the bridge, while the horizontal excitation was caused by tensioning the arch using a tugboat. The period of vertical oscillation varied from 0.3 s to 0.45 s, and the dumping ratio ranged from 0.065 to 0.135, while in case of horizontal oscillations the period varied from 0.25 s to 0.2 s in both directions. Detailed testing revealed that the bridge behaviour is technically acceptable and that the bridge can be opened to traffic for the design load [2].

3. Bridge testing and repair

3.1. Chronology of bridge inspections

Topographic surveying started immediately after completion of construction work. Geometric instability of the bridge occurred due to usual long-term deformation of concrete (creep). Rectification works were conducted in 1981 and the reinforced-concrete structure inspection, conducted in the same year, revealed some realisation errors [4].

In 1985, Civil Engineering Institute prepared the program entitled "*Instructions for monitoring and maintenance activities on the Tito's Bridge*" and, based on these instructions, the first detailed inspection of this bridge was conducted in 1986. The inspection revealed cracks and initial reinforcement corrosion at main girders, corrosion damage at inclined struts, bracings and arch springs, and cracking at piers, abutments and bottom contour of the deck slab. The chloride level in concrete was low, and the protective layer thickness and compressive strength of concrete were satisfactory.

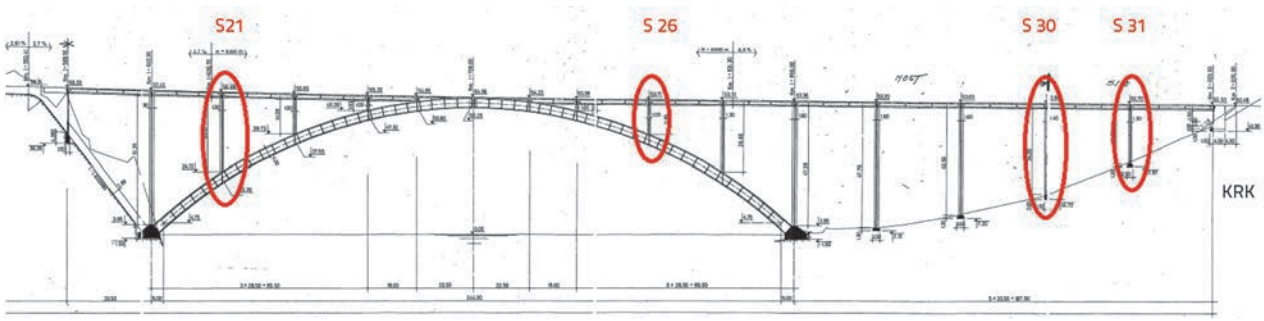

Figure 5. View of small arch piers that suffered greatest damage

Urgent repair and protection measures were defined. These measures included repair of main girders, protection of cracked areas by coating, asphalt repair, closing openings in arches, applying corrosion protection, and improving water drainage from pavement [2].

The second detailed bridge inspection was conducted by *Croatian institute for bridges and structures* in 1993. The segments and elements repaired in the period between two inspections were inspected, and a particular emphasis was placed on those parts that were exposed to aggressive maritime influence. Based on a number of non-destructive tests, the decision was made to conduct repair work on the most damaged parts, i.e. on small arch piers S21, S31, S26 and S30 (Figure 5), already in the ensuing year [4].

The condition of concrete and reinforcement, i.e. their physicomechanical properties, were tested for the first time in 1994, also in order to prepare an appropriate repair design, and to protect the piers that suffered greatest damage. It was established that the concrete is of high quality, with a low gas-permeability and capillary absorption coefficient. The carbonation was still observed in the surface layer only, while the chloride penetration was variable [4]. Concrete test results and visual inspection results for the smaller arch were combined in the final report issued in 2000. The following main conclusions were made:

- The concrete tested in piers, arches and pavement structure is characterised by a high compressive strength (of approximately 80 N/mm^2), but it also exhibits a high absorption rate (of approximately 1,0 kg/m^{2}h^{0,5}) in the surface layer, and low resistance to freezing, which is due to the presence of chlorides.
- Critical chloride concentration was attained in the reinforcement zone in joints and at haunches of lateral arch elements where the protective layer of concrete is too thin, at piers in reinforcement zone at pier bases closer to the sea, at piers closer to St. Mark Island, and at porous and cracked concrete parts of all piers, which is especially pronounced at abutments. The chloride concentration in the deck slab did not attain a critical value.
- Static cracks were visible at some structural elements, while corrosion cracks up to several cm in length were visible at most piers.
- The repair campaign conducted in 1988 slowed down further chloride penetration into repaired elements.
- High quality concrete and slag cement, which reduced the cement hydration heat release rate, slowed down penetration of chloride and extended useful life of the structure [2].

Furthermore, the following conclusions were made based on the big arch testing, initiated in 2001, the results of which are presented in Volume 1 [6], Volume 2 [7] and Volume 3 [8]:

- General condition of the big arch of Krk Bridge is much better compared to that of the small arch.
- Capillary absorption and gas permeability are more favourable compared to small arch, which is due to more favourable local micro-site conditions and a higher quality of construction work.
- Compressive strength corresponds to that registered at mall arch.
- Local chloride penetration was most pronounced at arch springs, at deck slab above St. Mark, and at some piers that were already singled out during preliminary testing.
- It was estimated that the structure can remain in that conditions for another decade, considering the situation regarding the design stability and safety.
- The occurrence of cracks 0.5 mm to 0.8 mm in size at deck slab elements was a sign that traffic speed limit at the bridge must be limited, and that cracks due to shrinkage, and static and dynamic load, must urgently be repaired [2].

Considering the slow progress of repairs and protection of the reinforced-concrete structure, an additional inspection was made, which revealed a progress in chloride penetration and corrosion of locally exposed reinforcement. The results are presented in reports, i.e. in Volume 4 [9] and Volume 5 [10] (2006./2007.), and it was concluded that the condition of the structure deteriorated in the period between the two inspections. However, chloride concentration remained the same, which is probably due to the difference in the testing and sampling methodology [2]. In the light of the above, the chloride content determination procedure was verified and additional testing was conducted. The results of this testing are presented in Volume 6 [11], as summarized below:

- Both chloride testing and sampling procedures, i.e. the one conducted according to British standards and the one based on Croatian standard HRN EN 14629, provide similar results.
- The bridge protection conducted in the late 1980s failed to prevent chloride penetration, i.e. It only succeeded in slowing down the process.
- Much better results were obtained by the protection conducted in the early 2000s, which involved application of polymer coating onto some parts of the structure [2].

Underwater diving inspections are also an important form of prevention against greater bridge damage. These underwater inspections were conducted in 1982, 1984, 1989, 1990, and 2001. According to the report issued by IGH in February 2002, the presence of shellfish does not endanger stability of the structure and has not greatly progressed over the past decade. However, it is stated in the report that chloride penetration is significant, i.e. that critical concentration was registered at the depth of 4 cm, which is the main reinforcement zone. At all samples, the contact between concrete and reinforcement was black in colour, instead of the healthy grey, which pointed to the presence of active corrosion. In addition, it was estimated that the inclined struts protection, either traditional or cathodic, is obligatory [4].

3.2. Chloride protection at small arch of Krk Bridge

The first detailed inspection was conducted already in 1986, and it was concluded that some poor structural solutions must urgently be improved, and that the structure must be protected against chloride penetration. The bidding documentation was prepared during the ensuing year, but none of the offered solutions complied with requirements, and so the decision was made to conduct tests in smaller zone of the structure (Figure 6).

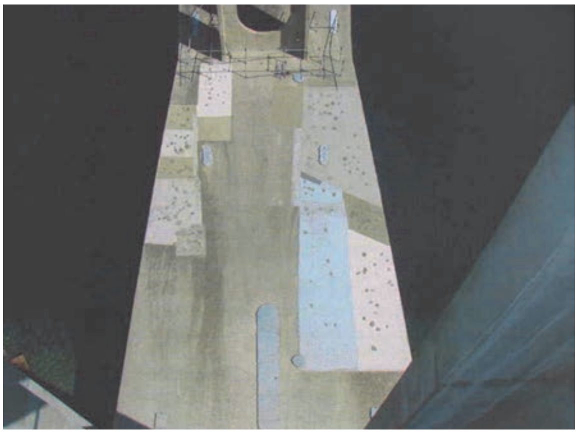

Figure 6. Test areas [2]

The mentioned comparative testing revealed that only three out of twenty protection systems installed in 1988 and 1989 only partly meet the repair criteria, and so it was concluded that the practice of remedying chloride exposed structures by polymer cement coats must be abandoned [2].
In 1998, the Croatian Road Administration signed a contract for the remedy and protection of four spandrel piers at the small arch bridge. In parallel with this initiative, a six-member expert group was formed in order to develop an appropriate strategy for the repair and protection of the reinforced-concrete structure. Thus a protection system was selected, and this system was applied in three phases: application of shotcrete by dry method, application of the impregnation and levelling coating, and application of the final polymer coating in two layers. The works on pier S28 started in the late 1998 and they lasted for two years. The designer and the investor were not satisfied with the works because of unsatisfactory adhesion and compressive strength, and due to introduction of galvanized guides - installed by contractor at its own initiative - which endangered the remedial activities. The works were also conducted at piers S29, S30, and S31 [2].
The design documentation consisting of five Volumes [12], was prepared in 2000s, and it comprised static and dynamic analyses, repair of twelve bearing points on the St. Mark - Krk bridge, solution for repair of piers S20 and S27, and solution for the repair and protection of the arch, deck slab and abutments. Two additional volumes with additional design solutions were later on added, and the second waterproofing system to be used in the repair was accepted. The system includes four realisation phases:

1. reprofiling mortar, wet application
2. basic coating
3. elastoplastic levelling compound
4. Protective and decorative acrylic paint

In Volume 7, the designer proposed the use of contract funds to raise the small bridge protection from 15 above the sea to 25 m above the sea, and continuation of works on the repair and protection of piers S18 and S9, which were in critical condition. The chloride penetration was slowed down considerably by the use of this repair system.
The repair of other damaged piers (S21 and S27) was agreed on already in mid 2001. The repair of pier S21 represented a particular challenge due to required repair of the head beam on top of the pier, and installation of neoprene bearings. A special scaffold, aimed at assuming pier load during repair work, was designed for that purpose (Figure 7). The repair process itself was not highly demanding mainly because of the use of the relieving scaffold whose design lasted almost a year, and due to accessability of the site. The fibre reinforced concrete with steel fibres, silica fume, superplasticiser and slag cement, was used in the repair of pier S27 [4].

Figure 7. Load relieving scaffold at pier S 26 [4]

The repair of piers S20 and S26 started immediately after completion of works on piers S21 and S27 [4]. Simultaneously with preparation of the design for the repair and protection of small arch of the Krk Bridge, appropriate investigations were conducted in order to determine condition of the reinforced-concrete structure of the big arch of the Krk Bridge. The obtained results were analysed and used to prepare a detailed repair & protection design [4].

3.3. Chloride protection at big arch of Krk Bridge

Due to variable micro-climate conditions, and hence an unpredictable penetration of chlorides, and considering a relatively complex foundation method used, the repair problem relating to the big arch of the Krk Bride proved to be more complex comapred to repairs at the small arch.
As to penetration of chlorides into the bridge structure, the focus was on selection of a good quality polymer-based surface protection. Five distinct systems were tested for the undersea protection of inclined struts for foundations. Three of these systems met requirements regarding easy undersea installation and adhesion. Furthermore, chloride penetration tests conducted in the period from 2001 to 2003 revealed that the greatest big arch damage is situated at bracing sides and at arch springs where 2-3 cm of protection had to be removed, and at the bottom part of the arch at St. Mark toward Rijeka where 1-2 cm had to removed at the first ten meters of the arch, and 0.5-1 cm at the remaining arch length. 1-2 cm of the degraded repair mortar had

to be removed from the top area of the bracing and from the side and spring of the arch toward Crikvanica at St. Mark. At the arch side, such depth was estimated at 0.5-1 cm [2].

An appropriate solution that would stop further penetration of chlorides had to be developed for the remaining parts of the big arch of the Krk Bridge, where critical chloride concentration was situated within the first two centimetres. As the described testing confirmed that the condition of the reinforced-concrete structure of the big arch bridge is similar to that of the small arch bridge, the decision was made to adopt the same design solutions for both bridges.

After a number of unsuccessful attempts to find the most favourable system that would ensure proper cathodic protection of the bridge structure, a solution provided by a French company was finally accepted. This solution involved superficial anodic protection for inclined strut parts situated above the water level, and disk-based anodic systems each with 12 titanium anodes activated by a layer of abrasion resistant electricity conductive ceramics, for the segments situated under the water level (Figure 8) [2].

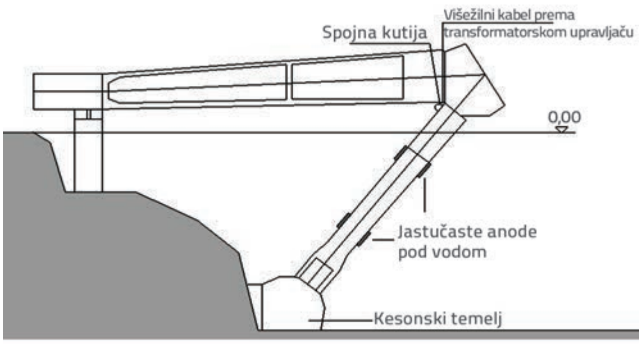

Figure 8. Schematic view of designed cathodic protection of inclined-struts at big-arch foundations [2]

Piers S18 and S19 were repaired and protected using the system that was accepted for the small arch, and the same system was also used to repair abutments U3 on the big arch and abutments U4 and U5 on the small arch. The polymer cement binding and levelling course of higher pH value was used for the repair of concrete surfaces at the sides of the bottom part of the big arch (up to 25 m above the sea level), and at arch springs and bracings on the mainland.

3.4. Description of design solution from Volume 6

Guidelines for further repair work are presented in Volume 6. A detailed visual inspection of the structure and hammer inspection was proposed so as to determine places at which concrete has separated from the reinforcement due to corrosive action. The areas in which a critical concentration of chlorides was determined were treated using the hydro-demolition procedure (demolition by water pressure ranging from 2,000 to 2,500 bars), while places of easy detachment were additional tested usilng the pull off method. The adhesion strength of the blinding concrete prepared for repair and protection was not to be lower that 2 N/mm^2 [13]. Other (sound) areas of concrete at arches and deck slab were cleaned by hydrodynamic method (at water pressure ranging from 1,000 to 1,500 bars) to remove the old surface coating. Then the concrete surface was washed clean, and all protrusions were levelled down by polishing [13]. The corroded reinforcement was cleaned down to metal gloss, i.e. until a clean contact with concrete was reached. In cases where the cross section of distribution steel was reduced by corrosion for more than twenty percent, this reinforcement was replaced by new bar and linked by overlap to sound (undamaged) parts of the old reinforcement [13].

Local zones of open concrete were filled with reprofiling mortar (either by hand or by spraying). It was important to include in this repair all places of exposed reinforcement and to fill such places with mortar no less than 15 mm in thickness. In addition, zones repaired with mortar were carefully smoothed down so that a continuous polymer protection could be applied. To this end, these zones were adequately protected against evaporation immediately after repair. The repair mortar had to comply with requirements specified in HRN EN 1504-9, as well as with the following additional requirements:

- adhesion ≥ 2,0 N/mm^2
- Compressive strength ≥ 50,0 N/mm^2
- Tensile strength ≥ 4,0 N/mm^2
- Specific coefficient of gas-permeability ≤ 10^{-13} cm^2
- Resistance to freezing and deicing salt ≥ 56 cycles [13].

Properties of mortar were tested on samples at 28 days, except for adhesion which was tested by breaking samples 50 mm in diameter, cut down to blinding concrete at the structure. The prepared concrete surface was treated by corrosion penetration inhibitor. The concrete surface prepared in this way was protected against further penetration by polymer-cement and polymer coating presenting the following properties:

- Continuously elastoplastic binding and levelling polymer cement layer no less than 2 mm in thickness with an average adhesion to blinding concrete of ≥ 1,0 N/mm^2 (or ≥ 0,7 N/mm^2 in individual cases)
- final continuously elastoplastic polymer coating 0.7 mm in thickness defined in HRN EN 1504-2 as a 5 % fractile, with an average adhesion to binding layer of ≥ 0,8 N/mm^2 (or ≥ 0,5 N/mm^2 in individual cases) [13].

The entire system had to have the following minimum properties:

- Average adhesion ≥ 0,8 N/mm^2 (≥ 0,5 N/mm^2 in individual cases)
- Crack repair tested acording to the procedure described in HRN EN 1062-7, opening ≥ 1,0 mm
- Capillary absorption ≤ 0,01 kg/m^{2}h^{0,5}
- Resistance to freezing and deicing salt according to HRN 1128 ≥ 56 cycles.
- Resistance to ageing tested according to HRN EN 1062-11 ≥ 10 years [13].

4. Repair of small arch at the Krk Bridge (2013-2014)

Prior to the start of works, the structure was inspected and areas to be repaired were defined in an appropriate report. The sum of these areas was by approximately 40 m^2 greater than the sum of

Figure 9. Bottom flange of the main girder in the U4-S20 zone after removal of poor-quality concrete [14]

Figure 10. Side of main girder in the S20-S21 zone at pier S21 after removal of poor-quality concrete [14]

Figure 11. Deck slab bottom contour in the S31-S30 zone next to pier S31, moisture due to seepage at joint after hydrodemolition of damaged concrete [14]

Figure 12. Seepage through joint at pier S30, Crikvenica sidei [14]

Figure 13. Bottom contour at the first third of deck slab in the U5-S31 zone after removal of damaged concrete [14]

Figure 14. Bottom contour at the first third of deck slab in the U5-S31 zone after placement of the repair system [14]

Table 1. Average values of adhesion strength testing by pull-off method (surface, coating, mortar) and coating thicknesses in the U5-S31 zone [14]

Date of testing	Place of testing		Tested material	Average tensile strength [Mpa]	average coating thickness [mm]
9.5.2014.	U-S31	tunnel* Crikvenica - slab	repair mortar R4	2.42	2.84
		girder Crikvenica	coating	0.97	3.14
		tunnel* Crikvenica - slab	repair mortar R4	2.03	3.41
*tunnel - bottom contour of the slab bounded by central, longitudinal and edge girders, and by transverse girder)					

Figure 15. Deck slab bottom contour in the U5-S31 zone after application of the final coat of paint [14]

Figure 16. Deck slab bottom contour – S31-S30 zone - application of the final coat of paint [14]

areas included in the Repair Design from 2010. The areas were treated as shown in design solution contained in Volume 6. The following time schedule was adopted:

- Hydrodemolition of damaged concrete down to the sound zone (Figures 9, 10 and 13)
- Hydro-dynamic washing of all bottom contour areas and saturation of concrete surface by penetrating corrosion inhibitor.
- Placing repair mortar in zones from which concrete was removed (Figure 14)
- Hydrodynamic washing as a preparation for application of coating
- Application of two coats (minimum 2 mm in dry thickness).

Application of two coats of final paint (minimum 0.7 mm in dry thickness) (Figures 15 and 16). During realisation of repair works, inspection of deck-slab bottom contour areas has revealed moist zones next to piers S31, S30, S29, S28, S20 on the side toward St. Mark, while in the expansion joint zone at pier S27 moisture is present at both sides of the pier. Moisture at bottom contour of the deck slab and longitudinal and transverse girders along piers is due to rainwater seepage through expansion joints (Figures 11 and 12). Local seepage from deck slab was also observed in the cantilever zone on the Rijeka side, while moisture was registered at top girder flange in external zones from pier S30 to pier S29. New seepage tubes were installed in the local seepage zones, while connections were placed in the zones of the existing tubes so as to prevent seepage on the concrete surface. The tubes placed in this way also serve as marks showing position of seepage points [14].

4.1 Testing

The current testing included adhesion measurement by pull-off method according to HRN EN 1542:2001 for determining tensile strength of the prepared concrete surface and for determining adhesion of paint coats and mortar layers, while the coating thickness was tested by penetration needle. Based on testing conducted on the structure, it was concluded that the quality of works is compliant with requirements specified in the design. The same methods were used in control tests. Some results obtained during control tests, with average tensile strength and coating thickness values, are presented in Table 1 [14]. The following conclusions were made based on control test results:

- adhesion of repair mortar is satisfactory (design value is ≥2,0 N/mm^2)

- adhesion of the surface protection system onto the blinding concrete is satisfactory (design value is ≥1,0 N/mm^2 (average value) and ≥0,7 N/mm^2 (individual value)); at test points, the surface protection system's material mostly separates within itself, which means that its adhesion to the blinding concrete is higher
- measured coating thickness values are satisfactory (design calls for no less than 2.7 mm of the total surface protection thickness) [14].

5. Conclusion

The chronology of inspection and repair activities conducted at the small and big arches of the Krk Bridge is presented in the paper. It has been demonstrated that the basic problem, besides the aggressive environment, is an inadequate thickness of protective layer. Chlorides still have not reached the main reinforcement, but they have damaged the reinforcement devoid of protective layer, which is due to construction error. It can be concluded from the chronology of activities that many years and great expertise were necessary to define protection system capable of safeguarding main functions of this structure. Periodic repairs have been made to remedy local deficiencies i.e. to repair points where concrete has deteriorated, and where corrosion and detachment of protective layer of concrete has started. All other surfaces are treated by inhibitor, which slows down the corrosion process and negative action of chlorides. Surface protection systems involving the use of appropriate coatings are applied to protect the structure against further damage by chlorides. The repair design prepared in 2010 introduced overall bridge inspections every two years, during which a special emphasis is placed on the already repaired and protected areas. Attempts have also been made to determine the remaining durability of the Krk Bridge structure, and this through a number of tests aimed at determining chloride content in concrete samples, and through analyses based on appropriate mathematical models. Continuous investments in terms of financing and other contributions and expertise are considered necessary to ensure good quality maintenance of the Krk Bridge, i.e. to preserve basic functions of this extremely valuable structure.

REFERENCES

[1] Simović, V.: Dvadeseta obljetnica mosta kopno - otok Krk, 52 (2000) 8, pp. 431-442.
[2] Beslać, J., Bleiziffer, J., Ille, M.: Pregled aktivnosti sanacije i zaštite Krčkog mosta od 1980. do 2010., 2010.
[3] Stojadinović, I.: Glavni projekt broj: 1153; Dispozicija mosta
[4] Vujić, D.: Radovi na izvanrednom održavanju Krčkog mosta, *Građevinar*, 56 (2004) 9, pp. 547-553.
[5] Brojenje prometa na cestama Republike Hrvatske godine 2015.
[6] IGH d.d.: Izvještaj, Knjiga 1 za kosnike, broj: 2131-70, 2002.
[7] IGH d.d.: Izvještaj, Knjiga 2 za razupore i stupove, broj: 2131-93, 2002.
[8] IGH d.d.: Izvještaj, Knjiga 3 za luk i kolničku konstrukciju, broj: 2131-95, 2003.
[9] IGH d.d.: Izvještaj, Knjiga 4 broj: 2100-2300, 2006.
[10] IGH d.d.: Izvještaj, Knjiga 5 broj: 2100-2367, 2007.
[11] IGH d.d.: Izvještaj, Knjiga 6 broj: 2100-1794, 2008.
[12] IGH d.d.: Projektna dokumentacija sanacije i zaštite mosta velikog luka; Knjige 1-5, 2003.-2008.
[13] IGH d.d.: Knjiga 6 - Radovi iz Knjige 4 Projekta preostali nakon izvršenja ugovora HAC d.d. – Viadukt d.d. , 2010.
[14] Balagija, A.: Izvješće nadzornog inženjera o provedenim radovima na podgledu kolničke konstrukcije (nosači i kolnička ploča), 2014.